

6 *Computer Applications in Mining & Processing*

Mathematical Modelling of the Roadheader's Cutting Process

M.Dolipski, MJaszczuk, P.Cheluska & P.Sobota

Institute of Mining Machinery, Faculty of Mining and Geology, Silesian University of Technology, Gliwice, Poland

ABSTRACT: The roadheader's cutting system is a complex process characterized by continuous distribution of the mass, with its concentration being visible in such elements as; die rotor of the driving motor, the disks of the flexible coupling, the gear wheels and the cutter heads. The moment of load forces on the shaft of the cutter head is the effect of the action of the roadheader on the rock mass when cutting the room being driven. The forced excitation of vibrations in the cutting system results from resistances to cutting of the rock. Recognition of the physical essence of the process of mining the rock in the course of particular movements of the boom and the modelling of cuts taken by conical cutting tools of the cutter head are starting points for determining the run of such forces.

1 DYNAMIC MODEL

The roadheader's cutting system consists of an asynchronous motor, a flexible coupling, reduction gear and cutter heads. The system can incorporate two transverse cutter heads or a longitudinal one. This complex system is characterized by a continuous distribution of the mass with its concentration being visible in such elements as: the rotor of the driving motor, the disks of the flexible coupling, the gear wheels and the cutter heads. The design of the road-

header's cutting system is conducive to the construction of a physical model featuring a discrete structure (Fig. 1). Thus, it is composed of rotating concentrated masses with moments of inertia I that are connected to each other by means of weightless viscoelastic elements, the specific torsional rigidity of which is k and the damping coefficient is c . In Figure 1, the following items have been marked: rotor of the asynchronous motor (index W), disks of the flexible coupling (index K), n - stage reduction gear and cutter heads (index G). The physical model

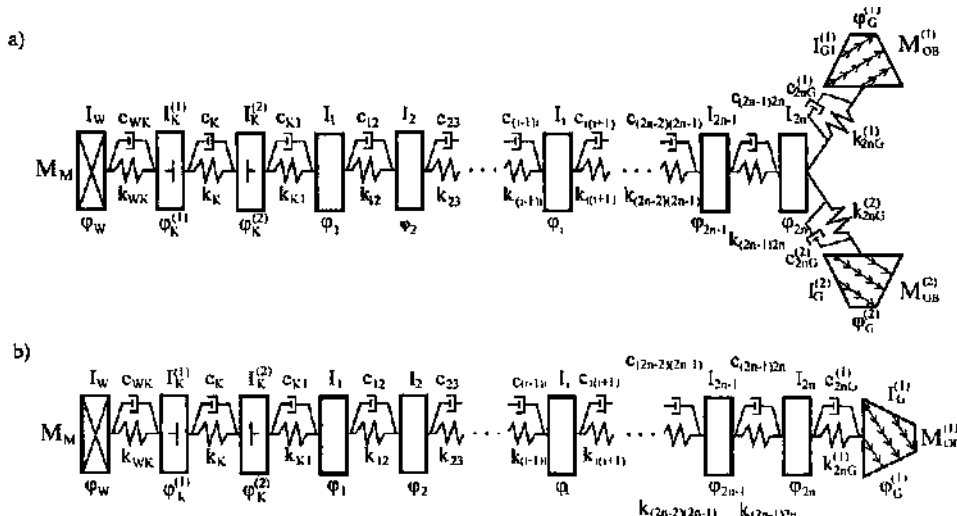


Figure 1. Physical model of roadheader cutting system: a) with transverse cutter heads, b) with a longitudinal cutter head.

of the roadheader's cutting system is subjected to the action of external loads in the form of a driving torque M_M and a moment of load forces of the cutter head MOB (Dolipski & Cheluszka, 1999).

Motion in the physical model of the roadheader's cutting system is described by a system of ordinary differential equations of the second order (Table 1). The quantity WG stands for a number of cutter heads ($WG = 1$ corresponds, in this case, to a roadheader equipped with a longitudinal cutter head, $WG = 2$ signifies a roadheader with transverse cutter heads). A reduced driving torque applied to a shaft of the cutter head MM is determined by means of the relationship given in a previous paper (Dolipski, 1993). The moment of load forces acting on a shaft of a cutter head MOB is an effect of the action of cutting tools on the rock mass when mining the road head being driven. It is necessary to model the process of mining the rock mass with cutter heads so that a run of such loading can be determined.

2 MODELLING OF THE CUTTING PROCESS EFFECTED BY MEANS OF CUTTER HEADS

Modelling of the rock-cutting process with cutter heads covers the following phases:

- I. finding out the cutting tools arranged on a cutter head which take part in the process of mining the road head of the roadway being driven;
- II. establishing cutting zones for tools engaged in the cutting process determined by: the value of the angle at which the tip of a cutting tool enters a cutting zone δc and of the angle at which the tip of the cutting tool leaves the cutting zone δa ;
- III. the projection of cuts taken by cutting tools for preset parameters: the mechanical properties of the rock being cut, the stereometric features of the cutter head, cutting tools and boom as well as the operational parameters of the roadheader,
- IV. defining the kinds of particular cuts and determining the function runs relating to the depth of cuts taken during the revolution of a cutter head $g = f(VG)$
- V. determining a run of components of the load of the cutting tools: cutting forces $P_s = f(pG)$, pressing down forces $P_i = f(cj)$ and side force $P_b = f(c)$,
- VI. determining a run of the moment of load forces of the cutter head $M_{ob} = f(pG)$ which is the forced excitation of torsional vibrations in the roadheader's cutting system.

As the basic technique used for driving the roadway consists of the mining of a road head by extracting the layers parallel to the floor, there are

three movements of the boom involved in the process of rock mining which must be taken into consideration:

- displacement of the boom in a direction parallel to the longitudinal axis of the roadway,
- swinging of the boom in a plane parallel to the floor,
- swinging of the boom in a plane perpendicular to the floor in the vicinity of one or the other side-wall of the roadway.

The displacement of the roadheader's boom in the direction parallel to the longitudinal axis of the roadway is connected with the sumping of the cutter heads in the rock. With a roadheader which incorporates transverse cutter heads, there are three technological variants to be distinguished (Dolipski & Cheluszka 2000):

- I. sumping in when the boom is being displaced in a direction parallel to the longitudinal axis of the roadway at a speed v_p (Fig. 2a),
- II. sumping in when the boom is being displaced in a direction parallel to the longitudinal axis of the roadway at a speed v_p along with one-side swinging of the boom in a plane parallel to the floor effected at the same time at a speed v_m (Fig. 2b),
- III. sumping in when the boom is being displaced in a direction parallel to the longitudinal axis of the roadway and swung in a plane parallel to the floor at the same time (Fig. 2c).

When transverse cutter heads are advanced towards a road head, the cutting tools move along plane curves having the form of cycloids. This results from the composition of vectors of two speeds, i.e., of a speed of the displacement of cutter heads in a direction parallel to the longitudinal axis of the roadway, and of a tangential velocity of cutting tools rotating around the axis of rotation of the cutter heads. The vectors of these speeds lie in the same plane. During the displacement of transverse cutter heads in a plane parallel to the floor towards a side-wall of the roadway, cutting tools move along screw lines circumscribed on a side surface of the torus. In this case, the speed vectors in question are perpendicular to each other.

The sumping in of a longitudinal cutter head is of a typical boring character (Fig. 3). A hole made by the tips of the cutting tools arranged over the smallest radii is gradually extended by means of the tips of successive cutting tools, while the tips are describing circles with greater and greater diameters. The cutting tools move in this time along screw lines described on a side surface of the cylinder.

The basic working movement accompanied by the process of the mining of a roadheader covers swinging of a boom in a plane parallel to the floor at

Table 1. Equations of motion in a physical model of the roadheader's cutting system

$I_W \cdot \ddot{\varphi}_W$	$+ k_{WK} \cdot (\varphi_W - \varphi_K^{(1)})$	$+ c_{WK} \cdot (\dot{\varphi}_W - \dot{\varphi}_K^{(1)})$	$= M_M(\ddot{\varphi}_W)$		
$I_K^{(1)} \cdot \ddot{\varphi}_K^{(1)}$	$+ k_{WK} \cdot (\varphi_K^{(1)} - \varphi_W)$	$+ c_{WK} \cdot (\dot{\varphi}_K^{(1)} - \dot{\varphi}_W)$	$+ k_K (\varphi_K^{(1)} - \varphi_K^{(2)})$	$+ c_K \cdot (\varphi_K^{(1)} - \dot{\varphi}_K^{(2)})$	$= 0$
$I_K^{(2)} \cdot \ddot{\varphi}_K^{(2)}$	$+ k_K \cdot (\varphi_K^{(2)} - \varphi_K^{(1)})$	$+ c_K \cdot (\dot{\varphi}_K^{(2)} - \dot{\varphi}_K^{(1)})$	$+ k_{K1} (\varphi_K^{(2)} - \varphi_1)$	$+ c_{K1} \cdot (\dot{\varphi}_K^{(2)} - \dot{\varphi}_1)$	$= 0$
$I_1 \cdot \ddot{\varphi}_1$	$+ k_{K1} (\varphi_1 - \varphi_K^{(2)})$	$+ c_{K1} \cdot (\dot{\varphi}_1 - \dot{\varphi}_K^{(2)})$	$+ k_{12} \cdot (\varphi_1 - \varphi_2)$	$+ c_{12} \cdot (\dot{\varphi}_1 - \dot{\varphi}_2)$	$= 0$
$I_2 \cdot \ddot{\varphi}_2$	$+ k_{12} \cdot (\varphi_2 - \varphi_1)$	$+ c_{12} \cdot (\dot{\varphi}_2 - \dot{\varphi}_1)$	$+ k_{23} \cdot (\varphi_2 - \varphi_3)$	$+ c_{23} \cdot (\dot{\varphi}_2 - \dot{\varphi}_3)$	$= 0$
\vdots	\vdots	\vdots	\vdots	\vdots	\vdots
$I_i \cdot \ddot{\varphi}_i$	$+ k_{(i-1)i} \cdot (\varphi_i - \varphi_{i-1})$	$+ c_{(i-1)i} \cdot (\dot{\varphi}_i - \dot{\varphi}_{i-1})$	$+ k_{i(i+1)} \cdot (\varphi_i - \varphi_{i+1})$	$+ c_{i(i+1)} \cdot (\dot{\varphi}_i - \dot{\varphi}_{i+1})$	$= 0$
\vdots	\vdots	\vdots	\vdots	\vdots	\vdots
$I_{2n-1} \cdot \ddot{\varphi}_{2n-1}$	$+ k_{(2n-2)(2n-1)} \cdot (\varphi_{2n-1} - \varphi_{2n-2})$	$+ c_{(2n-2)(2n-1)} \cdot (\dot{\varphi}_{2n-1} - \dot{\varphi}_{2n-2})$	$+ k_{(2n-1)2n} \cdot (\varphi_{2n-1} - \varphi_{2n})$	$+ c_{(2n-1)2n} \cdot (\dot{\varphi}_{2n-1} - \dot{\varphi}_{2n})$	$= 0$
$I_{2n} \cdot \ddot{\varphi}_{2n}$	$+ k_{(2n-1)2n} \cdot (\varphi_{2n} - \varphi_{2n-1})$	$+ c_{(2n-1)2n} \cdot (\dot{\varphi}_{2n} - \dot{\varphi}_{2n-1})$	$+ \sum_{j=1}^{WG} k_{2nG}^{(j)} \cdot (\varphi_{2n} - \varphi_G^{(j)})$	$+ \sum_{j=1}^{WG} c_{2nG}^{(j)} \cdot (\dot{\varphi}_{2n} - \dot{\varphi}_G^{(j)})$	$= 0$
$I_G^{(1)} \cdot \ddot{\varphi}_G^{(1)}$	$+ k_{2nG}^{(1)} \cdot (\varphi_G^{(1)} - \varphi_{2n})$	$+ c_{2nG}^{(1)} \cdot (\dot{\varphi}_G^{(1)} - \dot{\varphi}_{2n})$	$= -M_{OB}^{(1)}(\ddot{\varphi}_G^{(1)})$		
\vdots	\vdots	\vdots	\vdots		
$I_G^{(WG)} \cdot \ddot{\varphi}_G^{(WG)}$	$+ k_{2nG}^{(WG)} \cdot (\varphi_G^{(WG)} - \varphi_{2n})$	$+ c_{2nG}^{(WG)} \cdot (\dot{\varphi}_G^{(WG)} - \dot{\varphi}_{2n})$	$= -M_{OB}^{(WG)}(\ddot{\varphi}_G^{(WG)})$		

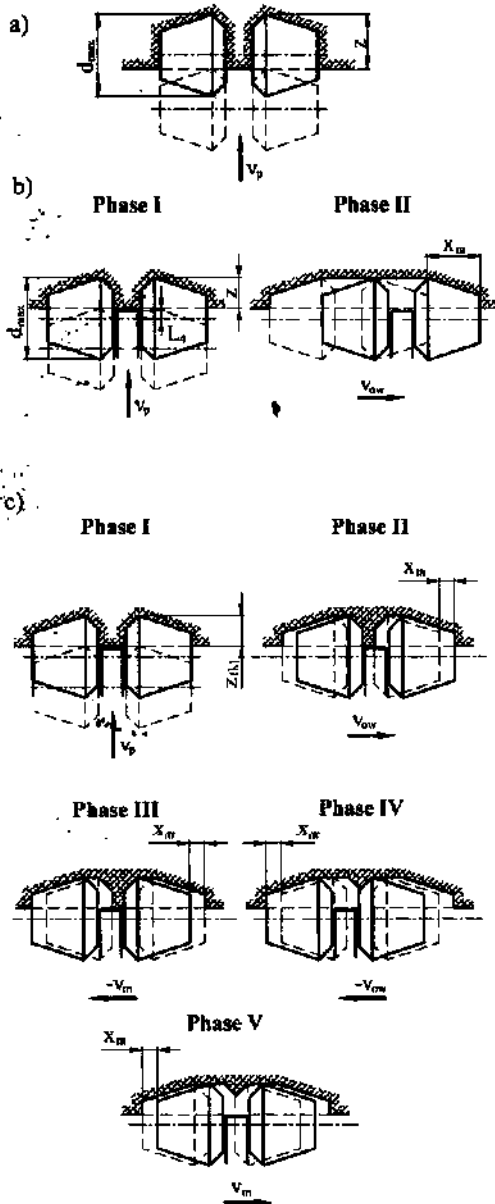


Figure 2. Sumping of transverse cutter heads in rock: a) technological variant I, b) technological variant II, c) technological variant III.

an angular velocity ω . The rock is then mined by slicing the layers of height h with web z (Fig. 4). The course of cutting done by means of cutting tools arranged on transverse cutter heads during the above movement of the boom has the form of screw lines (Gehring 1989; Haaf 1992; Knissel & Wiese 1981). When a longitudinal cutter head is used for mining

purposes, cutting tools move along cycloids. The differences are attributed to the dissimilar models of operation of the two types of cutter heads:

- with transverse cutter heads in working motion, a vector of tangential velocity of the boom swinging is perpendicular to the plane of rotation of a cutting tool tip (plane perpendicular to the axis of rotation of the cutter head running through the cutting tool tip),
- in the case of a longitudinal cutter head, a vector of tangential velocity of the boom swinging is parallel to the plane of rotation of a cutting tool tip.

The swinging of the boom in a plane perpendicular to the floor is an auxiliary movement which makes it possible to pass to the next layer. It is the determinant of the height of the layer extracted during the working movement. When cutter heads are displaced towards the roof or the floor of a roadway under drive at the tangential velocity v_{pw} , the cutting tools of both the transverse cutter heads and longitudinal cutter head move along cycloids.

When cutting tools are in contact with the rock mined, i.e., in a zone of cutting, they take cuts when penetrating the rock. The shape and size of these cuts depend on:

- the mechanical properties of the rock mined (compression strength, breakability number, angle of side breaking),
- the geometry of the cutting tools,
- the position of the cutting tool taking a given cut in relation to the cutting tool taking the preceding cut,
- the operational parameters of the road header (angular velocity of cutter head, speed of the boom displacement, web, and height of the layer extracted).

In order to determine a run of load on particular cutting tools engaged in the process of the mining of a road head, it is necessary to make a projection of cuts taken by particular cutting tools. The projection of cuts resolves itself into the modelling of the shape of particular cuts and of the shape of the initial break cross-sectional area (before beginning the process of mining) and that of the final break cross-sectional area (after termination of the process of mining). With regard to cutter heads equipped with conical cutting tools, there are three kinds of cuts, distinguished as opening cuts, half-open cuts and open cuts (Wiese, 1982).

The way in which cutting tools are displaced has an effect on the shapes of the cuts and their sequence as well as influencing the run of their depth. As a result, it also determines the state of the load on the cutting tools and, thus, the character and magnitude of the dynamic load in a roadheader's cutting system (Frenyo & Lange, 1993; Mahnen et al., 1990).

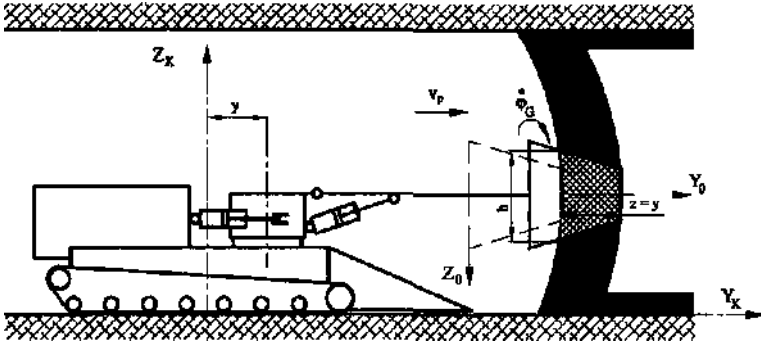


Figure 3. Sumping in of a longitudinal cutter head

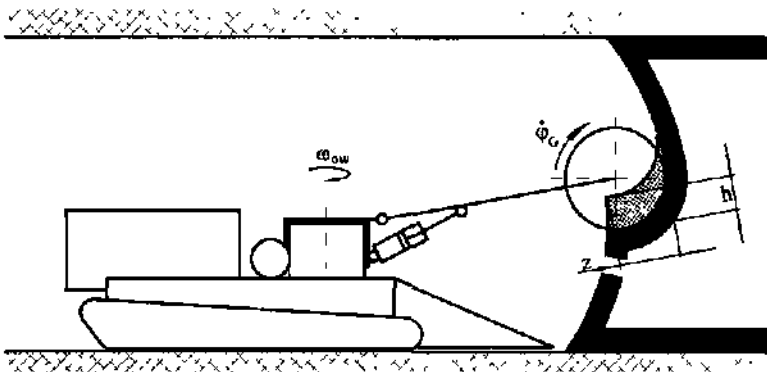


Figure 4. Extraction of a layer parallel to the floor

Whenever cutting tools are displaced along screw lines, the cuts taken by these tools are characterized by (approximately) constant depth (Dolipski & Cheluszka, 1993). A practically constant mean load is the effect. The depths of cuts taken when cutting tools are moving along cycloids vary as a function of the angle of rotation of the cutter head (ρ) (Dolipski & Cheluszka, 1995).

A cutting tool load, corresponding to the reaction of the rock to penetration of the tip of the cutting tool, is a vector sum of three components which are perpendicular to each other, i.e., of the cutting force P_c , holdmg-down force P_d and side force P_s . The spatial orientation of these forces depends on the shape of the movement trajectory of the tips of the cutting tools. Both the type of cutter head (transverse or longitudinal) and the mode of displacement of the boom in the course of the mining of the road head of the roadway under drivage have an effect on this orientation.

Depending on the depth of cut, the mean value of the cutting force is determined on the basis of Evans' theory of cutting with a conical cutting tool (Evans, 1984). From the analysis of the dynamic phenomena in a roadheader's cutting system, it ap-

pears that it does not suffice to assume loading of a cutting tool with cutting resistances at the level of the mean value for a given depth of cut. In reality, it varies within a wide range, even when a cut of constant depth is taken. Therefore, a method for determining a run of load on the cutting tools has been worked out for the purpose of investigation of the dynamic phenomena occurring in a roadheader's cutting system (Dolipski & Cheluszka, 1998)

The overall moment of load forces of a cutter head is equal to a sum of moments of load forces on cutting tools in a zone of cutting at a given moment. In the case of transverse cutter heads, furnished with N cutting tools each, a moment of load forces is expressed by the formula:

- during displacement of a boom in a direction parallel to the longitudinal axis of a roadway:

$$M_{OB}(\varphi_G) = \sum_{i=1}^N W_i(\varphi_G) [P_{c_i}(\varphi_G) \cdot \cos(\sigma_i) + P_{d_i}(\varphi_G) \cdot \sin(\sigma_i)] r_i \quad (1)$$

wherein.

$$\sigma_i = \arcsin \left[\frac{v_p \cdot \cos(\varphi_G - \vartheta_i)}{v_{Si}} \right] \quad (2)$$

The function $W_i(\varphi_G)$ assumes values:

$$W_i(\varphi_G) = \begin{cases} 1, & \text{cutting tool is in a zone of cutting,} \\ 0, & \text{cutting tool is not in a zone of cutting} \end{cases} \quad (3)$$

$\cdot \hat{P}^*$ during swinging of the boom in a plane parallel to the floor:

$$M_{OB}(\varphi_G) = \sum_{i=1}^N W_i(\varphi_G) \cdot [P_{si}(\varphi_G) \cdot \cos(\rho_i) + P_{bi}(\varphi_G) \cdot \sin(\rho_i)] \cdot r_i \quad (4)$$

wherein:

$$\rho_i = \arctg \left(\frac{v_{ow}}{\varphi_G \cdot r_i} \right) \quad (5)$$

$\cdot \hat{P}^*$ during swinging of the boom in a plane perpendicular to the floor:

$$M_{OB}(\varphi_G) = \sum_{i=1}^N W_i(\varphi_G) \cdot [P_{si}(\varphi_G) \cdot \cos(\xi_i) + P_{di}(\varphi_G) \cdot \sin(\xi_i)] \cdot r_i \quad (6)$$

wherein:

$$\xi_i = \arcsin \left[\frac{-v_{pw} \cdot \sin(\varphi_G - \vartheta_i + \alpha_V)}{v_{Si}} \right] \quad (7)$$

where: M_{OB} - forced excitation of torsional vibrations, N - number of cutting tools on a cutter head, P_s - instantaneous value of cutting force, P_a - instantaneous value of holding-down force, P_b - instantaneous value of side force, r, ϑ - coordinates of cutting tool tip in a polar system, v_p - speed of displacement of boom in a direction parallel to the longitudinal axis of the roadway, v_m - tangential velocity of swinging of the boom in a plane parallel to the floor, v_{pw} - tangential velocity of swinging of the boom in a plane perpendicular to the floor, v_s - cutting speed, α_V - angle of swinging of the boom in a plane perpendicular to the floor, φ_G - rotational coordinate of cutter head, and φ_G - angular velocity of cutter head.

3 COMPUTER SIMULATIONS OF THE PROCESS OF MINING WITH A ROADHEADER

Figures 5, 6 and 7 show computer simulation of the process of sumping of transverse cutter heads in the rock, carried out according to the second technological variant (Fig. 2b). The simulation has been performed for rock the compression strength of which is equal to 65 MPa. In the first phase of sumping in, the cutter heads penetrate into the surface and road head until they reach a web of 0.075 m. In this case (Fig. 5).

The speed of displacement of the boom in the direction parallel to the longitudinal axis of the roadway amounts to 0.05 m/s. The dynamic load in the coupling of the cutting system initially increases and after reaching the maximum value, it decreases (Fig. 6). The peak value is 2615.9 Nm, while the amplitude is equal to 2899.4 Nm.

In the second phase of sumping in, the boom is swung from the axial position to the right at an angular velocity $\omega_{ow} = 0.031 \text{ rad/s}$ (Fig. 7). The distance covered by the cutter heads in this phase of sumping in results from the width of the rib between the cutter heads. The dynamic load in the coupling of the cutting system is here more stable in character. It ranges from 1323.1 Nm to +3488.4 Nm (Fig. 6).

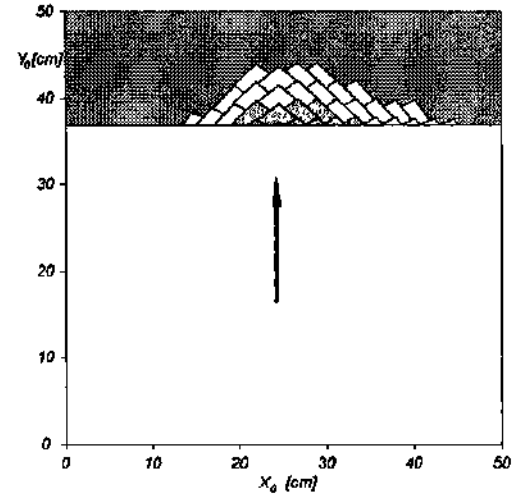


Figure 5. Break cross-sectional area made by cutting tools of the right-hand cutter head in the first phase of sumping in.

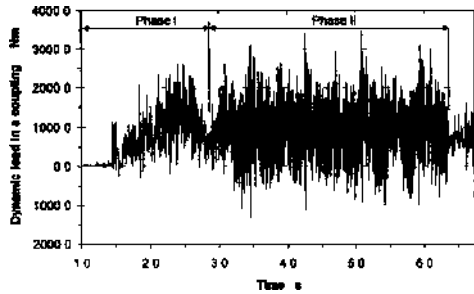


Figure 6 Run of dynamic load in coupling of the cutting system during sumping of transverse cutter heads in rock

The course of the process of mining by means of the longitudinal cutter head during swinging of the boom in the plane parallel to the floor is shown in Figures 8 and 9. The mining of a rock layer of 60 MPa in compression strength with a web of $z = 0.30 \text{ m}$ was simulated. The longitudinal cutter head was then displaced at the tangential velocity $v_{ov} = 0.04 \text{ m/s}$. The run of the dynamic load in the coupling of the cutting system is characterized by great variability (Fig. 9). The peak value of dynamic load in the coupling of the cutting system reaches 3100 Nm , while the amplitude of this load is equal to 4270 Nm .

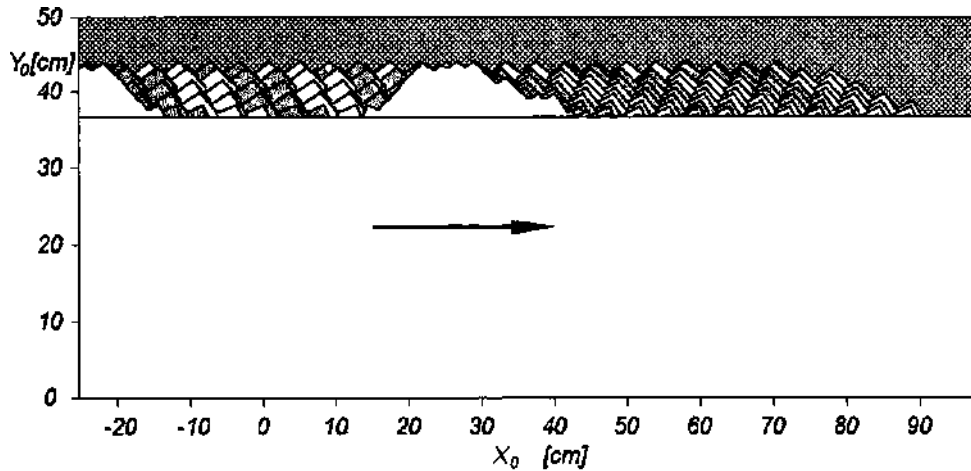


Figure 7 Shapes of cuts taken by cutting tools of the right-hand and left-hand cutter head in the second phase of sumping in

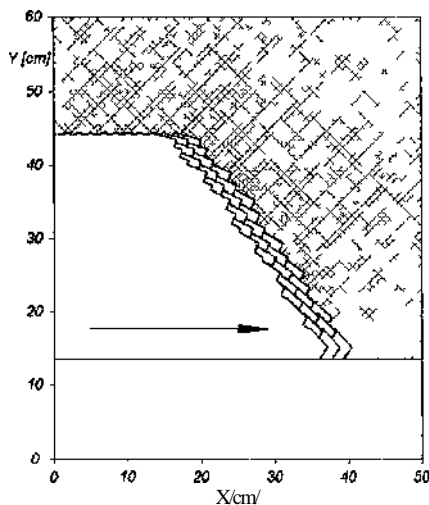


Figure 8 Break cross-sectional area made by cutting tools of longitudinal cutter head displaced parallel to the floor

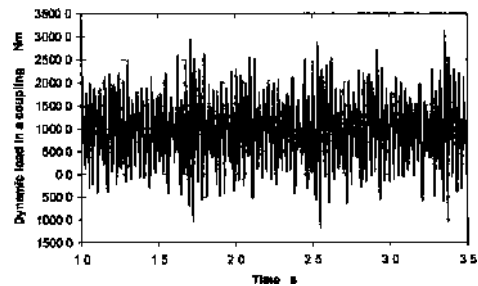


Figure 9 Run of dynamic load in coupling of the cutting system during mining by means of longitudinal cutter head displaced parallel to the floor

4 CONCLUSIONS

The dynamic model of the roadheader's cutting system developed has been experimentally verified on the basis of dynamic characteristics recorded under real operating conditions. Having been accepted, the

model has successful application in research and design practice. In particular, it allows:

- graphics of break cross-sectional areas made by a cutter head to be computer generated in order to determine the depths and sectional areas of cuts, the volumes of the material cut and the performance of mining;
- dynamic loads in all elements of the cutting system to be determined when taking any technological variant being realized into consideration;
- dynamic phenomena occurring in the cutting system of roadheaders produced at present to be investigated by means of computer so that conclusions resulting from experiments can be facilitated;
- computer investigation of the process of mining to be carried out, while making it possible to change freely the values of particular parameters of the roadheader and of strength properties of the rock to determine the optimum parameters relating to mass, elasticity, damping of the cutting system as well as the operational parameters of the roadheader;
- computer analysis to be performed at the stage of the designing of roadheaders which incorporate cutting systems of the new generation, without the necessity of building expensive prototypes;
- the design of cutter heads for roadheaders and the selection of them for definite mining and geological conditions to be computer aided;
- the demand for energy in the process of mining the rock to be stated when designing the technical equipment of a road head to be suitable for the given mining and geological conditions;
- the process of mining to be automatically controlled in respect of reducing the dynamic loads and specific energy consumption of mining as well as allowing work safety to be enhanced.

The dynamic model presented finds successful application in the process of designing the cutter heads and subassemblies for roadheaders made by the REMAG Company - a leading manufacturer of these machines in Poland. The development of novel cutter heads for the R-100 roadheader, characterized by the arrangement of cutting tools along screw Unes with a small helix angle, is, among others, a result of many years of comprehensive computer investigations (Fig. 10). The rock is here cut by the tips of cutting tools of successive groups entering the zone of cutting. Cutting is realized so that in each successive group of cutting tools, the tip of the cutting tool situated on the smallest radius starts the process and the tip of the cutting tool situated on the greatest radius finishes it. In this case, the load of the cutting tools is visibly lower due to the additional area of exposure. This leads to reduction of the dynamic load and to a decrease in the specific energy consumption of mining. The comparison tests carried

out in underground workings of coal mines show that a roadheader equipped with the new cutter heads, characterized by screw lines with a small helix angle, consumed less energy than the conventional solution. The average specific energy consumption of mining by means of the new cutter heads was 5% lower than the average specific energy consumption typical for mining with the aid of standard cutter heads, although the compression strength of the rock being mined increased by 60%.

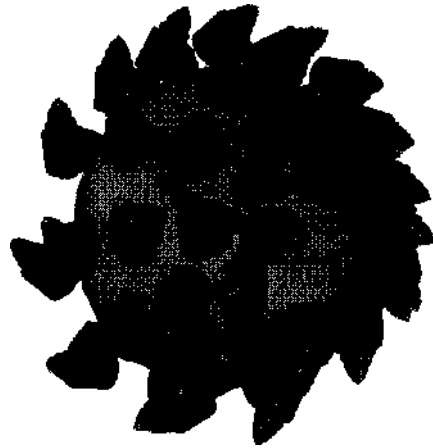


Figure 10. Novel cutter head with screw lines characterized by small helix angle.

REFERENCES

- Dolipski M., 1993. Dynamic model of coal plough. *Archives of Mining Sciences* 3:315-330.
- Dolipski M., Cheluszka P. 1993. Belastungsmoment des Schneidkopfes einer Teilschnittvortriebsmaschine. *Bergbau* 5:198-202.
- Dolipski M., Cheluszka P. 1995. Vergleichende Untersuchungen an Längs- und Querschneidköpfen in einer Vortriebsmaschine. *Bergbau* 4:154-159.
- Dolipski M., Cheluszka P. 1998. Bestimmung der Form des Schnittkraftverlaufs an Kegelmeißeln von Vortriebsmaschinen. *Glückauf-Forschungshefte* 4:123-127.
- Dolipski M., Cheluszka P. 1999. Dynamic model of a roadheader's cutting system which incorporates transverse cutter heads. *Archives of Mining Sciences* 1:113-146.
- Dolipski M., Cheluszka P. 2000. Dynamik des Einschneidevorgangs einer Teilschnittmaschine mit Querschneidkopf. *Glückauf-Forschungshefte* 2:53-65.
- Evans I. 1984. Basic Mechanics of the Point-Attack Pick. *Colliery Guardian* 5: 189-193.
- Frenyo P., Lange W. 1993. Die Auslegung von Schneidköpfen für optimale Löseleistung. *G/wc*flw/7:524-531*.
- Gehring K.-H. 1989. A cutting comparison. *Tunnels and Tunneling* 11:27-30.
- Haaf J. 1992. *Das Verschleiß- und Drehverhalten von Meißeln für Teilschnitt-Vortriebsmaschinen*. Diss. TU Clausthal.

- Kmsel W , Wiese H-F 1981 Möglichkeiten zur Verbesserung des Losevorgangs von Teilschnitt-Vortriebsmaschinen *Glückauf* 1360-1366
- Mahnen U , Gerhardt H , Bellman A 1990 Rechnergestützte Optimierung der Arbeitsweise von Schneidköpfen an Teilschnitt-Vortriebsmaschinen *Glückauf-Forsch ungsh efte* 6 277-282
- Wiese H -F 1982 *Grundlagenuntersuchung zur Optimierung der Losearbeit von Teilschnitt-Vortriebsmaschinen mit Querschneidkopf* Diss TU Clausthal

A New Computer Program for Cutting Head Design of Roadheaders and Drum Shearers

B.Tiryaki

Department of Mining Engineering, Hacettepe University, Ankara, Turkey

M.Ayhan & O.Z.Hekimoglu

Department of Mining Engineering, Dicle University, Diyarbakır, Turkey

ABSTRACT: This paper is concerned with a new computer program developed for the design, of the cutting heads employed on mechanical excavation machines. Computer aided design (CAD) technique was proven to improve the performance and life span of these machines, when used in designing cutting beads. A number of computer programs are utilized in practice, none of which considers the aspects of multi-tracking. A series of laboratory and In-situ experiments were carried out through comparing a triple tracking arrangement that is widely employed on three-start shearer drums worldwide, to a single tracking arrangement in an effort to close this gap in this field. The data gained from these experiments were evaluated and embedded into the current computer program VAP (Vibration Analysis Program), and the new computer program was developed. The results of computer analysis for the both tracking arrangements were found to be in good agreement with those of laboratory and in-situ studies.

1 INTRODUCTION

Mechanical rock and coal excavation machines such as roadheaders, drum shearers and continuous miners excavate the rock material by a number of picks mounted on their cutting heads or drums with various shapes. The design of trie cutting head is of crucial importance since it comprises the machine-rock interface in mechanical excavation. Cutting power installed on the machine is transferred from the motors to rock by the interactive motion of picks relieving each other. Additionally, the machine vibrations during excavation significantly depend on the cutting head design. Vibration induces the damages on machine units, resulting in machine downtimes that increase the operating cost. These damages may require costly repairs, and in a further stage, the machine typically of high capital cost may be discarded, unless the proper cutting head design is employed. As the picks, pick holders and geometry of the cutting head are selected by considering the geomechanical properties of rock, proper disposition of the picks on a cutting head improves the overall performance of mechanical excavators (Roxborough & Rispin 1973, Hurt 1980, Hurt & McAndrew 1981b, 1985, Hurt et al. 1982, 1986, 1988, Hurt & McStravick 1988, Hekimoglu & Powell 1990).

Therefore, selected cutting head for a particular operation must be evaluated in terms of cutting efficiency and vibrations prior to its mounting on machine. Some computer programs related to design and performance evaluation of cutting heads were developed by world's leading companies in mechanical excavation sector, research institutes, and universities. However, practical investigations and literature surveys revealed that, these computer programs did not consider the aspects of the tracking cutter arrangement or setting the number of picks required on each cutting line on a cutting head. Researches showed that, when the picks were arranged in multi-tracking, the machine performance could be affected conversely, and therefore single tracking arrangement was recommended for efficient cutting (Evans & Pomeroy 1973, Brooker 1979, Hurt 1980, Hurt & McAndrew 1981a, b, Hekimoglu 1984). However, it is known Üiat, in current computer programs, pick forces, i.e. cutting, normal and sideway forces, likely to be experienced by individual picks during cutting operation are estimated considering the single tracking arrangement, although the pick lacing follows the multi-tracking arrangement. This may be due to the lack of information obtained from the long-term comprehensive in-situ studies combined with laboratory simulation experiments.

This paper aims to present a new computer program for the cutting head design of roadheaders, drum shearers and continuous miners considering the effects of multi-tracking arrangements on pick forces, along with the other design parameters. Before the development of the new computer program, detailed laboratory rock cutting simulation experiments were carried out in an attempt to clarify the aspects of tracking cutter arrangement. Long-term comprehensive underground trials were conducted with drum shearers employed in Çayırhan Lignite Mine, during actual production operations. The results from laboratory experiments and underground trials were utilized in developing the new computer program. The brief description of this program and the results of computer analysis applications on some cutting heads and shearer drums were presented.

2 COMPUTER AIDED CUTTING HEAD DESIGN

There are a number of scientific and commercial softwares that help scientists and engineers overcome the problems encountered throughout the cutting head design process in mechanical excavation. Many researchers reported that the performance of mechanical excavators could be improved significantly through utilizing computer assistance in cutting head design (Holt et al. 1984, Hurt & Morris 1985, Hurt et al. 1986, Kadiu 1995). Essentially, this improvement results from the softwares that are available to estimate the possibility of excessive cutting vibrations and inefficient cutting conditions due to the positions of picks on cutting heads. Where the possibility of the above-mentioned problems are estimated, it is likely to avoid die vibration induced damages on mechanical excavators and the machine downtimes due to these damages, and to utilize the installed power on these machines effectively in practice, by selecting appropriate pick lacing arrangements.

2.1 *Computer programs in use*

Intensive and consistent studies on cutting head and shearer drum design carried out at Mining Research and Development Establishment (MRDE) of National Coal Board (NCB) yielded the first and well-known CAD package for roadheaders and drum shearers (Morris 1980, NCB 1984, Holt et al. 1984, Hurt et al. 1986). This package is based on the idea of employing pick-lacing arrangements that make almost all picks to be subjected to the equal forces in order to prevent excessive vibrations and to have

efficient cutting conditions (Hurt 1980a, Hurt & McAndrew 1981b). However, the studies at MRDE did not clarify all aspects of maintaining the picks on a cutting head with equal forces.

There have been several investigations leading to development of a CAD package, following that of MRDE, Kadiu et al. (1991) developed a package named PC DRUM for drum designs of continuous miners and drum shearers. Cordelier & Kadiu (1991) then improved PC DRUM and developed a new package named SIMHEAD for both cutting heads and shearer drums.

Price and Jeffrey (1992) reported to succeed in developing a CAD package for performance evaluation of drum shearers, which uses the results of the linear cutting tests carried out on actual rock materials by full-scale picks in order to estimate pick forces. This package is known to result similar performance predictions to those obtained from MRDE package for given drum design parameters.

A comprehensive computer program was developed during the investigations for utilizing roadheaders in excavating rooms of a nuclear waste repository in welded tuffs at Yucca Mountain (Rostami et al. 1993). This program was developed through full-scale rock cutting tests by using a linear cutting machine (LCM) and model cutting trials by using the boom of a roadheader in laboratory, at the Earth Mechanics Institute (EMI) of Colorado School of Mines (CSM), for the roadheaders with transverse type cutting heads. Program is also available for the roadheaders with the axial type cutting heads when a few modifications are carried out.

Kadiu (1995) proposed to employ a knowledge base for design and performance calculations of shearer drums. By using this knowledge base, he has developed software named ARCHD for shearer drums.

Tiryaki (1998) from Hacettepe University proposed a cutting head and drum simulation program named VAP, depending on the principles of CAD package of MRDE, and the results of the long-term extensive underground trials carried out at Çayırhan Lignite Mine, for performance evaluation of drum shearers, continuous miners and roadheaders with both axial and transverse cutting heads.

It is also known that, world's leading cutting head and drum manufacturers such as Krummenauer, IBS, Krampe, Dosco, Kennametal, Eickhoff etc. use computer assistance for cutting head design. These commercial programs were generally developed through projects undertaken by universities or research institutes, which are understood to have the deficiencies similar to those of scientific programs.

2.2 Procedure followed in CAD of cutting heads

In general, computer aided cutting head design procedure begins with the evaluation of cutting efficiency and relative duties of individual picks by drawing breakout pattern for the selected pick lacing arrangement (Fig. 1). This pattern enables design engineer to see the picks that are under-utilized or overloaded and to realize if the picks tend to deepen an existing groove instead of effectively breaking the rock (Brooker 1979, Hurt 1980, Holt et al. 1984, Hurt et al. 1986, Hurt 1988). Design engineer enters the type and geometry of the cutting head, picks and pick holders, and the details of the pick lacing arrangement to the computer program as input data. Then computer program automatically draws the breakout pattern for a certain advance per revolution of the cutting head.

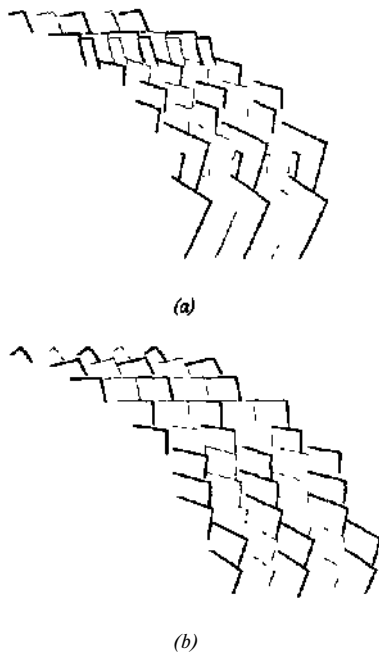


Figure 1. Breakout patterns drawn by MRDE's program for cutting heads with (a) poor design and (b) good design (NCB 1984).

The next step in design procedure is the prediction of the levels and fluctuations in horizontal, vertical and axial reaction forces acting on the cutting head and the shaft torque generated, which may be experienced during actual cutting operations (Fig. 2). In this step, the individual pick forces are estimated before the calculations for reaction forces

and shaft torque have been performed. The current scientific and commercial computer programs mentioned above relate the pick forces to only the cross-sectional rock area removed or the depth of penetration achieved by individual picks after one entire revolution of the cutting head is completed, regardless of tracking cutter arrangement in which the pick is laced. Therefore, these programs do not take into account of any differences between single tracking or multi-tracking arrangements in terms of individual pick forces.

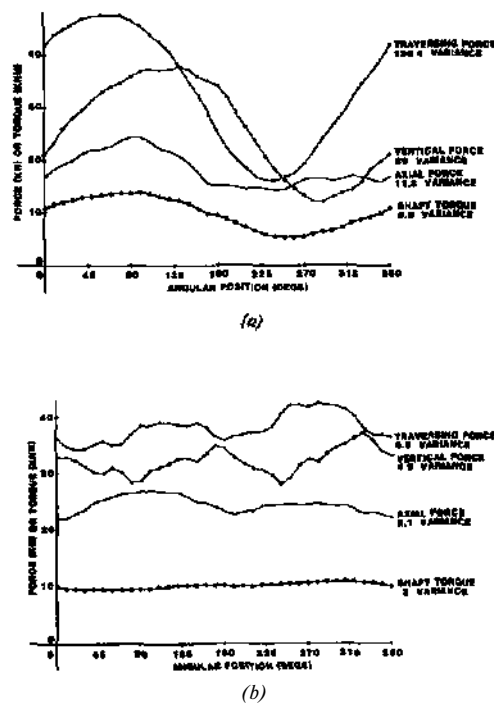


Figure 2 Vibration graphs drawn by MRDE's program for cutting heads with (a) poor design and (b) good design (NCB, 1984).

However, it was reported that the forces acting on a pick in a multi-tracking arrangement differ from the forces acting on a pick in a single-tracking arrangement, even if both picks removed the same rock area or achieved the same depth of penetration (Evans & Pomeroy 1973, Hurt 1980, Hurt & McAndrew 1981a, Hekimoğlu 1984). Consequently, current computer programs estimate similar values for reaction forces and torque acting on the cutting head, for both single and multi tracking arrangements, causing the accuracy of the performance evaluation of a particular cutting head

design to decrease.

The reaction forces and shaft torque are calculated, considering the active picks in cut sector at each defined angular interval of rotation of a specified reference pick on the cutting head in degrees, until one entire revolution of the cutting head is completed. Data gained from computer simulation are then subjected to statistical analysis and the fluctuations in these data are expressed in terms of variance, individually. Cutting heads with lower variance values for the calculated parameters are considered to be balanced in terms of cutting vibrations and the machines employing these cutting heads are expected to perform efficiently. In practice (Hurt 1980, Hurt et al. 1988, Hekimoğlu 1991, Tiryaki & Hekimoğlu 1998).

3 DESCRIPTION OF THE NEW COMPUTER PROGRAM

The new computer program was developed through modifying the existing computer program VAP, considering the results of laboratory investigations to formulate the effects of tracking cutters for pick force estimation, together with in-situ trials to investigate the effects of tracking cutter arrangement on machine performance under similar conditions.

3.1 Details of VAP

VAP is a scientific program consisting of two subprograms, one of which is for drawing the breakout pattern and the other is for generation of simulation values of reaction forces and shaft torque (Tiryaki '1998, 2000b). Prior to the program development, the motion of the picks on axial and transverse cutting heads and shearer drums during cutting was analysed both dynamically and kinematically in detail, so that the computer simulation could be achieved. Breakout pattern subprogram was developed by using AutoLISP programming language in order to utilize the drawing facilities of AutoCAD software. The data files including the design specifications of the cutting head and advance per revolution value desired for performance evaluation, must be prepared and stored in hard disk before the program execution, since this program was developed in batch-programming mode. When the program is run, the breakout pattern of the cutting head is automatically drawn and displayed on computer's screen, and then, the individual breakout areas for picks are determined by using the area function of AutoCAD. These values are stored in a data file for

further processing by the vibration evaluation subprogram that was developed by using Quick BASIC programming language. The vibration evaluation subprogram calculates the respective values of horizontal, vertical, and axial reaction forces and shaft torque, asking user for the additional information on type, sumping depth, cutting mode, and extraction height of the cutting head. Calculations are performed at one-degree angular interval until one entire revolution of the cutting head is completed. Program estimates the pick cutting forces, only depending on the cross sectional rock area removed by the pick as stated in a previous research by Hekimoğlu (1984), whereas pick normal forces are assumed to be 1.5 times the pick cutting forces. Reaction forces and torque are estimated considering the formulas proposed by Hurt et al. (1988).

3.2 Laboratory and in-situ investigations

Laboratory experiments were conducted on blocky rock samples, simulating the actual motion of the picks on a three-start shearer drum during cutting operation, when laced in both single and triple tracking arrangements, by using a linear shaping machine (Ayhan 1998). These experiments showed that the picks in a multi-tracking arrangement will be subjected to higher forces than those in a single tracking arrangement. Plotting the mean cutting force values that were measured during experiments, against the depth of cut for both tracking cutter arrangement individually, showed the superiority of single tracking on triple tracking (Fig. 3).

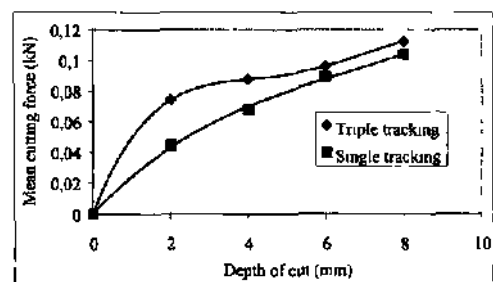


Figure 3 Variation of mean cutting force with depth of cut.

Specific energy values also reflected the same result. Statistical analysis of the results of laboratory experiments revealed the necessity of using a cutting force coefficient given in the equations below in order to have more accurate values of pick forces, considering the angular position of the pick in cut

sector for single and multi-tracking arrangements respectively.

For single tracking arrangement;

$$F = \left[(\sin \theta)^{0.642} \right] - 0.00724 \quad (1)$$

For triple tracking arrangement;

$$F = 1.185 \left[(\sin \theta)^{0.321} \right] - 0.05364 \quad (2)$$

where; F : Cutting force coefficient and θ : Angular position of the pick in cut sector (in degrees).

The cutting force acting on a pick for a given angular position θ is proposed to be calculated by multiplying the pick cutting force at maximum depth of cut by cutting force coefficient instead of $\sin \theta$, as used in current version of VAP regardless of tracking cutter arrangement.

In-situ experiments were carried out by using Eickhoff EDW 230-L type double-ended ranging drum shearers employed at Çayırhan Lignite Mine, during the actual coal production operations in lower seam that has thickness of around 1.70 m and average gradient of 15°. Shearer has a couple of three-start drums with 1.30 diameter and 0.85 m web depth. Pick lacing of the current shearer drums considering the triple tracking concept was changed and a new pick lacing was adopted considering the single tracking concept, while keeping the all remaining drum design parameters intact. The new pick lacing was applied on the drums at Central Workshop of Çayırhan Mine and the modified drums were produced. These drums were then compared to current drums under identical cutting conditions.

Throughout the underground trials, performance of the machine, when fitted with the current and modified drums at different periods of time, was observed and recorded in terms of pick consumption, life span of drums, power consumption, machine downtimes, and vibrations, until the drums reached the end of their service lives. The results of the in-situ trials showed that the overall performance of the shearer substantially increased with the modified drums, e.g. pick consumption, specific energy, machine downtimes, and machine vibration acceleration decreased by 45%, 35%, 30%, and 50% respectively and the life span of drums increased by 70%. Results of machine power consumption measurements implied that the picks on a drum with single tracking arrangement were likely to experience lower forces than those on a drum with triple tracking arrangement even at the

same cutting rate, confirming the results of the laboratory experiments (Fig. 4).

Design specifications of the drums that were put into underground trials and the detailed information on the results of these trials can be found elsewhere (Tiryaki 1998, Tiryaki & Hekimoğlu 1998, Tiryaki 2000a). Taking into account of the findings from in-situ experiments, VAP was modified through embedding the cutting force coefficient equations for both single and triple tracking arrangements into the program code.

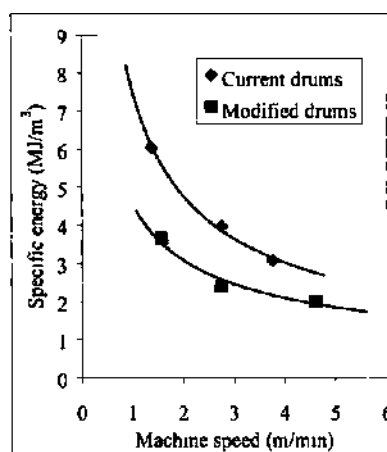


Figure 4. Variation of specific energy consumption with machine speed in upward direction

4 EXAMPLES ON THE APPLICATIONS OF THE NEW COMPUTER PROGRAM

Current and modified drums that were compared throughout the underground experiments were subjected to a performance analysis for 9 cm advance per revolution by using VAP. Breakout patterns showed the inefficiency of the triple tracking arrangement (Fig. 5).

Vibration evaluation graphs drawn for current and modified drums at 180° and 90° cut sectors were given in Figures 6 and 7, respectively. When individual variance values of reaction forces and shaft torques are considered, modified drums are understood to be better balanced than current drums. Mean values of calculated parameters indicate that the shearer is likely to experience lower reaction forces and torque with the modified drums than with the current drums, under the identical operational and cutting conditions, utilizing the available power installed on the machine efficiently.

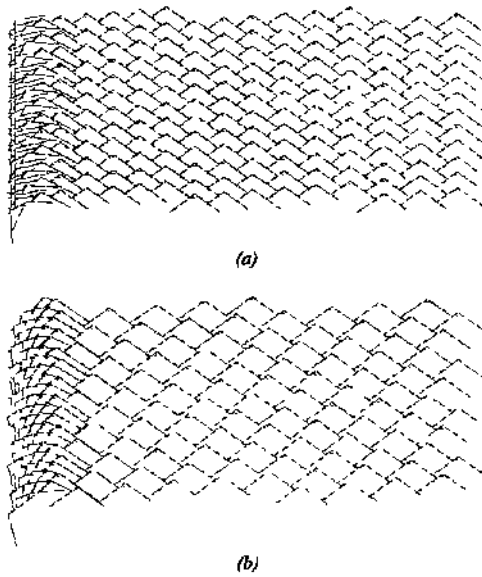
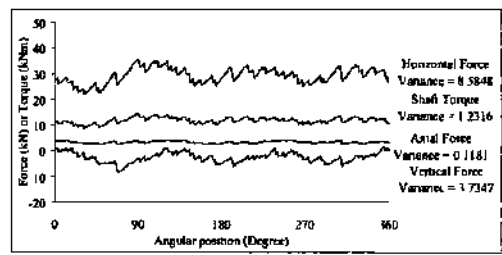
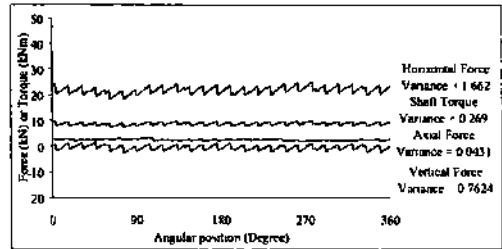


Figure 5. Breakout patterns drawn by VAP for (a) current and (b) modified drums.

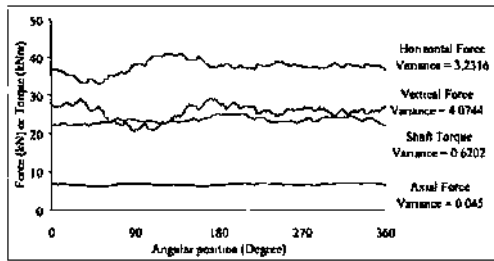


(a)



(b)

Figure 7. Vibration graphs drawn by VAP at 90° cut sector for (a) current and (b) modified drums.



(a)

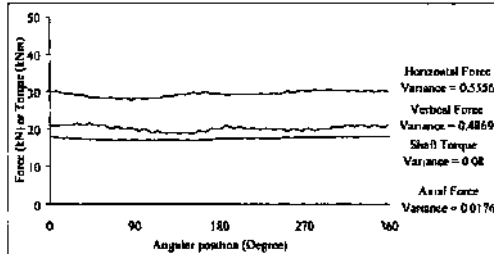
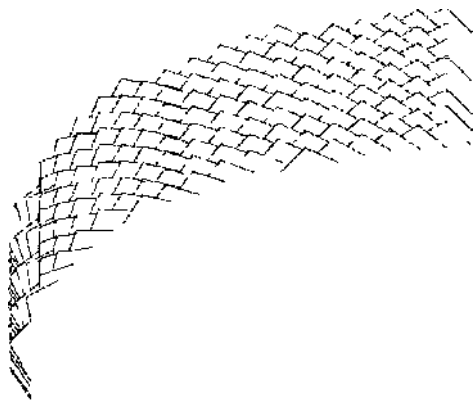


Figure 6. Vibration graphs drawn by VAP at 180° cut sector for (a) current and (b) modified drums.

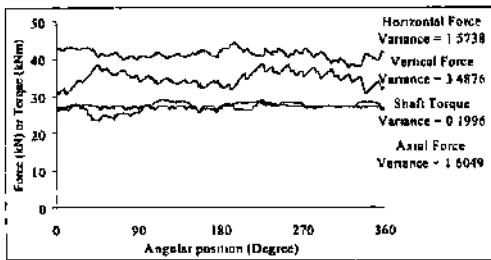
Results of computer evaluation for two tracking cutter arrangements are all in close agreement with

those of in-situ and laboratory experiments. Therefore, further computer analyses were carried out for the axial and transverse type cutting heads that have been employed on roadheaders. For these analyses, an axial type cutting head with 41 picks (Head-A) and a transverse type cutting head with 72 picks (Head-B) were selected, both were designed and manufactured by one of the world's leading cutting head and drum manufacturers. Head-A was analysed considering the 180° cut sector, while Head-B was analysed for 120° cut sector that was typical for transverse type cutting heads. Breakout pattern and vibration graph of Head-A for 9 cm advance per revolution are shown in Figure 8, while those of Head-B for 8 cm advance per revolution are shown in Figures 9 and 10, respectively.

Although cutting force coefficient equations enable the simulation of reaction forces and shaft torque for the drums fitted on shearers and continuous miners, to be achieved with a great accuracy, further practical investigations may be necessary to be conducted for their use in axial and transverse type roadheader cutting heads with different geometries. The mode of roadheader operation, geometry of the cutting head, and the boom carrying it make the motion of a pick on a roadheader cutting head to be more complex in nature than that of a pick on a shearer drum.



(a)



(b)

Figure 9. Results of performance analysis of Head-A produced by VAP (a) breakout pattern and (b) vibration graph.

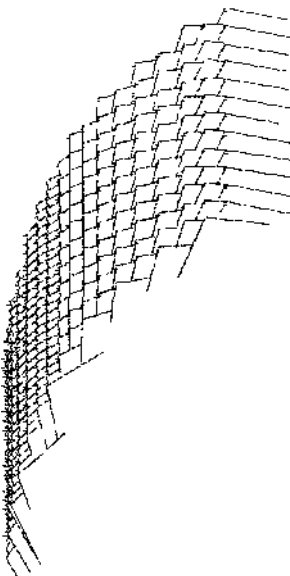


Figure 9. Breakout pattern drawn by VAP for Head-B.

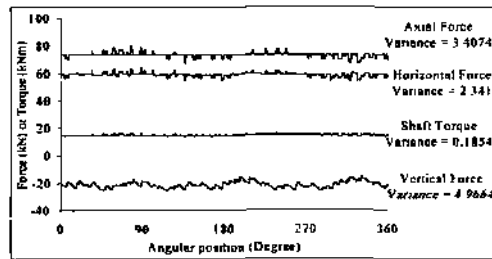


Figure 10. Vibration graph drawn by VAP for Head-B.

5 CONCLUSIONS

Theoretical and practical investigations on mechanical excavation machines indicated that these machines suffered from poor cutting head designs, which may prevent mine operators from obtaining the benefits offered by mechanical excavation. This may be due to the lack of conclusive information on some parameters that must be considered during the cutting head design process. The tracking cutter arrangement is one of these parameters. The effect of this parameter on individual pick forces is not included in current computer aided cutting head design programs used in practice. This situation can be regarded as a deficiency for these programs.

Extensive laboratory and underground investigations resulted in a reliable computer program for the cutting head design of roadheaders and drum shearers. This computer program is believed to enable the scientists and practising engineers to select the optimum design for the cutting heads with certain geometrical properties. The new computer program including the cutting force coefficient equations for pick force estimation succeeded to reflect the difference in pick forces between single and triple tracking, as seen throughout the laboratory and in-situ experiments. These experiments have also indicated the inefficiency of multi-tracking arrangements that have been persistently employed by the major cutting head and drum manufacturers worldwide, and single tracking arrangements were recommended to be employed on cutting heads.

Some additional features including specific energy prediction and the cutting head design selection in relation to geomechanical rock properties will also improve the functional properties of the new computer program. These improvements can only be achieved if the universities or research institutes undertake long-term research projects in cooperation with tunnel and mine operators.

ACKNOWLEDGEMENTS

The authors wish to thank to Turkish CoaJ Enterprises (TKI) for permission to carry out underground investigations, to Prof. Dr. Naci Bötükbaşı from Middle East Technical University for providing chart recorder and laboratory facilities, and to Prof. Dr. Nuh Bilgin from İstanbul Technical University for providing vibratiometer.

REFERENCES

- Ayhan, M. 1998. *Designing shearer drums and culling heads with the aid of a computer programme*. Ph.D. Thesis. Hacettepe University, Ankara, Turkey (Unpublished).
- Brooker, C.M. 1979. Theoretical and practical aspects of cutting and loading by shearer drums. *Colliery Guardian*. April: 41-50.
- Cordelier, P. & Kadiu, M. 1991. Roadheaders and continuous miners behavior modelling with regards to inclined pick-Evolution towards hard rock cutting. *Proceedings of the 1st International Symposium on Mine Mechanization and Automation*. 1-21/1-58.
- Evans, I. & Pomeroy C.D. 1973. *The strength, fracture and workability of coal*. London: Pergamon Press Ltd.
- Hekimoğlu, O.Z. 1984. *Studies in the excavation of selected rock materials with mechanical tools*. Ph.D. Thesis. The University of Newcastle Upon Tyne, England (Unpublished).
- Hekimoğlu, O.Z. & Fowell, R.J. 1990. From research into practice: In-situ studies for design of boom tunnelling machine cutting heads. *Proceedings of the 31st U.S. Symposium on Rock Mechanics*. 481-488.
- Hekimoğlu, O.Z. 1991. Comparison of longitudinal and transverse cutting heads on a dynamic and kinematic basis. *Mining Science and Technology*. 13:243-255.
- Holt, P.B., Morris, C.J. & Owen, R.J. 1984. Desk-top computers for design work. *The Mining Engineer*. 143(271): 485-489.
- Hurt, K.G. 1980. *Roadheader cutting heads: A study of the layout of cutting tools and a rational procedure for design*. MRDE Report No: 90. England (Unpublished).
- Hurt, K.G. & McAndrew, K.M. 1981a. *Roadheader cutting heads: How many tools per line?*. MRDE Report No: 96. England (Unpublished).
- Hurt, K.G. & McAndrew, K.M. 1981b. Designing roadheader cutting heads. *The Mining Engineer*. 141(240): 167-170.
- Hurt K.G., Morris, C.J. & McAndrew, K.M. 1982. The design and operation of boom tunnelling machine cutting heads. *Proceedings of the 14th Canadian Rock Mechanics Conference of CIM*. 54-58.
- Hurt, K.G. & McAndrew, K.M. 1985. Cutting efficiency and life of rock-cutting picks. *Mining Science and Technology*. 2: 139-151.
- Hurt, K.G. & Morris, C.J. 1985. Computer designed cutting heads improve roadheader performance. *Tunnels and Tunnelling*. March: 37-38.
- Hurt, K.G., Morris, C.J. & Mullins, R. 1986. Developments in coal cutting techniques. *The Mining Engineer*. 145(296): 467-477.
- Hurt, K.G. 1988. Roadheader cutting heads and picks. *Colliery Guardian* September: 332-335.
- Hurt, K.G., McAndrew, K.M. & Morris, C.J. 1988. Boom roadheader cutting vibration: Measurement and prediction. *Proceedings of Conference on Applied Rock Engineering*. 89-97.
- Hurt, K.G. & McStravick, F.G. 1988. High performance shearer drum design. *Colliery Guardian*. 236(12): 428-429.
- Kadiu, M., Sellami, H. & Demoulin, J. 1991. A new conception of clearance ring based on the study of inclined pick behavior. *Proceedings of the 1st International Symposium on Mine Mechanization and Automation*. 1-1/1-10.
- Kadiu, M. 1995. Organization of knowledge base in automatic design of drum cutting machines. *Proceedings of the 3rd International Symposium on Mine Mechanization and Automation*. IQ-2/10-30.
- Morris, C.J. 1980. The design of shearer drums with the aid of a computer. *The Mining Engineer*. November: 289-295.
- NCB, 1984. *Computer aided design of cutting drums*. Technical note. Staffordshire: Mining Research and Development Establishment.
- Price, D.L. & Jeffrey, I.C. 1992. Prediction of shearer cutting performance. *Proceedings of the 11th International Conference on Ground Control in Mining*. 660-666.
- Rostami, J, Neil, D.M. & Özdemir, L. 1993. *Roadheader application for the Yucca Mountain experimental study facility*. Final Report for Raytheon Services, EMI, Colorado School of Mines.
- Roxborough, F.F. & Rispin, A. 1973. A laboratory investigation into the application of picks for mechanized tunnel boring in the lower chalk. *The Mining Engineer*. 133:1-13.
- Tiryaki, B. 1998. *Optimisation of tool lacing parameters for drum shearers*. Ph.D. Thesis. Hacettepe University, Ankara, Turkey (Unpublished).
- Tiryaki, B. & Hekimoğlu, O.Z. 1998. Cutting vibration analysis for mechanical cutting machines. *Madencilik, Publication of Chamber of Mining Engineers of Turkey*. 37(3): 3-18.
- Tiryaki, B. 2000a. An investigation on the effects of pick lacing parameters on the performance of drum shearer-loaders. *Yerbilimleri, Bulletin of Earth Science Application and Research Centre of Hacettepe University*. 22: 237-246.
- Tiryaki, B. 2000b. Computer simulation of cutting efficiency and cutting vibrations in drum shearer-loaders. *Yerbilimleri, Bulletin of Earth Science Application and Research Centre of Hacettepe University*. 22: 247-259.

The Effects of Operational Parameters on the Output Efficiency of the Bucket Wheel Excavator

S.Ural

Department of Mining Engineering, Çukurova University, Adana, Turkey

ABSTRACT: In this study, the effects of operational parameters, such as slewing speed, bench height, terrace height, block width, etc., on output efficiency are discussed and the interrelationships between these parameters are investigated. The main theme of the study is the definition of the optimum values of operational parameters for the C-frame-type BWE Sch (2300 /5) x 32, which is in operation in Kislakoy open cast mine, Elbistan. A model is presented by means of which the optimal operational parameters may be selected. Finally, total efficiencies were calculated for two generalized bench geometries in which the slope height varied according to the necessary place between the bench belt conveyor and the toe of the side bench.

1 INTRODUCTION

The effective output of a mining system is based on the degree of utilization of its production capacity. This is the quotient of the effective to the optimum capacity. The effective utilization of a Bucket Wheel Excavator (BWE) mining system is defined as the product of the output efficiency and the time factor. The output efficiency depends on the effective output of the BWE and on the operation downtime of the transport and dumping systems. The time factor of a BWE system is expressed as net operating time divided by the total calendar time. Rasper (1975) shows that the output efficiency of the system is the product of the individual efficiencies. This is referred to as the total efficiency.

1.1 Symbols

The following symbols are used in this paper:

$T|E$ = efficiency of the BWE, (%)
 $T|T$ = efficiency of the transport system, (%)
 $T|D$ = efficiency of the dumping system, (%)
 $T|H$ = time factor, (%)
 Q_{eff} = effective output, (bank m^3/h)
 Q_{th} = theoretical output, (bank m^3/h)
 I = bucket capacity, (m^3)
 s = bucket discharges per minute (1 /minute)
 f = material swell factor, ($f=1 + \text{swell}$)
 V = volume of the excavating block, (bank m^3)
 $SUMT$ = total operating time, (s)
 $SSTS$ = time of slewing process, (s)

$SSTV$ = adjustment time for slice advance, (s)
 $STSE$ = adjustment time for terrace advance, (s)
 TBE = adjustment time for block advance, (s)
 TNS = time required for switch-on, (s)
 H_N = net operating time, (h)
 H_e = total calendar time, (h)
 H_s = slewing lime for one slice, (s)
 H_A = adjustment time for one slice advance, (s)
 HT = adjustment time for one terrace advance, (s)
 HB = adjustment time for one block advance, (s)
 N_s = number of slices,
 NTS = total number of slices,
 N_T = number of terraces,
 NB = number of blocks,
 NTB = total number of blocks,
 LT = length of slice, (m)
 L_A = length of block, (m)
 L_B = length of bench, (m)
 a = slew angle (degrees)
 α_{MIN} = min. slewing angle (degrees)
 T_{ws} = angle of working slope, (degrees)
 α_{MAX} = max. slewing angle (degrees)
 h_i = height of terrace, (m)
 h_s = height of working slope, (m)
 bo = width of slice at (a) angle, (m)
 b_a = depth of slice at (a) angle, (m)
 t_s = max. depth of slice, (m)
 t_x = direction of travel,
 to = depth of slice at (a) angle, (m)
 $to =$ depth of slice at (0°), (m)
 V_B = slew speed at (a) angle, (m/s)
 V_s = average slewing speed, (m/s)
 W_B = width of block (m)

2 DEFINITION OF OUTPUT EFFICIENCY OF BWE

Georgen (1983) designates the effective output of the BWE as the effective output divided by the theoretical output.

$$\eta_{(total)} = \eta_E \eta_T \eta_D \quad (1)$$

$$\eta_E = Q_{eff} / Q_{th} \quad (2)$$

$$\eta_H = H_N / H_C \quad (3)$$

The theoretical and effective outputs of the BWE can be expressed as follows:

$$Q_{th} = 1.560 / f \quad (4)$$

$$Q_{eff} = V 3600 / SUMT \quad (5)$$

Total operating time can be defined as follows:

$$SUMT = SSTS + SSTV + STSE + TBE + TNS \quad (6)$$

$$SSTS = H_S N_S N_T N_B \quad (7)$$

$$H_S = L_T / V_S \quad (8)$$

A terrace is formed when the advancement of the BW is repeated several times in a horizontal direction only between the limiting angles, while the height of the wheel position remains unchanged. The width of this terrace is the block width. The length of terrace (L_A) in the highest cut of the BW is determined by the boom length of the BWE and the inclination of the working slope (Figure 1).

The depth of slice must not exceed the largest cutting depth of the buckets (Durst & Vogt, 1988). For normal operation, the depth of a slice in the travel direction of the machine at slewing angle $\alpha = 0$, should not exceed 90% of max t_s .

$$t_\alpha = t_0 \cos \alpha \quad (9)$$

The cut area of a terrace cut is sickle-shaped. It is formed by two circles of the new and old cuts separated in a horizontal plane by the distance to resulting from the advance of the BWE with a slew angle α of 0° . Slice depths decrease continually with increasing slewing angles, away from the excavator travel direction, and become zero at a slewing angle of 90° (Figure 2). By introduction of the "cosine α control" in the slewing process, i.e., by increasing the slewing speed according to equation (10), by the

reciprocal value of $\cos \alpha$, higher efficiencies are obtained:

$$V_\alpha = Q_{th} / 60 h_T t_\alpha \quad (10)$$

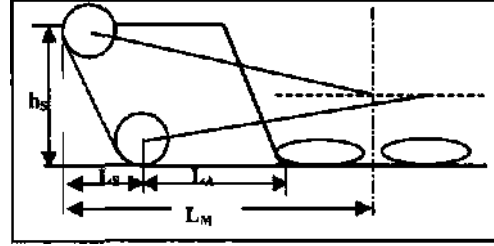


Figure 1. Length of terrace for face block excavation

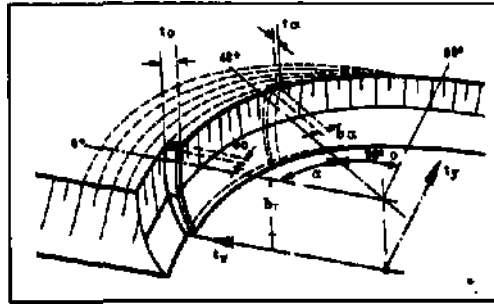


Figure 2. Reduction of slice depth with increasing slewing angle (Durst & Vogt, 1988)

The number of slices, number of terraces and number of blocks can be expressed as follows:

$$N_S = L_A / t_0 \quad (11)$$

$$L_A = L_M - L_S \quad (12)$$

$$N_T = h_S / h_T \quad (13)$$

$$N_B = L_B / L_A \quad (14)$$

The adjustment time for slice advance, adjustment time for terrace advance and adjustment time for block advance can be defined as follows:

$$SSTV = H_A N_{TS} \quad (15)$$

$$N_{TS} = N_S N_T N_B \quad (16)$$

$$STSE = H_T N_T \quad (17)$$

$$TBE = H_B N_{TB} \quad (18)$$

3 MODELLING OF OPERATING PROCESS

The parameters affecting the output efficiency of the BWE mining system can be divided into three categories. These are the material properties to be excavated and conveyed, the mechanical parameters of the mining equipment and the operational parameters. Panagiotou (1990) describes a mathematical digging model as the functions of geotechnical parameters of the ground to be dug (i.e., strength, fracture characteristics, etc.), the parameters of the excavated material (i.e., unit weight, swell factor, etc.), the operational parameters of the excavating equipment, the physical parameters of the excavating equipment (i.e., teeth and bucket geometry, available digging power, etc.) and the time during which changes in the excavation system take effect.

The purpose of the model created for this study is to match the physical and operational characteristics of the excavating equipment to the mode of excavation (Figure 3), based on the appropriate equations governing the geometry of the excavation and the operation of the equipment. The model requires the following input parameters:

Bench height,
Bench length,
Block width,
Block length,
Angle of working slope,
Time required for switch-on,
Adjustment time for one block advance,
Adjustment time for one slice advance,
Adjustment time for one terrace advance,
Depth of shoe at (0°),
Number of terraces,
Height of terrace,
Number of blocks,
Slewing speed,
Slewing angle of BW boom in horizontal direction,
Distance between bench belt conveyor and bottom of side slope,
Crawler width of BWE,
BW boom length.

3.1 Application of the Model

The model simulates the operation of the C frame BWE with a cordless-type boom, excavating according to the full block terrace cut method at the Kislakoy open cast mine, Elbistan, Turkey. The

mine is equipped with six identical bucket wheel excavators of the type Sch Rs (2300/5) x 32.

A set of constraints that express limitations resulting from interaction of the BWE and pit geometry is incorporated in the model. The crawler width of the BWE determines the dimensions of the box cut and the shifting distance of the bench belt conveyor. The maximum height of the working slope is 32 m. The maximum depth of slice at (0°) is 1.15 m. The minimum distance between the bench belt conveyor and the bottom of the side slope is 15 m. Possible slewing speeds are between 5 and 30 m/min. The slewing speeds to obtain the rated output (3000 bank m³/h) with respect to different terrace heights are given in Table 1. Other constraints direct the model to produce a logical design.

3.2 Determination of Optimum Operational Parameters

The effects of the different values of the block widths and terrace heights on the effective output of the BWE are investigated. In order to determine the optimum values of these parameters, the model shows that the effective output increases as the block width increases up to 58 m (Figure 4) and the terrace height increases up to 7 m (Figure 5). The first goal of the model proposed is to maximize the total efficiency of the BWE. For this reason, it is applied to the first bench of Kislakoy open cast mine to determine the optimum values of operational parameters. The model is based on the following assumptions: (1) the overburden formations in the first bench of the mine are diggable by the BWE; (2) the bench heights are multiples of 7 m; (3) the block width is 58 m; (4) the angle of the working slope is fixed at 54°; and (5) the efficiency of the transport and dumping system are assumed to be fixed.

Because the optimum values of the bench heights are multiples of 7 m, two different bench models are created - the bench height of the first scenario is 21 m and the bench height of the second scenario is 28 m. The development distance of the bench in the excavating direction is chosen as 240 m. The load factor, time factor and total efficiency are calculated for each scenario. Figure 7 and Figure 8 show the excavating sequences of BWE operation for the first scenario. The input data and the simulation run results are presented in Table 2 and Table 3. The results for the scenarios of the bench models are compared in Table 4.

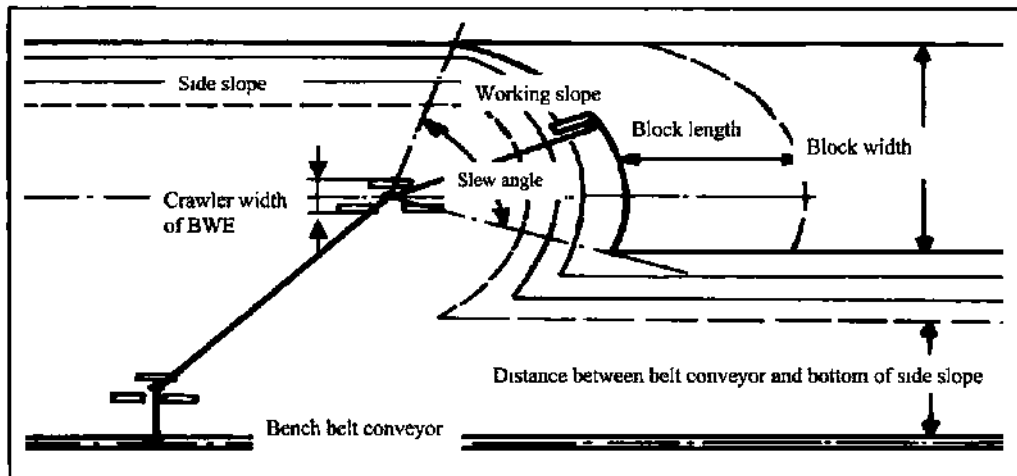


Figure 3. Physical and operational characteristics of the excavation.

Table 1 Slewing speeds to obtain rated output

Height of terrace (m)	Angle of slew (°)								
	0	29	34	40	46	55	65	75	80
9	5.56	6.35	6.70	7.25	8.00	9.69	13.15	21.47	63.74
8	6.25	7.15	7.54	8.16	9.00	10.90	14.79	24.15	71.71
7	7.14	8.17	8.62	9.32	10.28	12.45	16.90	27.60	81.96
6.125	8.16	9.33	9.85	10.66	11.75	14.23	19.32	31.54	93.66
6	8.33	9.53	10.05	10.88	12.00	14.53	19.72	32.20	95.61
5	10.00	11.43	12.06	13.05	14.40	17.43	23.66	38.64	114.74
4	12.50	14.29	15.08	16.32	17.99	21.79	29.58	48.30	143.42
3	16.67	19.06	20.10	21.76	23.99	29.06	39.44	64.40	191.23
2	25.00	28.58	30.16	32.64	35.99	43.59	59.16	96.59	286.84

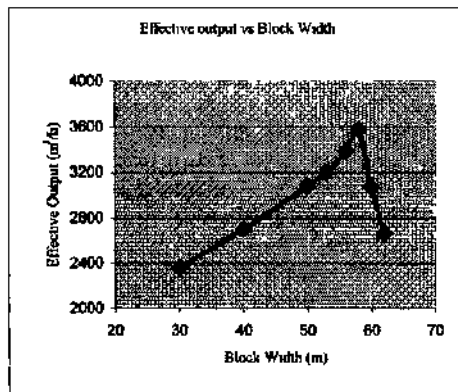


Figure 4. Effective output vs block width.

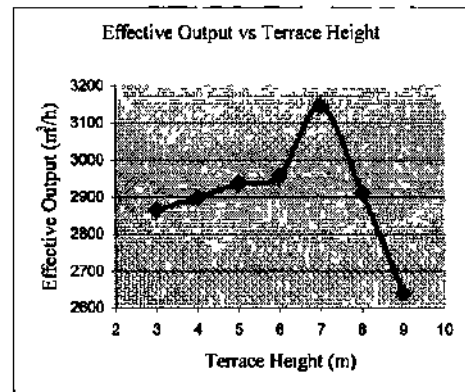


Figure 5. Effective output vs. terrace height.

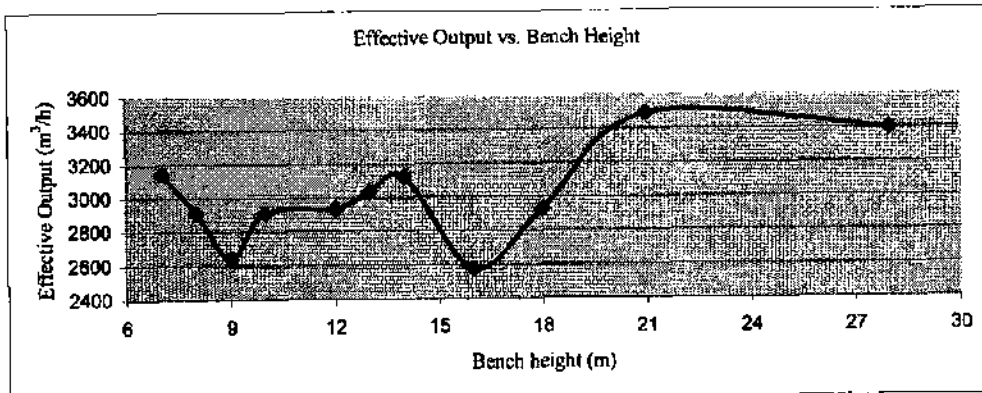


Figure 6. Effective output vs. bench height.

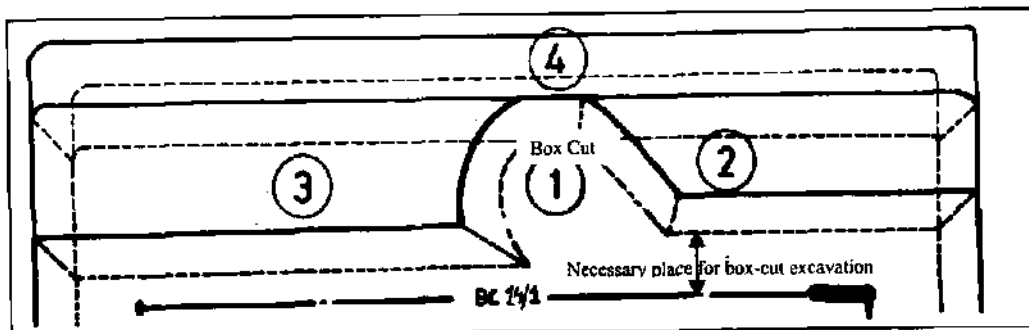


Figure 7. The excavation sequences of the first position of bench belt conveyor (14) for the 21-m bench height.

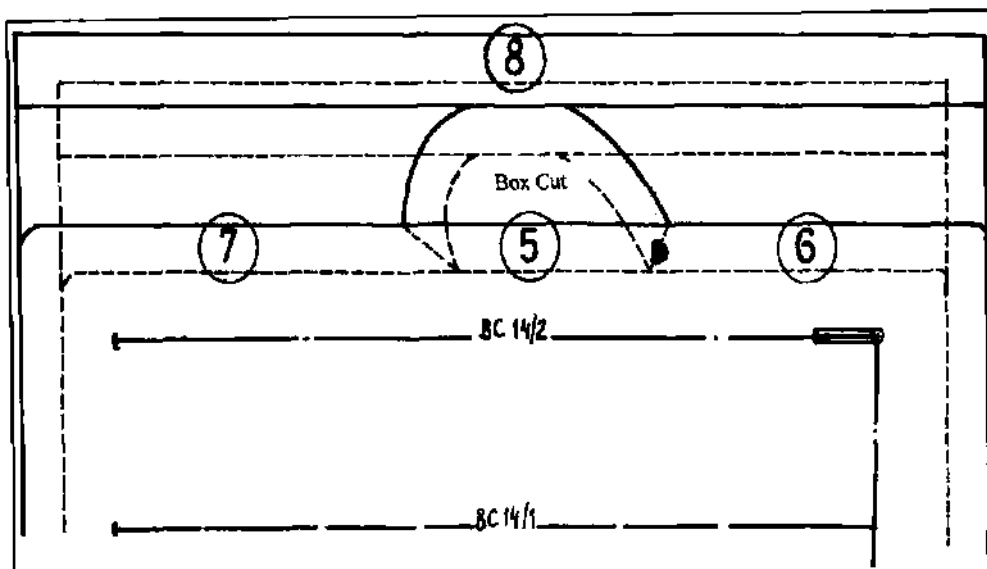


Figure 8. The excavation sequences of the second position of the bench belt conveyor for the 14-m bench height.

Table 2 Input data and the simulation run results for the 21-m bench height

Operation sequences	W_B (m)	V (m^3)	SUMT (h)	N_T	h_T (m)	Q_{if} (bank mVh)	IF (%)
Block 1	48	88704	30 35	3	7	2923	0 78
Block 2	53	222600	64 73	3	7	3439	0 92
Block 3	58	389760	11701	3	7	3331	0 89
Block 4	34	428400	155 27	3	7	2759	0 74
BC Shifting for 80 m (32 h)							
Block 5	48	88704	30 35	3	7	2923	0 78
Block 6	50	227052	70 54	3	7	3219	0 86
Block 7	50	619920	225 12	3	7	2754	0 73
Block 8	30	110124	63 64	3	7	1730	0 46
BC Shifting for 80 m (32 h)							
Blockt	48	88704	30 35	3	7	2923	0 78
Block 2	50	222600	64 73	3	7	3439	0 92
Block 3	50	389760	11701	3	7	3331	0 89
Block 4	30	428400	155 27	3	7	2759	0 74
BC Shifting for 80 m (32 h)							
TOTAL		3221064	1124 37			2865	0 76

Table 3 Input data and the simulation run results for the 28-m bench height

Operation sequences	W_H (m)	V (m^3)	SUMT (h)	N_r	h_r (m)	Q_{ciT} (bank nrVh)	π_E (%)
Block 1	48	118272	39 82	4	7	2970	0 79
Block 2	53	296800	92 90	4	7	3195	0 85
Block 3	58	519680	170 68	4	7	3045	0 81
Block 4	23	79856	47 70	4	7	1647	0 45
BC Shifting for 60 m (32 h)							
Block 5	48	118272	39 82	4	7	2970	0 79
Block 6	53	227052	71 07	4	7	3195	0 85
Block 7	58	599259	225 12	4	7	2662	0 71
BlockS	23	110124	63 64	4	7	1730	0 46
BC Shifting for 60 m (32 h)							
Block 1	48	345873	116 02	4	7	2981	0 80
Block 2	53	381901	116 68	4	7	3273	0 87
Block 3	58	417929	134 40	4	7	3110	0 83
Block 4	23	79856	47 74	4	7	1673	0 46
BC Shifting for 60 m (32 h)							
Block 1	48	118272	34 79		7	3400	0 91
Block 2	53	227052	69 62		7	3261	0 87
Block 3	58	619920	225 12		7	2754	0 73
Block 4	23	110124	63 64		7	1730	0 46
BC Shifting for 60 m (32 h)							
TOTAL		4370239	1558 76			2804	0 75

Table 4 Efficiency values of the first and second scenanos

	Excavation time 00	BC shifting time 00	He (h)	He (%)	HT (%)
1 Scenario (bench height - 21 m)	1124 37	96	1220 37	0 76	0 92
2 Scenario (bench height - 28 m)	1558 76	128	1686 76	0 75	0 92

4 CONCLUSIONS

The main findings of this study are the following:

There are strict relationships between slice depth (to), slewing angle (a) and terrace height (hy). Digging capacity can be constant only if the slewing speed is increased continuously by the reciprocal value of $\cos a$. Therefore, BWE operators should use the automatic cosine cp control process.

2. Possible slewing speed is limited to 30 m/min in view of the braking forces that occur when reversing direction. Therefore, the slewing angle should be limited up to 75° to obtain maximum digging capacity.

3. The terrace height should be selected so as to be as high as possible within the range of 6-8 m. Maximum digging capacity will be obtained if the terrace height is chosen as 7 m.

4. The block height should be chosen as a multiple of 7 m to obtain maximum BWE efficiency. The results obtained from the model indicate that block height is to be at least 21 m to ensure higher total efficiency of the BWE system.

5.-The necessary place between the bench belt conveyor and the toe of the side bench to begin the box cut after each belt conveyor operation strictly affects the shifting distance of the bench belt

conveyor. A distance of 30 m is enough between the bench belt conveyor and the toe of the side bench to begin the box cut up to a bench height of 24 m. If the bench height is greater than 24 m, the necessary place between the bench belt conveyor and the toe of the side bench to begin the box cut after each belt conveyor operation should be at least 40 m.

6. When the slope height is greater than 24 m, the bench conveyor shifting distance can be a maximum of 60 m. If a slope height between 14 m and 24 m is chosen, it is possible to obtain a bench conveyor shifting distance of 80 m.

REFERENCES

- Durst, W. & Vogt, W. 1988, *Bucket Wheel Excavator*. Clausthal-Zellerfeld: Trans Tech Publications
- Georgen, H. & Lu, Z. 1983. Beitrag zur festlegung der auslegungs und betnebsparameter von Schaufelradbaggern *Braunkohle*. 9:264-274
- Panagiotou, G. N. 1990. Assessment of open pit excavators* diggabüity. *Proc Ist Mme Planning and Equipment Selection*- 305-314.
- Rasper, L 1975. *The Bucket Wheel Excavator* Clausthal: Trans Tech Publications.

Simulation of Optimal Control for Mining Drilling Robot

E.Pop, M.Pop & M.Leba

Department of Informatics and System Control, University of Petrosani, Romania

ABSTRACT: In this paper, a system consisting of a mining drilling robot, microcontroller drives, and load model are considered. The drilling machine was modified to a three grades of mobility robot with rotation joints. Each joint is driven by a DC motor with power electronics. Control software is implemented in two parts of the system, one at high level in PC memory and the other at intermediary level in the microcontroller ROM memory as local BIOS. The mathematical model is determined as twelve transcendental equations written by the Denavit-Hartenberg methods. Inverting the equations with the software, three components of the position vector are determined. Thus, for each given position, it is possible to find the coordinates of the robot's elements. The gripper of the robot represents the electromechanical drilling machine, driven by an AC motor. A package of programs written in assembly language is implemented in a PC computer at high level. In order to optimize the drilling process, and implemented in the microcontrollers at intermediary level. The entire system was real-time simulated using a dSPACE kit.

1 INTRODUCTION

In this paper, a three grades of mobility robot with rotation joints is considered. These three joints are used for positioning the drilling machine.

This robot has a drilling machine on the last element and can be used for excavation in mining construction for increased safety of personnel (Fig.1).

To control the robot's joints, we use a SIEMENS CI67 16-bit microcontroller as a dedicated PLC to generate the movement trajectories according to optimal control algorithms (Anon., 1997).

To work in real-time we propose a distributed structure: a PC connected to a 16-bit microcontroller and power electronics at local level.

The software consists of two parts linked together with bi-directional data flow.

The first part solves the mathematical model to determine the rotation angles and the cutting speed (v_a) of the drilling machine.

The second part determines the new position of the joints and the rotation direction, converts the angles into pulses and sends these pulses to power electronics.

The entire process was simulated using a cinematic model according to the Denavit-Hartenberg method.

A program was written in assembly language so as to allow real-time working.

The programs run in real time, and ensure a high

level of flexibility in the robot.

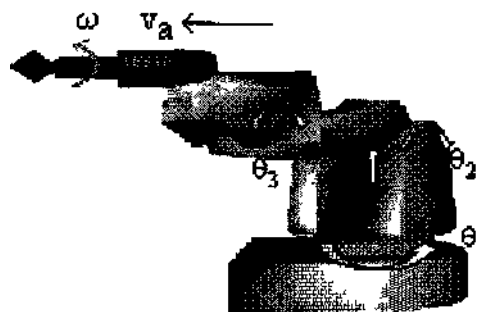


Figure 1. Drilling robot

In order to control the joints, the cinematic inverse problem was solved and then real-time simulated using dSPACE equipment with the expected results.

2 HARDWARE

The hardware consists of a PC, a SIEMENS CI67 16-bit microcontroller to control the joints, and a drilling machine operated by means of four power electronics modules (PE,) (Fig.2).

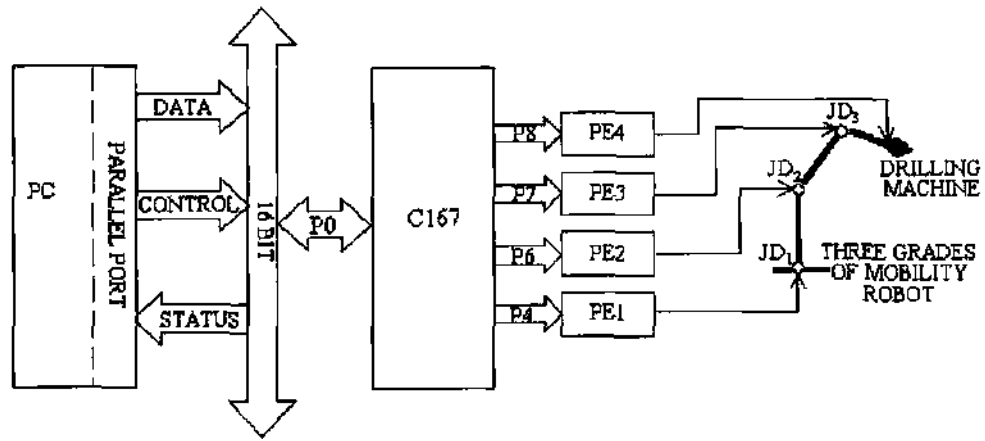


Figure 2. Hardware block diagram

The protocol data exchange is based on the hand-shaking principle. The process begins with the PC sending pooling data to identify each joint position. The parallel port of the PC, its 8-bit data section and two control bits and two status bits from the other two sections are used for this task.

These 12 bits represent the information for the 16-bit C167 microcontroller. The C167 decodes the information sent by the PC and determines the direction and angle value for each joint movement. This information is sent by means of four 8-bit output ports (P4, P6, P7, P8).

The signals generated by PE4 are to control the cutting speed of the drilling machine in order to optimize its efficiency.

This information is the input for the power electronics. The power electronics convert the received data into electrical pulses for the joint and drilling machine drives (JD).

3 MATHEMATICAL MODEL

The mathematical model of the three grades of mobility robot is determined by the following conditions: the first group of three rotation joints is for the positioning mechanism, and to the last element we fixed a drilling machine.

We consider that the rotation angles are θ_i ($i=1,3$) and the dimensions of the positioning elements are d_i ($i=1,2,3$). Then, the movement matrix $T_{0,3}$ is as follows:

$$T_{0,3} = \begin{bmatrix} n_{11} & a_{11} & a_{11} & d_{11} \\ n_{21} & o_{21} & a_{21} & d_{21} \\ n_{31} & o_{31} & a_{31} & d_{31} \\ 0 & 0 & 0 & 1 \end{bmatrix}$$

Using the Denavit-Hartenberg method, the 12 movement equations are:

$$\begin{aligned} \cos\theta_1 \cdot \cos(\theta_2 + \theta_3) &= n_{11} \\ -\cos\theta_1 \cdot \sin(\theta_2 + \theta_3) &= o_{11} \\ -\sin\theta_1 &= a_{11} \\ \cos\theta_1 \cdot \cos(\theta_2 + \theta_3) \cdot d_3 + \cos\theta_1 \cdot \cos\theta_2 \cdot d_2 &= d_{11} \\ \sin\theta_1 \cdot \cos(\theta_2 + \theta_3) &= n_{21} \\ -\sin\theta_1 \cdot \sin(\theta_2 + \theta_3) &= o_{21} \\ \cos\theta_1 &= a_{21} \\ \sin\theta_1 \cdot \cos(\theta_2 + \theta_3) \cdot d_3 + \sin\theta_1 \cdot \cos\theta_2 \cdot d_2 &= d_{21} \\ -\sin(\theta_2 + \theta_3) &= a_{31} \\ -\cos(\theta_2 + \theta_3) &= o_{31} \\ 0 &= a_{31} \\ d_1 - \sin(\theta_2 + \theta_3) \cdot d_3 - \sin\theta_2 \cdot d_2 &= d_{31} \end{aligned}$$

Inverting these transcendental equations, we obtain the angles θ_i :

$$\theta_1 = \arcsin\left(\frac{d_{21}}{d_{11}}\right)$$

$$\cos\varphi = \frac{d_{11}^2 + d_{21}^2 + (d_1 - d_{31})^2 + d_2^2 - d_3^2}{2 \cdot d_2 \cdot \sqrt{d_{11}^2 + d_{21}^2 + (d_1 - d_{31})^2}}$$

$$\cos(\theta_2 + \varphi) = \sqrt{\frac{d_{11}^2 + d_{21}^2}{d_{11}^2 + d_{21}^2 + (d_1 - d_{31})^2}}$$

$$\cos\theta_3 = \frac{d_{11}^2 + d_{21}^2 + (d_1 - d_{31})^2 - d_2^2 - d_3^2}{2 \cdot d_2 \cdot d_3}$$

To determine the optimum cutting speed, we use the equation:

$$\omega = k \cdot \frac{v_a}{s},$$

where k is constant, v_a is advance speed and s is the splinter width.

These equations represent the mathematical inverse model for determining the rotation angles and the drilling machine speed.

4 CONTROL ALGORITHM

For real-time simulation and digital control of the robot, the algorithm consists of several steps (Fig.3).

Given the input data, coordinates x, y, z and parameters of the drilling machine k, v_a , s, we determine the movement matrix TQ,3, then calculate the angles θ_i (i=1, ..., 3) and cutting speed ω . After this, we calibrate the six movement equations and determine the movement angles for each joint. All these steps are executed by the PC, which displays the robot position on the screen.

The next steps will be executed by the CI67 microcontroller as follows: taking the data of specific angles from the PC, this will be saved in the corresponding microcontroller RAM memory. Then the rotation direction will be found, the timing pulses corresponding to the specific equation of angles, and the pulses will be sent to the power electronics. In addition, the microcontroller sends feedback to the PC related to the position and other parameters of movement.

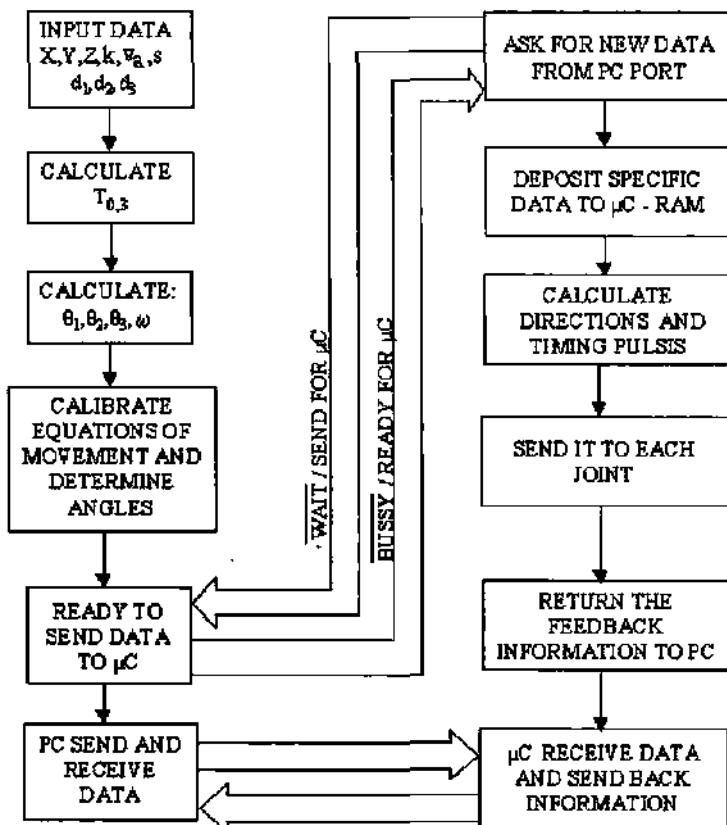


Figure 3. Control algorithm diagram

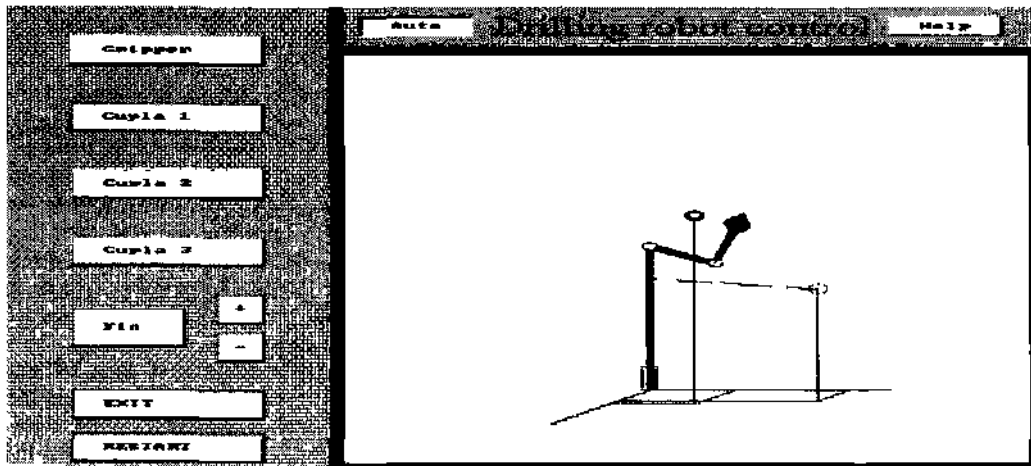


Figure 4 Assembly language program display.

5 SOFTWARE CONTROL

The software consists of two parts: at the PC level, there is a program written in assembly language for solving the inverse model and for graphic simulation. At the microcontroller level, there is a program written in C167 assembly language.

The PC software determines the movement angles, which are transmitted to the next level. It also displays a windows graphical simulation and control of the robot (Fig.4).

The microcontroller software generates the angle for each joint using its ports, compares it with the last position, and establishes the direction of movement according to the new position. Then, the microcontroller outputs the string of pulses to the power electronics.

The PC software written in 1-80X86 assembly language consists of over 2000 statements, of which the main program is;

```
start' call getcar
mov ax,0a000h
mov es,ax; initialize es=video address
mov ax,@data
mov ds,ax
mov ah,0; puts VIDEO mode
mov al,12h ; MODE=12h, 640x480
int 10h
call EnableMouse
redo: call HideMousePointer
call desenInit
call ShowMousePointer
callinit
call InversSursa ; calculates the inverse matrix
call scrieVal
call InversDestinatia
```

```
call desen
call buton ; polls the buttons
call TestButtonPress
cmp restart, 1
je redo; reinitializes the robot
mov ah,0; wait for a key to be struck
int 16h
mov al,3; clear display
mov ah,0
mov bh,0
int 10h
mov ax,4c00h ; exit to O.S.
int21h
end start
```

6 CONCLUSIONS

1. A robust three grades of mobility robot together with a drilling machine can become a drilling robot if it is software controlled.

2. In terms of hardware structure, the robot has a PC, a 16-bit microcontroller and corresponding power electronics for each joint.

3. The sophisticated software written in assembly language for the PC and microcontroller ensures a programmed drilling job, optimal control, high flexibility and user-friendly graphical support.

REFERENCES

- Pop, E., Leba, M. & Egn, A. 2001 Robotic control systems *Ed.Did & Pedagogica*
- Pop, E. & Pop, M. 1999. Assembly language programming for [-80x86 microprocessors. *Ed.Did & Pedagogica*
- Anon, 1997 CI 67 *SIEMENS Data Book*

Development of a Software Tool for the Prediction of Coal-Blending Efficiency

F.Pavloudakis & Z-Agioutantis

Department of Mineral Resources Engineering, Technical University of Crete, Hania, Greece

ABSTRACT; A coal-blending simulator for longitudinal stockpiles has been developed using the Visual Basic development platform for Windows®. The input to the simulator consists of the standard deviation and the autocorrelation of the coal property for which blending is attempted. The program initially creates a time series of property values for the coal delivered to the stockyard. Then, this input sequence is rearranged by simulating the operation of the stacking and reclaiming equipment. The output sequence of property values reflects the quality fluctuation of the coal fed to the power plant after blending. Results from the application of the simulator to the lignite mines of northern Greece show that coal-blending efficiency is a function of the capacity of the stockpile, the number of stockpile layers and the combination of the applied stacking and reclaiming methods.

1 INTRODUCTION

Coal quality control is a key factor in the improvement of overall coal combustion performance in terms of electricity generation costs and compliance with new stringent environmental standards. Various blending and mixing techniques have been proposed in order to reduce both the short- and long-term fluctuations of the coal quality characteristics. The capacity, shape and arrangement of the piles within the stockyard, the number of layers that are stacked in every pile and the applied coal-stacking and reclaiming methods are the major parameters that distinguish one technique from another. All of these parameters are closely related to the type of equipment that is installed in a stockyard.

2 COAL-BLENDING METHODS AND EQUIPMENT

The two main functions of a coal stockyard are buffering and blending. The successful design of a coal stockyard that can achieve high blending efficiencies requires the optimization of (i) the stockpile

length, (ii) the stockpile width, (iii) the number of stockpile layers, (iv) the quantity of coal per reclaimed cross-section, and (v) the position of the reclaimer in relationship to the stockpile. In order to properly select the above parameters, numerous factors relevant to the coal properties, the site-specific conditions and the specifications set by customers must be taken into account (Schofield, 1980).

The vast majority of coal stockpiles are longitudinal, arranged in series, in parallel or in series and in parallel. Circular piles are not common in the coal industry, although they have some important advantages (Zador, 1994).

The most commonly used stacking methods are the Chevron method and the Windrow method. According to the Chevron method, coal is stacked continuously along the central axis of the stockpile in such a way that a continuously growing triangular-shaped pile is formed (Figure 1). The Windrow method is applied in cases where high blending efficiencies must be achieved and the installed equipment does not allow the use of the Chevron method (i.e., where side-scrapers reclaimers exist). Less popular are the conical and the strata methods. The conical method is used in cases where blending is

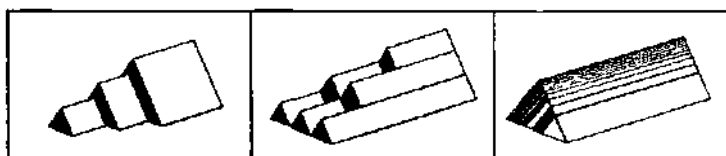


Figure 1. The Chevron, Windrow and strata methods of coal stacking.

not under consideration, while the strata method (Figure 1) is usually applied in stockyards where side-scraper reclaimers are installed (Zador, 1994).

The most widely used stockyard machinery is the boom-type bucket wheel stacker/reclaimer. Its traveling, slewing, luffing boom makes this machine flexible and easily adjustable even to special coal stockyard operations. Although it is a very versatile, high-capacity machine, it provides limited blending efficiency and at the same time it is difficult to automate its operations. Alternatively, reclaiming systems that dig material from the entire cross-section of the pile, such as bridge-type reclaimers with one or more bucket wheels, rotating drum reclaimers, disc-type reclaimers or chain-type scraper reclaimers, can be used. Other reclaiming systems may include the chain-type side scraper or the portal scraper reclaimers (Zador, 1994; Petersen, 1998).

3 PREVIOUS WORK ON BLENDING MODELS

The development of coal-blending simulation models started in the 80s. The traditional models were based on probability theory formulas, combining the blending efficiency with the number of stockpile layers, the mass of the stockpile and other characteristics. Recently-developed models also incorporate the autocorrelation function of the series of coal segments that have to be homogenized (Gerstel & Werner, 1996).

Nowadays, apart from the simulation models, there exist several commercial coal-blending optimization packages. Some of them are focused on the mining operation and usually incorporate linear programming techniques for the determination of the combinations of mine blocks that satisfy certain objectives, such as the maximum utilization of the material blocks and the minimization of the production costs of the specified ore quality (Mortensen & Hill, 1996). Other blending optimization packages have been developed for coal port terminals. They can handle the complex calculations involved in determining the lowest-cost blend when parameters, such as heating value and sulphur, moisture and ash content have to meet certain specifications, and when there is a multitude of coal qualities to choose from (Sehgal et al., 1997 - Jasper Comm., 1998).

4 DESCRIPTION OF THE SIMULATION MODEL

The simulation model that is presented in this paper was developed using the Visual Basic development platform for Windows®. The model consists of two parts. In the first part, a series of coal property values is generated based on the standard deviation and

the autocorrelation of actual property measurements. This is termed "input series of property values" and may be generated for any time interval. These values are subsequently used as input to the second part of the model, which simulates the stockpile operation. The output from the model is termed the "output series of property values". Considerable effort has been made in the development of a simulation model for the coal-stacking and reclaiming procedures in longitudinal stockpiles that is applicable to different site-specific conditions. It should be noted that this simulator is currently designed to handle a single coal property in each simulation run.

4.1 Model assumptions

In order to simplify the simulation process, the following assumptions have been implemented:

- *The coal-stacking and reclaiming rates are constant.* As far as the stacking procedure is concerned, this operational regime does not represent the real case, where stacking rates are related to the mine production rate. However, this assumption does not affect model performance, since the key variable in coal blending is not time but quantity. It can easily be understood that if coal sampling (and characterization) is performed every x tons of coal of variable stacking rate, this is equivalent to regular sampling of coal fed at a constant rate, in the sense that the coal property value will be assigned to the same block (quantity) of coal.
- *The coal contained in the conical ends of each pile is not reclaimed.* This technique is usually applied in stockyards whenever high blending efficiencies must be achieved in order to overcome problems arising from the irregular shape of coal layers within the conical ends of the piles.
- *The boundaries of each coal segment (input and output) are determined by two triangular sections perpendicular to the longitudinal axis of the pile.* Each stockpile segment that is stacked during a single pass of the stacker (at a constant boom angle) is conical and its inclination is equal to the angle of repose of the handled coal. When a series of such segments is stacked in sequence, each segment can be represented by a triangular prism. In addition, the boundaries of each reclaimed stockpile segment is determined by the geometry of the complex movement of the bucket wheel and the boom of the reclaimer. Again, this is modeled as a triangular or trapezoidal section. However, on average, and if the input series of property values has strong autocorrelation, (which means, for instance, that the calorific value of the n^{th} input segment will not differ considerably from the calorific value of the $(n+1)^{\text{th}}$ input segment), this assumption does not affect the accuracy of the calculations considerably.

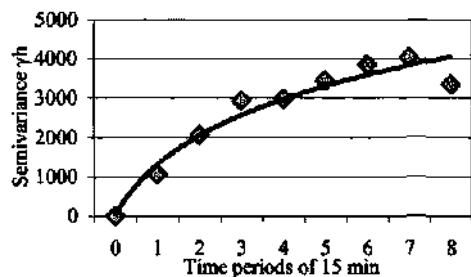


Figure 2. Comparison of the semivariance values of a generated NCV time series to the values obtained by actual sampling.

- *The size of coal particles is negligible compared to the dimensions of the stockpile segments.* The size segregation of coal particles (i.e., large particles roll to the stockpile base and fine particles remain at the top of it) during the stacking procedure is negligible.

4.2 Generation of the input series of property values

The first part of the model is designed to generate a time series of values regarding a single coal quality parameter, which will reflect the actual fluctuation of this parameter in the run-of-mine coal. Each value (element) in the data series corresponds to an average value for a given time interval, and assuming that the mine production rate remains constant, this value characterizes equal volumes of stacked coal (input elements or stockpile segments). The initial results that are presented in this paper are based on the use of the net calorific value (NCV) as the coal property to optimize through coal blending.

For effective application of a homogenization model, it is necessary for the input segments (stacking) to correspond to time intervals shorter than the time intervals that correspond to the output segments (reclaiming). The size of the input segments was chosen to be equal to the coal quantity consumed by the power plant in 15 min, based on the fact that the size of the output segments is equal to the coal quantity consumed in 1 hr. The size of the output segments was set so that it was equal to the so-called critical coal quantity of the boilers. The critical quantity (or period) is defined as the quantity of poor-quality coal (i.e., coal that does not meet the specifications) that can be burnt in a boiler without causing any drop in the power produced. The above-mentioned relationship between input and output element size ensures the contribution of at least 4 input segments for the formation of an output segment.

Therefore, to investigate the blending efficiency in a period of 1 month, the generation of property

values for 2880 input segments is required. Each element characterizes a stockpile segment with volume equal to the coal quantity received in the stockyard in a period of 15 min.

To generate the input series of the property value, the following data are required:

- 30 daily average net calorific values (d.a.NCV) of the run-of-mine coal, which is delivered to the stockyard within the investigated 1-month period.
- The standard deviation (sd) of the NCV of coal samples that represent fluctuations of the NCV with frequency equal to the size of the stockpile segments (i.e., 15 min).

These values are entered into a subroutine that generates pseudo-random numbers. The subroutine is available at the Internet site of NIST (NIST, 2000). For each d.a.NCV value, the subroutine returns 96 numbers, which follow a Gaussian distribution determined by the specified d.a.NCV and sd. Thus, each of these numbers corresponds to an NCV value that characterizes an input element, which contains the coal quantity consumed by the power plant in 15 min.

In order to ensure that the generated values are representative of the actual fluctuation of the NCV values of the run-of-mine coal, these 2880 values are rearranged, taking into account their autocorrelation. The autocorrelation function is an indication of the self-similarity between a series of spatially or temporally distributed measures of a property (Davis, 1986). The input series is rearranged several times and the resulting semivariograms are compared to a semivariogram which is considered to be representative of the actual fluctuations of the NCV (Figure 2). The latter semivariogram was determined by conducting a special sampling program at the South Field Mine of the Lignite Center of Ptolemais - Amynteon in northern Greece (Galetakis & Kavvouridis, 1999). This comparison is realized using a least squares comparing algorithm.

4.3 The blending simulation algorithms

The simulation of the blending procedure is based on the following parameters, which must be entered by the user of the simulator:

- the stockpile length,
- the stockpile width,
- the angle of repose of the handled coal,
- the coal quantity stacked within a 15-min period,
- the number of layers for coal stacking,
- the stacking method,
- the reclaiming method.

The simulation of the stockpile operation starts by assigning each of the 2880 input NCV values to a specified stockpile segment, which is accessed based on two coordinates: i, j . All the stockpile segments are included in an array with dimensions ixj , where i represents the stockpile layer and j represents the stockpile section (Figure 3).

6n	6n-1		5n+2	5n+1
4n+1	4n+2		5n-1	5n
4n	4n-1		3n+2	3n+1
2n+1	2n+2		3n-1	3n
2n	2n-1		n+2	n+1
1	2		n-1	n

Figure 3. Zig-zag placement of 3 x n input elements in a stockpile formed in 3 layers and n sections

Because of the zig-zag stacking of the stockpile layers, the following algorithm is used to calculate the position of the input elements within the stockpile (Gerstel & Werner, 1996):

$$\begin{aligned} \text{NCV}_{pile(i,j)} &= \text{NCV}_{input(i,j)} \text{ if } i \text{ is odd} \\ \text{or} \\ \text{NCV}_{pile(i, n+1-j)} &= \text{NCV}_{input(i,j)} \text{ if } i \text{ is even} \end{aligned} \quad (1)$$

where:

$\text{NCV}_{pile(i,j)}$, the NCV of the stockpile segment,
 $\text{NCV}_{input(i,j)}$, the NCV of the input element.

4.3.1 The Coal-Reclaiming Method of Sections

In the case of coal reclaiming using the Method of Sections, the output elements are triangular shape and their dimensions are determined from the height of each pile and the coal quantity that is fed to the power plant silos every hour.

The simulation procedure is modified according to the relative length of the output elements and the stockpile sections formed during the stacking procedure. As the number of layers increases, the length of the sections also increases and may become longer than the length of the output segments.

The length of the output elements and the length of the stockpile sections are calculated based on the stockpile geometry.

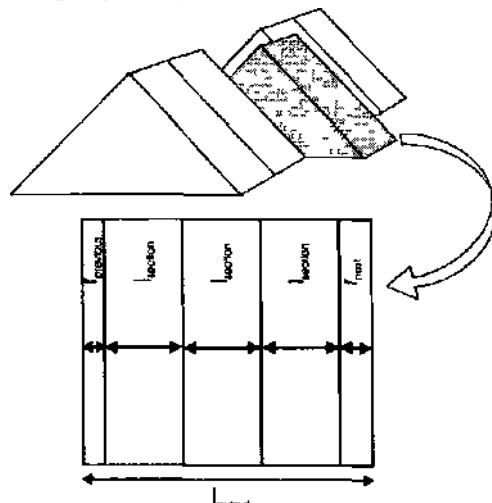


Figure 4 Schematic representation of a stockpile reclaimed using the Method of Sections

The calculations of the stockpile sections' length are modified according to the applied stacking method. The NCV value of each stockpile section is given by the following equation:

$$\text{NCV}_{section} = \left\{ \begin{aligned} &\sum_{i=1}^n \frac{\text{NCV}_{pile(i,j)}}{B} \\ &+ \sum_{i=1}^{n'} \frac{\text{NCV}_{pile(i,j)}}{2(n-0.5n')} + \sum_{i=n'+1}^n \frac{\text{NCV}_{pile(i,j)}}{n-0.5n'} \end{aligned} \right. \quad (2)$$

where the first sum corresponds to piles formed using the Chevron method and the second sum corresponds to piles formed using the Windrow method.

After the calculation of the NCV of the stockpile sections, it is possible to calculate the NCV of the output elements by calculating the average NCV value of all the stockpile sections that are included in the output element (Figure 4). The following general equation can be applied:

$$\begin{aligned} \text{NCV}_{output} &= \sum_{j=1}^J \left(\frac{l_{section}}{l_{output}} \text{NCV}_{section}(j) \right) + \\ &+ \frac{l_{previous}}{l_{output}} \text{NCV}_{section}(j_0 - 1) + \frac{l_{next}}{l_{output}} \text{NCV}_{section}(j_1 + 1) \end{aligned} \quad (3)$$

where:

NCV_{input} , the NCV of the output segment (reclaimed section),

j_0 , the first section of the pile which belongs completely to the specific output segment,

j_1 , the last section of the pile which belongs completely to the specific output segment,

l_{output} , the length of the output segment,

$l_{section}$, the length of each section if $l_{section} < l_{output}$, or the length of the output segments if $l_{section} > l_{output}$,

$l_{previous}$, the length of the part of the pile section that remains out of the previous output segment, and

l_{next} , the length of the part of the pile section that is partly contained in the specific output segment.

Furthermore, this equation is modified according to the following parameters:

- the relative length of the stockpile sections and the output segments of the stockpile, which are determined by the lignite quantities contained in the input and output segments, respectively, and
- the exact location of the boundaries of each output segment in relationship to the boundaries of the stockpile sections.

4.3.2 The Coal-Reclaiming Method of Benches

According to the Method of Benches, the reclaimer digs up above a fixed elevation in the stockpile on the entire length of the stockpile, thus creating a bench. The most economical way to accomplish this is to use 3 levels.

The simulation of coal reclaiming using the Method of Benches is based on the calculation of the

volumetric ratio for each layer in each bench. This ratio is calculated from the percentage of the bench cross-sectional area which is covered by each one of the layers (Figure 5). In the case of Chevron stacking, this area is calculated using the following equation, whose first part is valid for trapezoidal cross-sections and whose second part is valid for triangular cross-sections of layers:

$$E(i, k) = \begin{cases} \frac{(2\delta - \varepsilon)h'}{2} - E(i-1, k), & \text{if } y > h' \\ \frac{\delta y}{2} - E(i-1, k), & \text{if } y \leq h' \end{cases} \quad (4)$$

where:

i, k , the i.d. number of the stockpile layer and the bench, respectively,

h' the height of each bench, which is equal to 1/3 of the stockpile height,

y , the height of the part of the layer that is contained within the bench, which is calculated using the following equation (ϕ is the angle of repose):

$$y = \sqrt{iE \tan \phi} - (k-1)h' \quad (5)$$

δ , the width of each layer at the base of each bench, which is given by the equation:

$$\delta = 2y / \tan \phi \quad (6)$$

ε , the difference in the widths of each layer at the base and at the top of each bench (the difference of the two bases of a trapezoid), which is given by the equation:

$$\varepsilon = 2h' / \tan \phi \quad (7)$$

$E(i-1, k)$, the area of the portion of the previous layer which is contained within the current bench that can be calculated by the following equation:

$$E = \frac{d^2 \tan \phi}{4n} \quad (8)$$

where n is the number of layers and d is the width at the base of the whole stack.

It must also be noted that the length of output elements coming from different benches is not constant since the volume of the output elements must be kept constant and the cross-sectional areas of the three benches are different (Figure 5).

For the formulation of the output segments, equations similar to equation (3) are used. The difference between the two reclaiming methods is that while in the case of the Method of Sections there is one NCV value corresponding to each stockpile section, in the Method of Benches there are three NCV values that correspond to the three parts of the section that belong to each one of the stockpile benches.

Another difference between the two coal reclaiming methods is that in the Method of Sections no transition between segments on different benches is required, while in the Method of Benches special

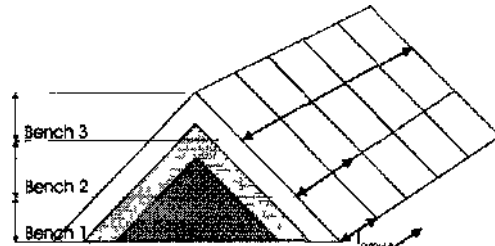


Figure 5. Cross-sectional view of a stockpile stacked using the Chevron Method and reclaimed using the Method of Benches.

algorithms have been developed to handle this transition. In the latter case, since every bench does not always consist of an integer number of output segments, at the end of each bench there usually exists a piece of coal that contains less coal quantity compared to the size of the output segments. In this case, in order to complete the last output segment of the bench, a piece of the next bench is added (Figure 6).

The length of the part of the next bench that must be reclaimed in order to complete the output segment that remained uncompleted at the end of the current bench is calculated by the following equation:

$$l_{next} = \frac{(Q-q)}{\frac{h'^2}{\tan \phi} (7-2(k+1))} \quad (9)$$

where Q is the coal quantity in an output segment, and q is the coal quantity which is contributed by the previous bench to this specific output segment. The latter is given by the following equation:

$$q = (l_{next} - c_{l_{output}}) \frac{h'^2}{\tan \phi} (7-2k) \quad (10)$$

where:

l , the length of the stockpile,

l_{next} , the length of the first stockpile segment of the lower bench, which was used to complete an output element during the transition of the reclaiming procedure from the current bench to the lower one. It is obvious that during the reclaiming transition from the 1st bench to the 2nd, l_{next} is equal to 0.

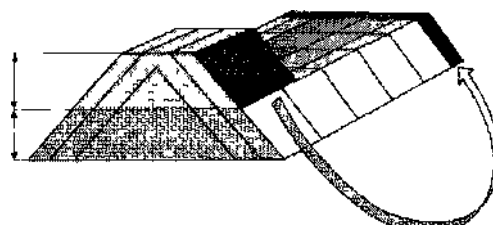


Figure 6 Output sequence for reclaiming a stockpile stacked using the Chevron Method and reclaimed using the Method of Benches

c, the number of output elements which were reclaimed from the current bench.

In the case of the Windrow Method of coal stacking, the algorithm for the calculation of the NCV of the output segments is based on the geometry that governs the coverage of each layer in the cross-sections of the three stockpile benches. Assuming that all the rhomboidal layers can be divided into two sublayers with a triangular cross-section (Figure 7), the following equation is valid if the entire sublayer with triangular section belongs to the bench:

$$E_1 = \frac{y^2 / \tan \phi}{\left(2d - (4k - 2) \frac{h}{3 \tan \phi}\right) \frac{h}{6}} \quad (11)$$

where h is the height of the stockpile.

Four other equations have been derived, depending on the geometry of the cross-section.

5 RESULTS

The model, which was developed as discussed previously, was initially applied for the evaluation of a coal-blending procedure applicable to the lignite stockyards of the Lignite Center of Ptolemais - Amynteon, in northern Greece. Furthermore, the simulator was used to conduct several parametric analyses for different stockpiling/reclaiming options for the lignite produced at the South Field Mine in that area.

The input series of property values was generated based on the results of the daily average samples of the lignite that was burnt in Agios Dimitrios Power Plant within a period of one month. The autocorrelation function was determined by collecting a series of special samples using a sampling period of 15 min.

Thus, 2880 input elements were generated from the first part of the model. After the simulation procedure was completed, the model returned 720 output elements, each one corresponding to an NCV value of the lignite reclaimed from a stockpile

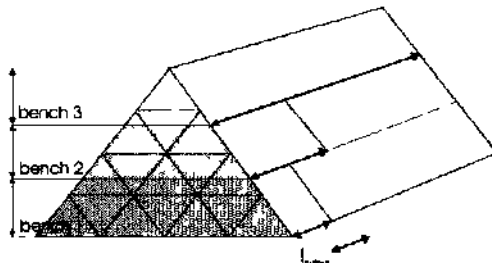


Figure 7. Cross-sectional view of a stockpile formed with the Windrow Method and reclaimed with the Method of Benches

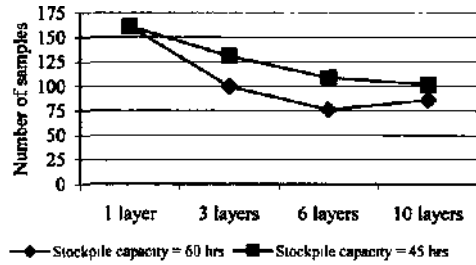


Figure 8. Reduction of the number of lignite samples with NCV below the power plant specifications, which results from the increase in the stockpile capacity

within a time period of 1 hr.

The results of the blending evaluation procedure are summarized in Figures 8, 9 and 10. The reduction in the number of lignite samples (occurrences) with an NCV lower than the power plant specifications, which results from the increase in the stockpile capacity, is presented in Figure 8. The reduction of the standard deviation of the NCV of the lignite, which results from the increase in the number of layers that form the stockpiles, is presented in Figure 9. It must be noted that the comparison was based on two different standard deviations. The first corresponds to the total number of lignite samples of the investigated period of 1 month (sd of 720 output elements). The other sd is calculated as follows: the simulator determines the number of stockpiles that were generated from these 720 elements; then, one sd is calculated for each group of elements comprising one stockpile; finally, the average of these sd values is compared to the first sd value which corresponds to the total number of output elements.

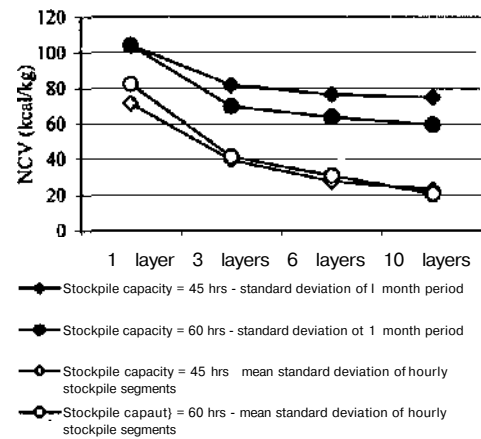


Figure 9. Reduction of the standard deviation of the NCV, which results from the increase of the number of layers that form the stockpiles

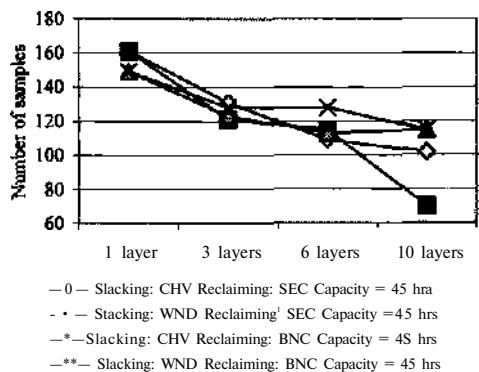


Figure 10. Differences in the number of samples that deviate from the specified lower limit of NCV, which result from four different combinations of stacking and reclaiming methods {CHV= Chevron, WND=Windrow, SEC=Method of Sections, BNC= Method of Benches}

The differences in the number of samples that deviate from the power plant specifications, which result from four different combinations of stacking and reclaiming methods, is presented in Figure 10.

The results can be summarized as follows:

- stockpiles consisting of 6 or 10 layers have approx. 50% smaller number of samples that do not meet the lower NCV specifications of the power plant. The standard deviation of the NCV of the lignite reclaimed from the same stockpiles is also considerably reduced;
- a stockpile capacity increase of 33% results in approx. 20% reduction in both the number of lignite samples that do not meet the lower specification of the fuel and the standard deviation of the NCV;
- the section method of reclaiming, when combined with the Windrow method of stacking in stockpiles consisting of 10 layers, gives significantly improved blending efficiency.

6 CONCLUSIONS

Nowadays, coal quality control is considered the primary tool for improving coal combustion performance in the power plants of the Ptolemais area. As a result, the overall cost of electricity generation can be significantly reduced.

The model which was presented in this paper is innovative since it can predict the coal quality fluctuation, taking into account both the statistical characteristics of the nm-of-mine coal quality data and the geometry of the stockpiles and of the stockyard machinery movements. Thus, this model can contribute considerably to the reliable evaluation of

different coal-handling scenarios applicable in coal stockyards.

This is particularly interesting for the stockyards of the mines and power plants of the Ptolemais area, which were initially designed to provide lignite-buffering storage, rather than a coal-blending facility.

Finally, the model was used for a parametric analysis regarding possible improvements on the lignite-handling procedure that is applied to the lignite produced from the South Field Mine of the Ptolemais area. The results show that there is room for improving current stacking/reclaiming practices at that mine.

ACKNOWLEDGEMENTS

This paper is based on research work conducted in the framework of a project entitled "Development of an automated system for lignite quality control and homogenization applicable in the mines and the thermal power plants of Ptolemais, Greece", funded by the "Program of Research Scholarships" of the General Secretariat for Research & Technology of the Greek Ministry of Development.

REFERENCES

- Davis, J.C., 1986, *Statistics and data analysis in Geology*, 2nd edition, John Wiley.
- Galetakis M., & C. Kavouridis, 1999. "Homogenization of quality of lignite mined from Ptolemaes-Anyndeon lignite basin", *Tech. Chron. Sci. J. TCG*, V, No 1-2, pp. 41-52 (in Greek).
- Gerstel, A.W., & J.W. Werner, 1996. Computer simulation program for blending piles, *Bulk Solids Handling*, Vol.16, Nr. 1, Jan/Mar 1996, pp.49-58.
- Jasper Communications, Inc., 1998. *PerfectBlend Software*, <http://www.jasper.com>.
- Luttekens, E., & G. Prins, 1994. New Developments in Storage Yard Systems, "The Best of Bulk Solids Handling: Stacking, Blending & Reclaiming of Bulk Materials" - B/94, Trans Tech Publications.
- Mortensen, AH. & S. Hill, 1996. FLS PC-Blend: A PC-based system for pile control and tactical production monitoring, *Proceedings, 1st International Symposium on Mine Simulation via the Internet (MINESIM 96)*, Balkema.
- NIST, 2000. Guide to Available Math Software, <http://gams.cam.nist.gov>.
- Petersen, F., 1998. *Raw Materials Handling Process and Equipment*, F.L. Smidth & CO. A/S - Materials Handling Division.
- Schofield, C.G., 1980. *Homogenization/blending systems design and control for mineral processing*, Trans Tech Publications.
- Sehgal, R., A. Hickinbotham, & D.L. Hill, 1997. Coal Blend Automation System for Power Plants, presented at: *Air and Waste Management Association's 90 Annual Meeting & Exhibition*, June 8-13, 1997.
- Zador, A.T., 1994. Technology and Economy of Blending and Mixing, "The Best of Bulk Solids Handling: Stacking, Blending & Reclaiming of Bulk Materials" - B/94, Trans Tech Publications.

Computer Modelling of Geomechanical Processes in Underground Working of Coal Seams

B.V.Vlasenko

Institute of Coal and Coal Chemistry, Siberian Branch of Russian Academy of Sciences, Russia

ABSTRACT: A new methodology of experimental-analytical approach has been developed. It is used in the building of an information geomechanical monitoring system (Gm MS) for computer modelling of geomechanical (Gm) processes during the working of coal seams. The approach synthesizes experimental (in-situ) measurements of rock pressure manifestation at separate points, methods of numerical modelling of processes on the rock boundary with goaf and seam, and analytical calculations of the spatial strained state of the rock mass.

1 INTRODUCTION

For the building of an information geomechanical monitoring system (Gm MS), a new methodology is used. It is the methodology of experimental-analytical modelling of Gm processes at the working of coal seams. Experimental-analytical modelling in mining geomechanics means the use of data as boundary conditions in solving problems with analytical methods, namely: adjoining rock shift, measured experimentally or calculated through momentary measurements in mine conditions. Such synthesizing is conducted on the basis of the worked-out model of shift (overhang) formation of adjoining roof rock and of the experimental-analytical method of determination of changes in the rock mass Gm state at the working of coal seams.

2 THEORY OF ROCK MASS KINEMATICS

Adjoining rock shifts during seam working present an integral characteristic of the rock mass geomechanical state and are an informative and simple form of rock pressure manifestations (BnaceHKo,1993). According to data from mine instrumental observations on adjoining rock movements in the locality of coal faces during seam working, It has been found that rock roof shift results from face advance in coal winning and temporary processes in the rock.

The schemes of formation of the working excavation given in Figure 1 show the one-type development of various forms of workings. The

main element of the development is the face movement along the front line. A trapezoidal form of working excavation (Figure 1b) may be considered more general. From this, workings of rectangular (a), triangular (c) and other forms are carried out, including workings with a skew angle line of the extraction front. One of these forms is the formation of a working excavation of compound form, for example, with a broken front line (Figure 1c), and the description algorithms of configurations of cavities having compound forms with a broken face line at the working of the seam are simple enough. In coal workings, individual face advances cause shifts of roof points in its locality. The geometrical place of normal-to-seam shifts of roof boundary points presents the surface of shift increments as a result of face advance (Figure 2d, e).

Surface of shift increments due to track working and die advance of the extraction front is formed as a result of face movement along the front line on shift surfaces due to individual face advances. Shift surfaces as a result of front advance, forming the coal face, constitute the final surface of roof shifts due to panel mining. Surfaces of shift increments and of final shifts are elements of roof boundary shifts. Surfaces of shifts due to face advance, which can be determined as an individual surface of shifts or an element of rock pressure manifestations (Figure 2d, e), are characterized by the parameters: location coordinates, direction and rate of face advance; maximum value of shifts and location relative to the face; degree of the decrease in shifts about die face. These physical parameters are applied to the analytical description of shift

formation are general enough for various determining parameters and computing from technologies (from the point of view of strata control observations in situ, methods) of seam workings and are suitable for

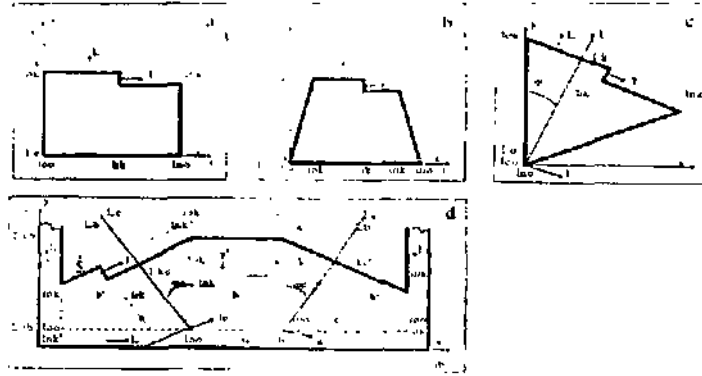


Figure 1. Schemes of coal face forming (a - straight shape; b - trapezoid shape; c - triangular shape (as a type of trapezoid) with inclined front line; d - compound shape with non-straight front line and development workings).

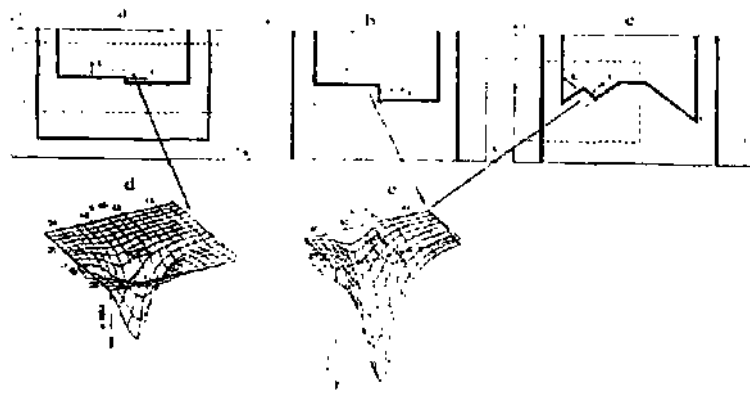


Figure 2. Elements of rock pressure manifestation in coal faces (a - longwalls with narrow web face; b - in longwalls with wide web face; c - in longwalls with non-straight wide web face; d,e - surfaces of shifts increments due to individual advances of narrow web (d) and wide web (e) faces; l^*j - calculation range of rock pressure

The worked-out method of calculation of rock shift surface formation (Bjiacemco, 1993) is a generalizing description and interpretation of shift experimental investigations most commonly used in the research of rock pressure manifestations during the mining of seam deposits. The calculation method provides an opportunity to work out a method (metJiodics) of shift modelling for different technological schemes of working. Taking basic increments of shifts due to individual face advance

for a known face scheme, for example, during the movement of a narrow web face (Figure 2a, d), it is possible to design a shift element due to individual face advance with set parameters, for example, of a wide web face (Figure 2b, c, e), and calculate shift surfaces for designed technological schemes of working.

Figure 3 shows the results of computer modelling of roof rock mass kinematics for spatial systems of working with different schemes of coal seam mining.

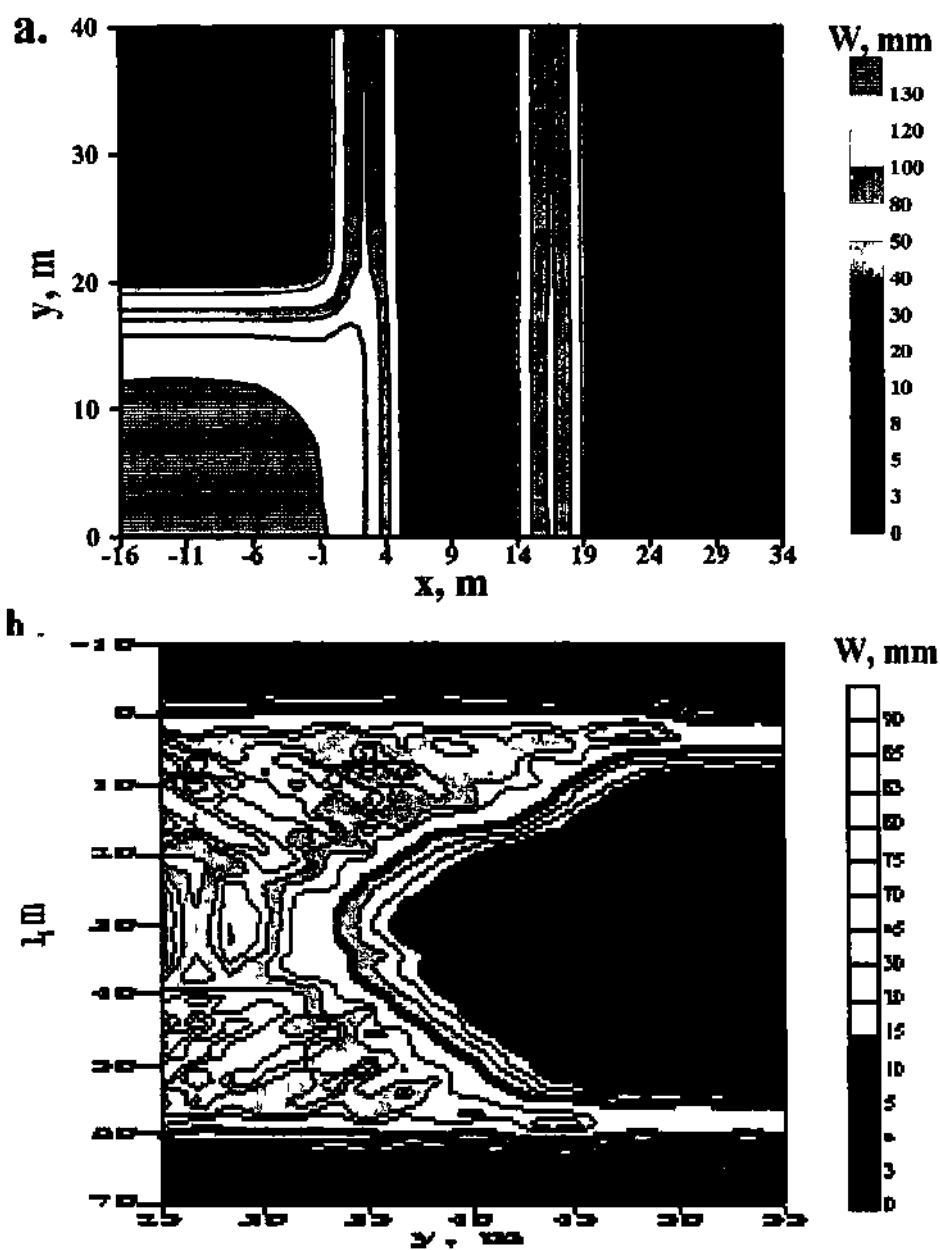


Figure 3 Picture of lines of surface levels of roof rock shifts in the neighborhood of coal face and development working system at the mining of coal seam by technological schemes with a pillar (a) and a non-straight (convex) wide-web face

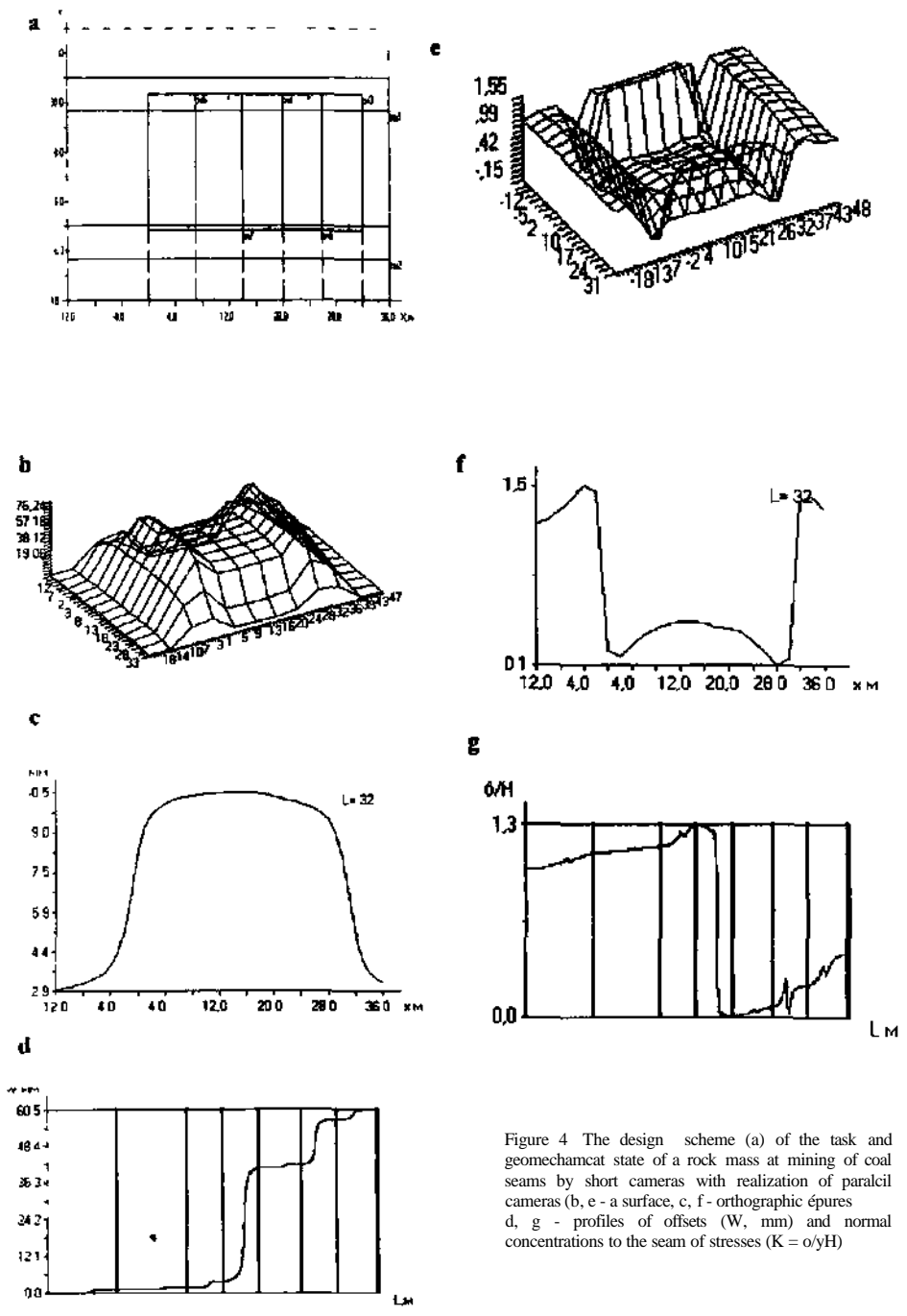


Figure 4 The design scheme (a) of the task and geomechanical state of a rock mass at mining of coal seams by short cameras with realization of paracil cameras (b, e - a surface, c, f - orthographic épures d, g - profiles of offsets (W, mm) and normal concentrations to the seam of stresses ($K = \sigma/yH$))

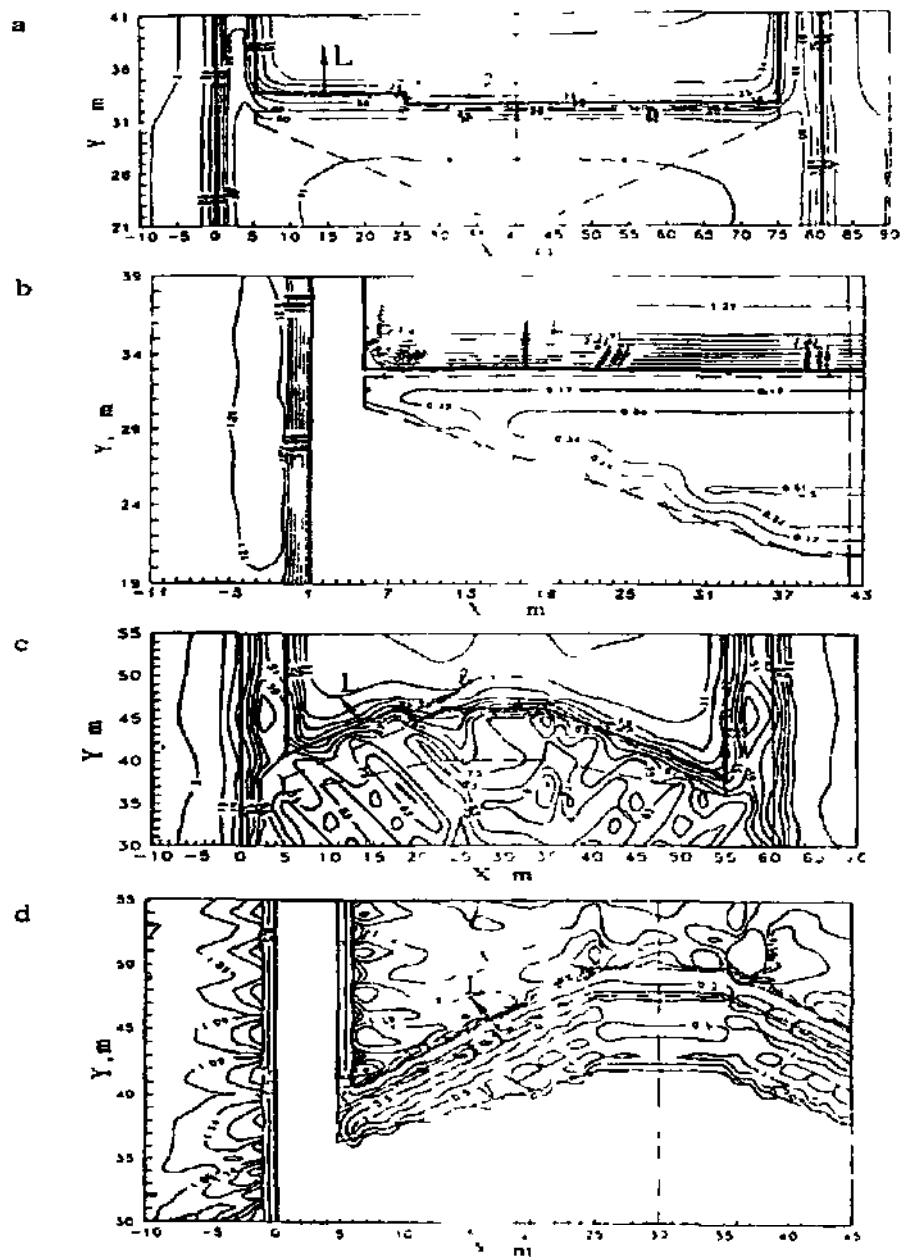


Figure 5 Rock pressure manifestations in longwalls with straight narrow web (a b) and non-straight (concave shape) wide web faces (a, e - lines of levels of roof surface, mm b, d- isolines of concentration surface of abutment pressure upon seam and of reaction support, $K \cdot a / \gamma H$)

3 EXPERIMENTAL ANALYTICAL METHOD OF INVESTIGATIONS

The processes of change in the rock mass Gm state in underground raining may be investigated not only with different methods or a combination of methods, but also by means of an experimental-analytical method, i.e., using analytical methods of investigation on the basis of experimental data (BjaceHKO, 1995).

The new method of mining geomechanics of computer experimental-analytical simulation of the geomechanical state of a rock mass is developed during the mining of a coal seam.

Analytical solutions to problems of rock mechanics are performed using experimental measurement results or calculated values of adjoining rock shifts as boundary conditions. The advantages of such an approach are in the use of real manifestations of geomechanical states under certain mining conditions and in the opportunity to overcome difficulties in the solution of spatial problems.

General solutions to spatial problems of the strained-deformed state of the rock mass in the vicinity of the face have been obtained on the basis of formulated statements under boundary conditions in the form of set surfaces of shifts. (Jalevsky & Vlasenko, 1998).

The method, algorithms and the programs of the accounts make it possible to:

- display the spatial design scheme of the task for any technological scheme of the mining and dynamics of the development of coal face works with the help of units of wall advance and front of operations;
- automate both the construction of the design scheme of the task, and account for the spatial stressed and deformed state of a rock mass and processing of the account results;
- present visually with the help of standard programs the machine profiles the obtained results as (Fig. 4) spatial pictures, maps of isolines, and orthographic épures of the surface offsets and stresses, and temporary profiles of changes in offsets and stresses during the development of a seam.

The advantages of the developed computer method of simulation have not been obtained previously in mining geomechanics, either in simulation by analytical methods (for example, the method of boundary integral equations, finite element methods, etc.), or in physical simulation (for example, with the help of equivalent or photo-elastic materials).

In Figure 5, the modelling results of the rock pressure manifestations are shown. They were modelled for schemes of seam working with the use

of a narrow-web cutter-loader and a cutter-loader at broken front lines of works. The pictures of rock roof shifts (roof subsidence) (Figure 5a, c), calculated over them the pictures of abutment roof pressure on a coal seam and the reaction support within the goaf (Figure 5b, d), give the opportunity to understand and compare rock mass geomechanical states for different schemes of working at one-type formation of deformation processes in roofs.

The accounts of the stressed-deformed status of rock massif in the vicinity of systems of mine workings in a coal seam were carried out at the rectilinear and non-rectilinear forms of the front of working faces, essentially the spatial schemes of the complex configuration of the workings. It has made it possible to begin the creation of a directory of geomechanical status and conditions for basic elements of new and traditional technological schemes of coal seam mining.

4 CONCLUSIONS

The use of kinematic theory, experimental analytical methods of determination of the geomechanical state and geographical information systems enable a system of dynamic computer modelling of geomechanical processes within the rock mass to be worked out.

Dynamic computer modelling of geomechanical processes in the mine information monitoring system is designed to calculate the geomechanical conditions within panels during planning and development as well as during mining, i.e., to enable long-term prediction, in-line control and short-term prediction of rock pressure manifestations.

Such a monitoring system can be used as a basic part of the system in order to facilitate scientifically proven technical and technological solutions in seam working.

REFERENCES

- Jalevsky V.D., Vlasenko B.V. 1998. Geomechanical evaluation of method for long room mining of coal seams *APCOM'98 27-th international Symposium on Computer Application* in the Mining Industries. Paper* presented at the 'APCOM'98' confèrent, organized by the Institution of Mining and Metallurgy in London, United Kingdom from 19 to 23 April, 1998* 429-440
- BjaceHKO. S.B. 1993. *Pa3pa3OTKa MCTOYOB yponio-nyoBaniDi iipoaueHHt roptopo JWBICIIIUI JUIS coMexamiccKoi o Moumopmira m ypojuuu* uiaxrax (Working out of predicted methods of rock pressure manifestation for geomechanic monitoring at coal mines). *Atmnpaipepam Ouccepmaittu ua coucKwrite mentm cmeiemi oonmopu merimecKax HIQL. KCMCDOBO: HV CO PAH.**

Dziacek K. E. D. 1995. ЗкнепрнМЦјТа.уно - аајтн-нл'фсцКос
МОЈСЛНрОВАилле прОСрпайСТВШНОИ I-COMCхaim'CCгеОП
оџсгаиодКН прН Мошгго-ршпге іта ут<uu>ну\ уиа\іа\
Proceedings of the 12th International dnjertme on
Atulm In Mining 13-15 091995 75-80 Olnvice
Poland.

Improving Safety in Open Pit Mines Using RTK - Differential GPS

A.Nieto & K.Dagdelen

Department of Mining Engineering, Colorado School of Mines, Colorado, USA

ABSTRACT. The National Institute of Occupational Safety and Health (NIOSH), has reported that, more than twenty-five fatal accidents related to dumping tasks and more than 23 fatal accidents related to vehicle collisions have occurred in USA since 1990. GPS technology is being used efficiently in large open pit mines in the area of truck dispatch systems and field surveying. In large open pit mines, the pit maps and dump maps are being built in real time and can be transferred directly to the on-board computers of the trucks. With the existing GPS equipment already on board, one can quickly determine exact coordinates of a given truck within sub-meter accuracy and evaluate if a given truck is dangerously close to the dumping edge of a waste dump. At Colorado School of Mines, Mining Engineering Department there is an ongoing research project on improving truck safety and productivity through GPS and wireless mobile network system using a state-of-the-art 3D interface, which could access SQL compatible databases. This paper presents the current progress on this work and discusses various issues that are needed to overcome in development of a rugged, reliable system.

1 INTRODUCTION

Coordinating several pieces of heavy equipment in an open-pit mine is not a easy task, the complexity factor is increased when this equipment scales up to house size trucks.

More than 25 fatal accidents have occurred when truck drivers performed dumping tasks since 1990 just in USA. This process requires the driver to move backwards toward the edge of a cliff tens of meters deep, and, over a surface composed of material that has been recently deposited, making this soil unpredictable for failure.

The requirement of a system to improve such conditions needs to be developed: the objective of this project is to develop a real time tracking system for these trucks so an intelligent system could automatically warn the driver, if he/she gets too close to the edge of the dumpsite, as well as, to indicate risk of surface-collapse.

Creating a virtual buffer safety-zone on the dump will permit the truck to move safely and efficiently in accordance with soil and truck characteristics in realtime.

The use of an accurate GPS system, which can handle sub-meter accuracy, is required to keep track on any movement of the truck respect to the edge of the dump, thus a differential GPS is used along with RTK (Real Time Kinematics) technology.

It is very important to remember that, differential mode using code phase is called DGPS. Using carrier phase is called *Carrier Phase Differential* (CPD). Real-time carrier phase differential has been called *Real-Time Kinematic (RTK)*.

Potential implementation of this system is the monitoring of pit ramps surface conditions using vibration sensors on the truck, Collision Warning, improving safety on shovel-truck loading tasks, and in the near future: real-time dispatching driverless systems.

2 DESCRIPTION

This project involves mining operation and safety, and particularly focuses on the dumping process of mine trucks in open pit operations. During the last years the Department of Labor MSHA (Mine Safety and Health Administration) and NIOSH, have followed statistically the number of accidents that have occurred due to this dumping task (1990 to 1996), resulting in 23 and 25 fatal accidents related to vehicle collision and off-highway, which also has caused losses of millions of dollars in equipment and opportunity costs.

Due to a large number of accidents that occur while a truck dumps a load at the edge of a waste dump, attention was focused on the danger

associated with the proximity of the truck to the dump edge and the potential ground failure due to the high truck weight and the material strength of the waste dumps.

If soil conditions are safe for dumping this project is also taking into consideration factors like poor visibility or driver error. Figure 1 shows a open pit mine in Peru using GPS.

Thus this project focuses on creating a system involving state-of-the-art technologies available today such as:

- RTK differential GPS
- Better and more reliable radio communication, like Bluetooth local wireless networks.
- TCP-IP protocol for Internet compatibility using VRML Virtual Reality Modeling Language, and.
- Potential use of pseudolites



Figure 1. Mine in Peru using GPS technology.

3 SOFTWARE DESCRIPTION

These technologies must be put together in a simple and friendly form that can be quickly interpreted by the truck driver and the main control office, and at the same, time this information must be shared in real time among other mobile equipment in the mine and even shared to offices located around the world.

In order to accomplish this task a visual two-dimensional interface written in Visual Basic language was developed, where the GPS data is read, collected, and compared with survey data and then displayed on a flat panel screen mounted on the truck.

A series of alarms (sound and visual) are also used to warn the driver if the truck is approaching a non-safe zone.

The safety zone is based on the soil conditions and on the truck size and load. The safety zone is represented by a series of lines distanced from the edge dump. This digital safety line is positioned with respect to the edge of the dump in real time depending on the truck and soil conditions, See Figure 2.



Figure 2. Cross section of a dumpsite showing the relative position of the truck represented by the dot against a buffer safety zone by the line

The Visual Basic algorithm takes in consideration the position of the truck in real time given by the GPS unit. It also reads the 2D survey map of the dumpsite zone and then creates a "safety buffer line" zone.

The next generation of this software; a three dimensional version of this interface is being developed based on VRML (Virtual Reality Modeling Language), which is described later in this paper.

Creating a virtual buffer safety-zone on the dump will permit the truck to move safely and efficiently in accordance with the soil and truck characteristics in real time. The current Visual Interface is shown next presenting three different scenarios where the mine truck is approaching the dump edge, and the safety buffer line: (See Figure- 3).

The use of a very accurate GPS system, which can handle sub-meter accuracy, is required to keep track of any movement of the truck with respect to the edge of the dump. Thus a RTK (Real Time Kinematics) differential GPS is used for this project. Utilization of GPS pseudolites (ground-based "pseudo satellites") next to the pit is also considered in order to increase reliability of the system and satellite constellation availability.

4 SOFTWARE DEVELOPMENT

Development of a Visual Interface is being carried out using the Visual Basic language, and consists on two main programs:

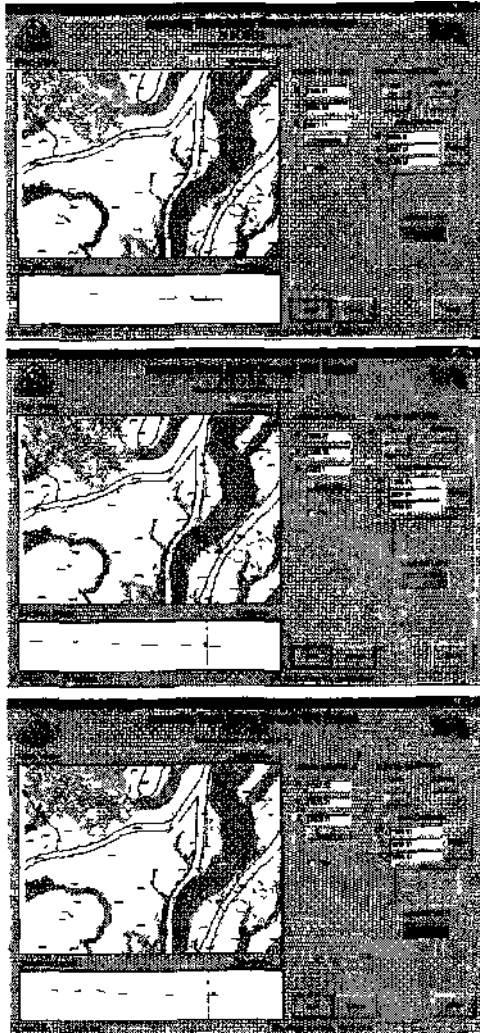


Figure 3 A series of snapshots showing the dumping process of a truck related to the dump edge and the safety zone

The first program consists of reading and interpreting data coming from the GPS receiver. GPS receivers commonly use NMEA (National Marine Electronics Association) protocol, which is the standard communication format, used in GPS.

4.1 NMEA code

Under the NMEA-0183 standard, all characters used are printable ASCII text (plus carriage return and line feed). NMEA-0183 data is sent at 4800 baud

The data is transmitted in the form of "sentences". Each sentence starts with a "\$", a two letter "talker ID", a three letter "sentence ID", followed by a

number of data fields separated by commas, and terminated by an optional checksum, and a carriage return/line feed. A sentence may contain up to 82 characters including the "\$" and CR/LF.

If data for a field is not available, the field is simply omitted, but the commas that would delimit it are still sent, with no space between them.

Since some fields are variable width, or may be omitted as above, the receiver should locate desired data fields by counting commas, rather than by character position within the sentence.

The optional checksum field consists of a "*" and two hex digits representing the exclusive OR of all characters between, but not including, the "\$" and "*". A checksum is required on some sentences.

The standard allows individual manufacturers to define proprietary sentence formats. These sentences start with "\$P", then a 3 letter manufacturer ID, followed by whatever data the manufacturer wishes, following the general format of the standard sentences.

4.2 Software Development

At the first stage of this project, a DeLORME GPS receiver unit was acquired to perform some preliminary communication tests between the receiver unit and the PC.

Unfortunately the DeLORME unit sends encrypted data coordinates and a "NMEA-Binary translator" device had to be used on the PC computer port.

Currently it is being used a TRIMBLE 4400 Dual Frequency GPS receiver unit which had to be reprogrammed to output NMEA-Code.

Once native a NMEA-code was received on the PC port, a small VB program was developed to read this data and extract the XYZ coordinates from the unit.

The VB program is a modification of a VB Modem Terminal, which consists of a text terminal that is connected to the COM1 of the PC. This program is able to read the output ASCII stream based on the NMEA code from the GPS unit, and extracts the XYZ coordinates. Figure 4 shows the terminal reading and extracting the longitude, latitude, and altitude.

The second part of the Visual Basic project, consists of a program for graphical visualization purposes, where a DXF reader module is incorporated into the VB routine in order to be able to import DXF maps from AutoCAD or any other CAD program.

This interface is to be installed on a LCD screen next to the truck driver controls (See Figure 5), so the driver can track his position with respect to the map in real time.

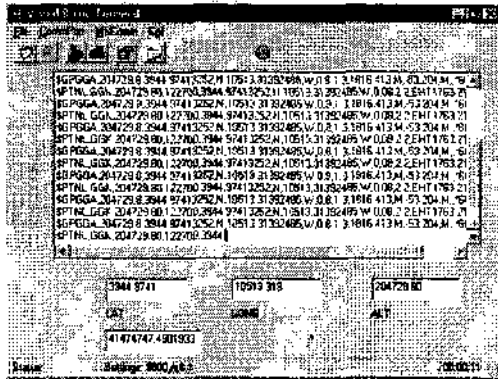
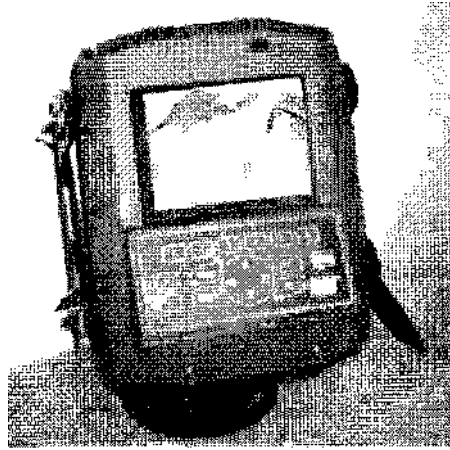


Figure 4. Shows a snapshot of the code and the terminal extracting the XYZ cords from the GPS unit.



panel, (digitally composed).

The 2D map software is designed such that two separate views of the dumpsite are generated in the graphical interface; The plan view on the top part of the screen and the equivalent section view just beneath Figure 6. Using this format the driver can track at the same time his vertical position with respect to the dumpsite as well as the horizontal position. The program also displays a virtual line representing the safety boundary of the truck with respect to the dumpsite. The line distance with respect to the edge of the dumpsite varies according to the truckload characteristics and also with respect to the soil conditions.

This information can be fed into the program from the engineering center office to the truck by a radio modem link or directly by the driver. Once the truck approaches this safety line a series of visual and sonic alarms start to act depending on the proximity of the truck to the virtual safety boundary line (See Figure 6).

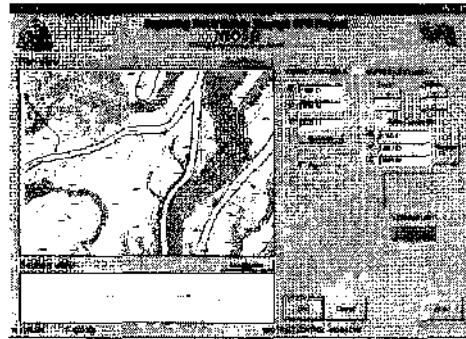


Figure 6. VB Interface monitoring truck position with respect to the dumpsite edge and the buffer safety line.

4.3 VRML Project, THE 3D Interface

In order to upgrade the above system from a 2D system into a Real Time 3D interface, the Virtual Reality Modeling Language VRML is being used.

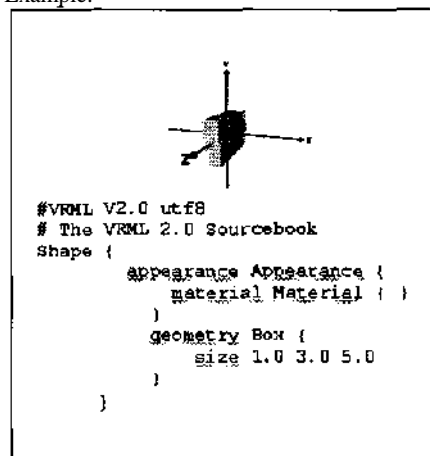
VRML is "an open standard for 3D multimedia and shared virtual worlds on the Internet."

Long before its official standardization VRML became the *de facto* standard for sharing and publishing data between CAD, animation, and 3D modeling programs; virtually every one of those programs now exports VRML or has a utility or plug in to convert its native file format to VRML. VRML is included or referenced in the upcoming MPEG-4 standard, Java3D, and in other developing standards.

Being able to talk and work in a 3D shared virtual space was one of the earliest motivations of the VRML pioneers. The VRML works has a whole section on Internet that talks about the work that's being done to realize this vision.

Unlike previous 3D applications, using the Internet to share 3D objects and scenes was built into VRML from the very beginning. The standard is even published in HTML.

Example:



The approach followed to construct a VRML world for this project was first to create a VB program, which could translate DXF files (contour lines in 3D poly-lines format) into a VRML 3D Lines.

Thus a mine map coming in a DXF format (which is the most common form), could now be visualized in a 3D view which can be dynamically viewed in real time, instead of using 2D sections.

The 3D visualization in VRML can be thought of as a VirtualWorld, or in this case: a VirtualMine since the user can move inside this "world" in real time using a standard keyboard or mouse. Eventually interactive devices like goggles and gloves will allow the user to immerse itself into this "VirtualMine" from any location since it is INTERNET based.

The first step to create this DXF to VRML translator was to create a program in VB to read the DXF file (ASCII file), and use it to determine the beginning of each individual poly line. Once this step was completed successfully, the program then was able to create 3D points in VRML floating in space representing the survey data coming from the mine map.

The next step was to "link" these points with lines to create 3D lines in VRML, thus creating a 3D map of the mine.

The next step is to create the 3D representation of the truck, which will be dynamically positioned in the map by following the XYZ coordinates coming from the GPS unit. The truck then interacts with the safety buffer zone represented by a 3D plane. Thus, if the truck approaches or crosses this plane, a series of alarms will be triggered.

Again, this safety buffer plane will be moving with respect to the edge of the dumpsite depending of the truck characteristics and soil conditions.

This program was, once again written in Visual Basic. As an example the same dumpsite map used in the 2D interface is now shown in an isometric view.

5 FUTURE DEVELOPMENT

GPS application in mining is becoming more and more reliable and less expensive, due to the implementation of new technologies like differential GPS and the relaxation of government policies, such as the recent announcement coming from the USA government in order to cancel GPS selective availability, as well as the use of the Russian GPS equivalent: GLONNAS.

Now, for the first time, it is economically feasible and reliable to monitor in real time any moving equipment in an open pit mine.

At Colorado School of Mines, Mining Engineering Department, we are using this GPS technology with a new state of the art visual interface based on VRML (Virtual Reality Modeling Language). The product code is named "Virtual Mine".

At this stage, "Virtual Mine" can translate DXF contour mine maps into VRML files (called virtual-worlds) (See Figure 7), so the user can interact through this 3D environment using a stand-alone visual basic interface or even a web browser from any "real-world" location.

Combining these approaches feeding the system with topographic DXF files and feeding the location of every equipment working in the pit from a GPS, it will be possible to virtually supervise a complete mine operation in real time, moving through this digital model of the mine, thus giving whole new approach in improving safety and productivity in mining operations.

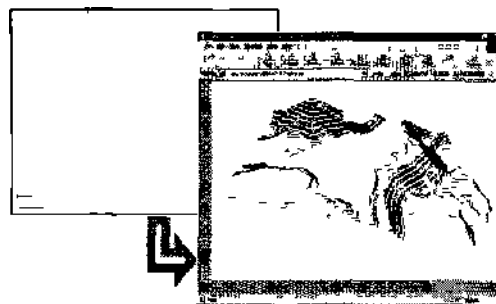


Figure 7. Translation from a DXF 2D contour map to a VRML 3D image, viewed using a web browser

Figure 8 shows the current interface where the dump map and a mine truck (represented by a 3D cube) interact in this 3D environment.

This system could be also integrated into the concept of "Collision Warning Systems" for surface mining equipment which is also being sponsored by the National Institute for Occupational Safety and Health (NIOSH) (Todd M. Ruff).

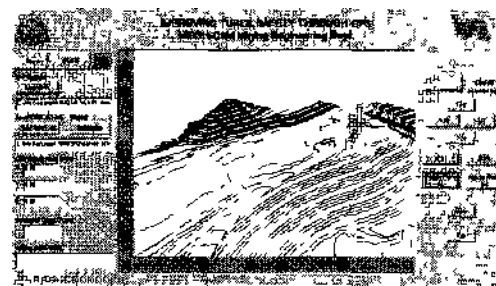


Figure 8. Snap Shot Showing a 3D representation of the dump site translated from a DXF file and a truck.

Other utility which is being incorporated into the system is "data access and transferring" (Figure 9); the system is intended to be capable of transmit and receive data from central office into any other vehicle in the mine in real time. This process will update a central database containing all data related to the mining operation. The system is also capable of query data from the central data base using the SQL.

The system uses TCP-IP upgraded radios (Currently Trimble TRIMCOMM 900) to broadcast GPS signal correction, however testing is being done to transmit the truck related data. Like: tonnage of ore/waste moved, grade, truck condition, road condition, etc.

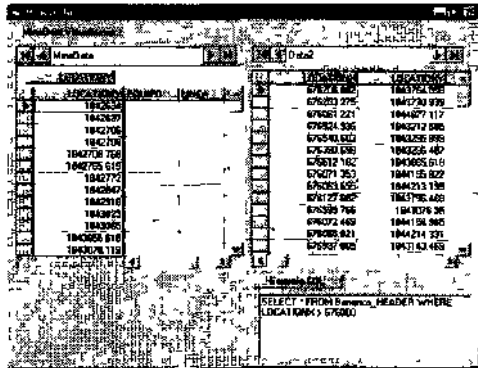


Figure 9. Database Interface used to transmit and receive data from central office to the truck

As mentioned other potential implementations of this system besides dumping tasks are:

- Collision Warning Systems
- Monitoring of surface condition in ramps or roads using vibration sensors on the truck.
- Improving safety on shovel-truck loading tasks.
- Improving preventive maintenance.
- And In the near future: real-time driverless dispatching

6 CONCLUSIONS

The Importance of the GPS applicability in mining is increasing since GPS technology is becoming more and more precise and reliable, thanks to the development of new technologies and the availability of systems like GLONASS.

New technologies like pseudolites and differential GPS based on geostationary satellites' have a great potential in GPS applied in open pit mining, since increases the reliability of the GPS system, at a

relatively low cost. Further investigation on the implementation of these technologies is suggested.

Fatal accidents related to dumping tasks are indeed occurring in a significant number, (Since 1991 -1999, 23 and 25 fatal accidents in vehicle collision and Off-highway). Differential GPS applied in this field can impact dramatically in reducing it.

This project, besides having an important impact on reducing accidents also has the potential to generate a new GPS tracking generation that very well could upgrade present GPS based systems, with better, more reliable, and cheaper systems.

REFERENCES

- Ruff, Todd M., Feb 2001, Test Results of Collision Warning Systems on Off-Highway Dump Trucks. Phase2, NIOSH. Report of Investigations 9654.
- Bennington, Ben, Johnson, David, and S lane 11 Dan 1999, "Mobile Communication System for the Construction and Mining Industry". Technical Report, Information Networking Institute, Carnegie Mellon
- Richard B. Thompson, 1998, Global Positioning System (GPS) The Mathematics of Satellite Navigation, available on the web MathCAD library, <http://www.mathsoft.com/appsmdex.html>.
- Dagdalen K., Alex Calderon A, May 2000, Geotechnical Investigation of Waste Dumps, Internal Report Mining Eng. Dept Colorado School of Mines.
- Jonathan M. Stone, Edward A. LeMaster, Prof. J. David Powell, 1999, GPS Pseudolite Transceivers -and their Applications. Internal Paper, Department of Aeronautics, Stanford University
- Trimble Navigation Limited, 1999, web presentation, All about GPS and Differential GPS <http://www.trimble.com/>
- Gilbert Strang, June 1997, The Mathematics of GPS, SIAM News, Volume 30, Number 5, available on the web, <http://www-math.mit.edu/~gs>
- Federal Radio navigation Plan, February 2000, U.S. Department of Transportation and Department of Defense Available on line from United States Coast Guard Navigation Center, <http://www.navcen.uscg.mil>
- Global Positioning System Standard Positioning Service Specification, 2nd Edition, June2, 1995. Available on line from United States Coast Guard Navigation Center, <http://www.navcen.uscg.mil>
- NAVSTAR GPS User Equipment Introduction. 1996 Available on line from United States Coast Guard Navigation Center, <http://www.navcen.uscg.mil/>
- MSHA, Department of Labor, Internet, Mine Safety and Health Administration, Fatality Information-Fatal Grams. <http://www.msha.gov/sitemdex/sitem.htm>
- Andrea L. Ames, Daved R. Nadeau and John L. Morelnad, 1997, VRML 2.0 Sourcebook Sand Diego Supercomputer Center
- Evangelos Petoutsos, 1998, Mastering Visual Basic 6 SYBEX Inc, Alameda, CA. number of 1285 pages.
- Anon, 1998, Trimble Users Conference Proceedings, CD Rom, available from Trimble, Inc. San Jose, CA

Predicting Horizontal Movement for a Tunnel by Empirical and FE Methods

M.Karakuş

Department of Mining Engineering, Inonu University, Malatya, Turkey

ABSTRACT: There are a number of benefits in constructing transport tunnels in highly populated areas for relieving traffic congestion and increasing the speed of travel for commuters. Instead of constructing a single tunnel, multiple tunnels constructed side by side offer more benefits. However, to avoid any adverse effects of tunnels on one another, more attention should be given to estimation of horizontal movement, which will ease not only support design, but also help to determine critical regions around a tunnel. Thus, a number of Finite Element Methods (FEM) as well as empirical analyses were conducted in this research to estimate horizontal movement profiles for a tunnel. The results of both analyses were compared with field measurements as well as each other. The comparison showed that the empirical models could be used to estimate the far-field settlement profiles, but that they could not be used for the near-field ground response to tunnelling. However, finite element analyses were in very good agreement with not only far-field but also near-field ground response tunnelling.

1 INTRODUCTION

The tunnelling process is very complex and requires a robust design to ensure its own stability as well as the stability of other structures which are in interaction. In urban areas, tunnels have a greater potential for disruption due to their impact on surface structures when induced settlements exceed the tolerable limits for these structures.

To evaluate ground response to tunnelling without using large-scale trial tunnels, FEM and empirical models are widely used when designing a tunnel. However, it is a matter of selecting the best analysis method to estimate the horizontal movement more accurately around a tunnel. Thus, this work aimed to appraise and compare predictions of FEM and empirical models for horizontal displacement profiles of a tunnel.

A number of FE analyses and recently developed empirical models were applied and a comparison was made for a tunnel which was constructed in London clay in 1992. This tunnel is of particular importance due to its being the first New Austrian Tunnelling Method (NATM) in London Clay. Thus, the field measurements recorded during the construction of the Heathrow Express trial tunnel in London clay were extensively used throughout the research for comparison with the predictions.*

In order to reflect the non-linear elasto-plastic stress-strain behaviour of London Clay in the FEM analysis, the Modified Cam-clay soil model with non-linear porous elasticity was used for London Clay. The Drucker-Prager plasticity model was adopted for Thames Gravel and made ground because the model considers the effects of the intermediate principal stresses on the failure mechanism in the FEM analysis. The Hypometical Modulus of Elasticity (HME) soft lining approach was employed to consider the 3-D tunnelling problem as well as deformations prior to lining installation for finite elements.

2 FINITE ELEMENT ANALYSIS

2.1 Heathrow express trial tunnel

The Heathrow Express trial tunnel excavation was undertaken as part of the Heathrow Express Rail Link, which provides a 15-minute high-speed rail service between Paddington railway station in central London and Heathrow Airport. The main concern of the trial was to investigate the ability of NATM to control and limit settlement in London Clay. Thus, in order to establish the feasibility of NATM in London Clay, three different types of

excavation and support sequences were investigated with this trial tunnel.

The trial tunnel contract consisted of a 10.65m internal diameter x 25m-deep access shaft and 100m of 8.66m-diameter running tunnel. Excavation of the trial tunnel started with Type 1 (TS1), a double side drift sequence, which was followed by Type 2 (TS2), a single side drift sequence, and Type 3 (TS3), crown, bench, and invert face excavation (Figure 1). The trial work on the site was started in February 1992 and completed by June 1992. To ensure the stability of the surface structures and the existing tunnels at the site, the multiple excavation sequences were devised to reduce ground movements and settlement. Thus, this work provided a work process that reduced the ground movements. Moreover, the project aimed to provide information, as well as observation of the ground movements, to tunnel designers about the behaviour of London Clay when excavated. Each trial section progressed for at least 30m in order to obtain adequate and meaningful data over each section.

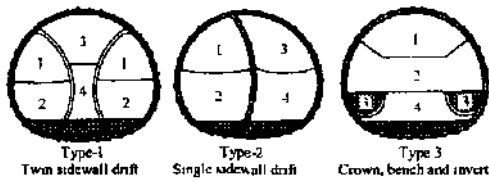


Figure 1. Heathrow Express Trial tunnels.

After completion of the three different types of excavation sequences, the data analysis proved that the maximum settlement occurring over the tunnel centre line for TS1, TS2 and TS3 were 27.9mm, 26.8mm, and 40.3mm respectively (TRL, 1992). Thus, only TS2 was included in this analysis as the final settlement was minimum.

2.2 Method of analysis

The finite element analyses were conducted by using the ABAQUS finite element program developed by Hibbit, Karlson & Sorensan, Inc. (1997). Conventional plane strain analysis was used in the analysis stage. In this case, the outer boundaries are located far away from the tunnel so that they are not influenced by the tunnel. The model geometry used in this work was 130m width and 50m height. The selected tunnel size was approximately 7.9m high x 9.2m wide. The model was fixed in the horizontal direction at each side, and the bottom part of the boundary was pinned so that neither vertical nor horizontal movements were permitted. The top surface of the model was free in both directions. Figure 2 illustrates the 2D-model geometry. Eight-node biquadratic reduced integration plane strain elements, CPE8R, were used for the continuum body and three-node quadratic curved beam elements, B22, were used for the lining throughout the two-dimensional analysis. The advantage of using the reduced integrated continuum element was a reduction in CPU time, leading to less cost for complex analyses, especially for three-dimensional cases.

The HME soft lining approach was used to consider the 3-D face effects and deformation occurring prior to lining installation. This technique was applied to the Heathrow Express tunnel design at Terminal 4 by Powell et al. (1997). This method was chosen due to its flexibility for multi-stage excavation simulation. The approach considers a lower elasticity modulus for the lining when the lining is in place just after the excavation stage. Thus, there will be deformation occurring due to lower elasticity modulus of the lining (HME). Then, the HME value is increased to the assumed short-term elasticity modulus of the lining. As a result, the use of this approach in a numerical analysis can control deformations and settlements due to tunnel excavation.

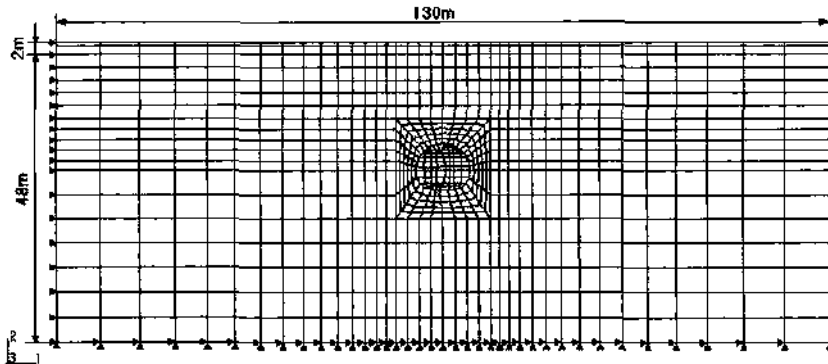


Figure 2. Finite element mesh and boundary conditions.

Tunnel excavation was carried out in nine steps in the analysis. The initial condition for each step in ABAQUS is the history of the analysis at the end of the previous step. Therefore, complex loading conditions, such as sequential tunnel excavations, can be conveniently analysed. Primary stress conditions in the ground representing a stage prior to excavation are a function of overburden, i.e., a function of the earth pressure at rest, and any additional surcharge because of the existing car park over the tunnel. Thus, all the analyses were covered in a preliminary run in the first step. However, deformations in this step are ignored since they are not related to tunnelling.

No interface was introduced between the lining and the ground because shotcrete is believed to provide perfect interlock between the ground and itself. In other words, slippage cases were ignored. However, this could be of crucial importance when concrete support is introduced, as in the case of shield tunnelling, or if a shotcrete-concrete interaction case is subjected to analysis. The detailed analysis procedures employed during this sequential excavation model (SEM) are as follows:

Step 1: The initial stress state was introduced to reach equilibrium before tunnel excavations begin. The beam elements representing the lining were deactivated, as there was no lining at the beginning of the analysis.

Step 2: The left sidewall top heading was excavated. Meanwhile, the lining elements for the top heading with lower elasticity modulus were activated. A 0.40GPa HME value was used for the lining, which was found from back analysis to obtain the required volume loss

Step 3: The stiffness of the beam element for the left top heading, i.e., the HME value, was increased

to 5GPa, which is the assumed short-term elasticity modulus of the lining.

Step 4: The continuum elements in the left sidewall bench and invert were removed and the beam elements with a 0.40GPa HME value for the bench and invert were activated.

Step 5: The HME value of the lining on the left bench and invert periphery was increased to 5GPa.

For the right sidewall excavation, the same procedure was applied as in steps 2,3,4 and finally in step 9 the value of HME was increased to 5GPa for beam elements on the right bench and invert periphery. At the same time, beam elements representing the central inner lining were removed and the simulation was completed.

2.3 Material properties at the site and constitutive law adopted for the model

The properties of the soils used in this analysis were obtained from Atzl & Mayr (1994), and Powell et al. (1997); they are given in Table 1. The materials encountered at the site consisted of London Clay at a depth of 4.2m overlaid by coarse gravel, with 0.3m of cement stabilised material and above this a bituminous car park, brick earth (Ryley & Carder, 1995). Beneath the London Clay are the clays and sands of the Woolwich and Reading Beds and the sands of Thanet Beds, which were reported by Bishop et al. (1965) with the sinking of the Ashford Common shaft four kilometres to the south of the trial site. London Clay is clearly dominant at the site and the construction of the trial tunnel was for the most part carried out approximately 16.8 m below the surface.

Table 1 Material properties at the site (Atzl & Mayr, 1994, Powell et al. 1997).

Parameter, Unit and Symbols	Value		
	London Clay	Made Ground	Terrace Gravel
Total unit weight (kN/m^3) (γ)	20	19	20
Log plastic bulk modulus (λ)	0.085	-	-
Log elastic bulk modulus (κ)	0.0085	-	-
Cohesion, (kN/m^2) (c)	0	0	0
Drucker-Prager outer circle (d) $d = 6c \sin \phi / (3 - \sin \phi)$	0	0	0
Effective friction angle (degrees) (ϕ)	-	35°	35°
Drucker-Prager outer circle $\tan \beta = 6 \sin \phi / (3 - \sin \phi)$ (degrees) (β)	-	54.8°	54.8°
Young's modulus (GPa) (E)	-	0.010	0.050
Poisson's ratio (ν)	0.15	0.3	0.3
Earth pressure at rest (K_0)	1.15	0.43	0.43
Moisture content, % (w)	30	-	-
Stress ratio at critical state $M = 6 \sin \phi / (3 - \sin \phi)$	0.9	-	-
Specific gravity of grains (G_s)	2.75	-	-
Parameter defining the size of the yield surface on the wet side of critical state (β)	1.0	-	-
Ratio of flow stress in triaxial tension to flow stress in triaxial compression (K)	1.0	-	-

Pore water pressure was not incorporated within the analyses. However, the undrained material properties of London Clay were adopted in order to conduct total stress analysis. The made ground, 0.5m thick, and Thames gravel, 1.5m thick, were modelled using the drained material properties with the linear elastic perfectly plastic Drucker-Prager failure criteria (Table 1).

As a constitutive model for London Clay, a non-linear porous elasticity model was adopted in which the pressure stress varies as an exponential function of volumetric strain with the Modified Cam-clay plasticity model (Roscoe & Burland, 1968). Anisotropy was disregarded in the analyses conducted.

For the shotcrete used as lining, a typical elasticity model was used in the FEM. The properties of the shotcrete adopted for the model are given in Table 2.

Table 2 Shotcrete properties used in the analysis (TRL, 1992)

Parameters for lining	Lining	
	Outer	Inner wall lining
Thickness, mm	250	150
Poisson's ratio	0.17	0.17
Unit Weight, kN/m ³	25	25
Elasticity Modulus, GPa	5	5

3 EMPIRICAL MODELS

As an alternative method, empirical models based on stochastic distribution analysis are widely used for surface and subsurface settlement analysis. These models assume that a constant volume of ground deformation occurs due to the loss of ground (Bowers, 1997). Attewell (1978), New & O'Reilly (1978), O'Reilly & New (1982) and O'Reilly (1988) developed empirical models to predict the far-field (one tunnel diameter beyond the tunnel periphery) settlement profiles induced by tunnelling. These models provide settlement patterns not only in the transverse direction to the tunnel axis but also in the longitudinal direction. It has been reported that the normal Gaussian distribution curve provides a good approximation to the shape of the ground settlement above a tunnel (Peck, 1969). Therefore, the settlement, S , at a point of transverse distance, y , from the tunnel centreline is given by the following expression:

$$S = S_{\max} \exp(-y^2 / 2i^2) \quad (1)$$

where S_{\max} is the maximum settlement at the tunnel centreline, and i is the standard deviation of the

curve. The value i defines the trough width and corresponds to the value of y at the point of inflexion of the settlement curve as shown in Figure 3.

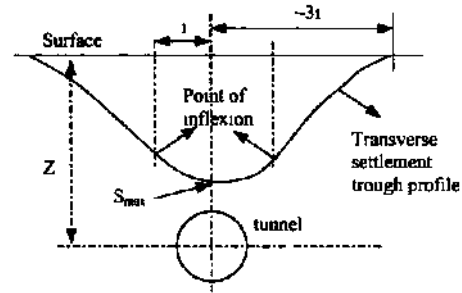


Figure 3. Tunnel settlement trough

The total half width of the settlement trough is given by approximately $2.5i$. O'Reilly & New (1982) proposed a linear relationship for the trough width parameter, i , as follows:

$$\text{(For cohesive soils)} \quad i = 0.43Z + 1.1 \quad (2)$$

$$\text{(For granular soils)} \quad i = 0.28Z - 0.12 \quad (3)$$

where Z is the depth. For most practical purposes, the value of i is simplified to the following form:

$$i = KZ \quad (4)$$

where $K = 0.5$ for cohesive soils and 0.25 for granular soils. For stiff clays and soft-silty clays, this value varies from 0.4 to 0.7 respectively.

The settlement induced by tunnelling is often considered by the term "ground loss or volume loss" and is expressed as a percentage of the notional excavated volume of the tunnel (Mair et al., 1993). When equation 4 is integrated, the volume of the settlement trough per meter of tunnel length, V_s , is calculated as follows:

$$V_s = \sqrt{2\pi} i S_{\max} \cong 2.5i S_{\max} \quad (5)$$

Then the generalised settlement can be given as:

$$S = \frac{V_s}{\sqrt{2\pi} KZ} \exp(-y^2 / 2(KZ)^2) \quad (6)$$

The displacement in the horizontal direction, $H_{(y)}$ can also be derived by using the relationship given below.

$$H_{(y,z)} = \frac{y}{z} S_{(r,z)} \quad (7)$$

Substituting Equation 6 into Equation 7, the following relationship is derived to calculate horizontal displacements around the tunnel:

$$H_{(y,z)} = \frac{V_s y}{\sqrt{2\pi} K z^2} \exp(-y^2 / 2(Kz)^2) \quad (8)$$

The method above, which was developed by O'Reilly & New (1982), is known as the *point sink radial-flow* model. The method assumes that the displacement flow is directed towards a "sink", which is located at a point below the axis level of the tunnel.

The response of the ground to tunnelling is evaluated in two zones. The first is the far-field response to tunnelling, which is at least one tunnel diameter beyond the tunnel periphery. The second is the near-field response to tunnelling, which is within one tunnel diameter. The tunnel diameter in some cases is so large that the near-field environmental impacts cannot be ignored. The point-sink radial-flow model can model the far-field tunnelling response efficiently. However, New & Bowers (1994) concluded that the point-sink radial-flow model fails to predict the pattern of movement in the near field. Thus, they proposed the *"ribbon-sin"* model, whose predictions are much better than the point-sink model for near-field movements. However, Bowers (1997) concluded that as a relatively simple method to calculate volume loss in the near field, this model has a major disadvantage, in that there is no clear relationship between the sink shape and the tunnel geometry.

As a recent alternative approach to the prediction of near-field settlement, Mair et al. (3993) proposed the "variable-K point-sink model". This model is a modification of the point-sink model and considers the value of the trough width parameter, K , which varies with depth. They proposed the following relationship for K

$$K = \frac{0.175 + 0.325(1 - z/z_0)}{1 - z/z_0} \quad (9)$$

Where z is the depth of the point considered and z_0 is the depth of the tunnel axis below the ground surface. Incorporating Equation 9 into Eqs. 6 and 8, displacement in both the vertical and the horizontal directions are calculated. The relationship given above, however, is dependent on the ground conditions and it can vary within a wide range. This is the major drawback of this model.

New & Bowers (1994) proposed circle-sink and disk-sink models to analyse the near-field tunnelling response as accurately as possible and provide recognisable parameters to understand the near-field ground response. They, however, concluded that both the ribbon-sink and the variable-K models provide very good fits to field measurements, circle-sink and disk-sink models produce greater settlement curvature in the near field, which results in greater horizontal strains and angular distortion than with the other models. Thus, only the point-sink radial-flow and variable-K models were used to predict horizontal movement using Eq. 8 in this research.

4 EVALUATION OF EMPIRICAL AND FE ANALYSIS RESULTS

As stated earlier, the measurements recorded during the Heathrow Express trial tunnel, type-2, single-wall excavation were used to evaluate both the empirical and FE analysis predictions. The instrumentation methodology which was used for the trial work is given in Figure 4. In-tunnel and surface settlement evaluations were omitted as they are beyond the scope of this paper.

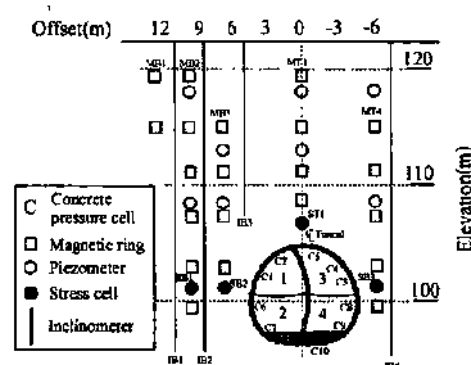


Figure 4. Subsurface and in-tunnel instrumentation around tunnel type 2.

Figures 5-8 show the comparative horizontal movements in the transverse direction to the tunnel predicted by the stochastic models and the sequential excavation finite element model. The range in the predictions by the point-sink model and the variable-K model are not in very good agreement with the field measurements. Even the trend of the movement did not show a close relationship to the field measurements. Both of the empirical models failed to predict the horizontal displacements accurately. However, the predictions of these models for the

surface settlements are very close to the measurements, as discussed in detail elsewhere by Karakuş (2000). Therefore, these models need to be subjected to further investigation. The relationship between surface settlement and horizontal movement given in Eqs. 6 and 8 could be related to different parameters such as tunnel size, excavation pattern and support elements.

On the other hand, the finite element predictions for the horizontal movements are in close agreement with the field measurements. The pattern of the movements also matches the measurements well. Thus, the empirical models examined in this research were found to be inappropriate for horizontal movement analysis of a tunnel.

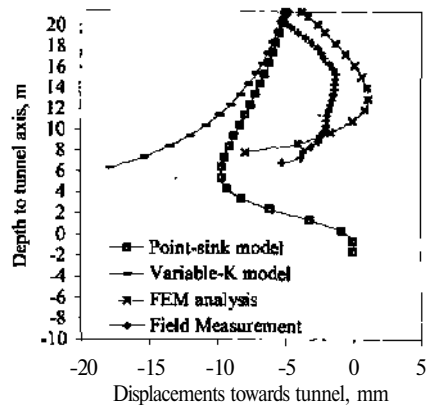


Figure 7. Horizontal movements 4.35m from tunnel centreline.

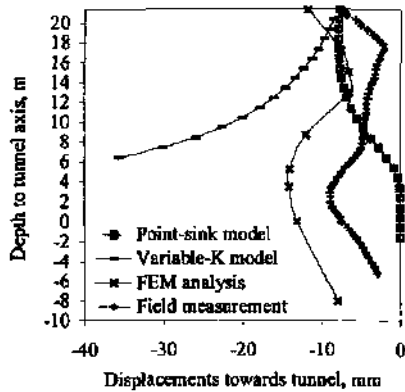


Figure 5. Horizontal movements 9.63m from tunnel centreline.

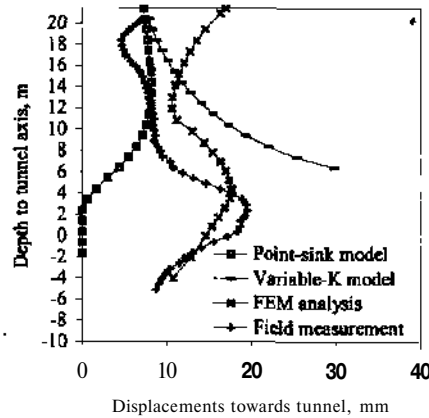


Figure 8. Horizontal movements -7.69m from tunnel centreline.

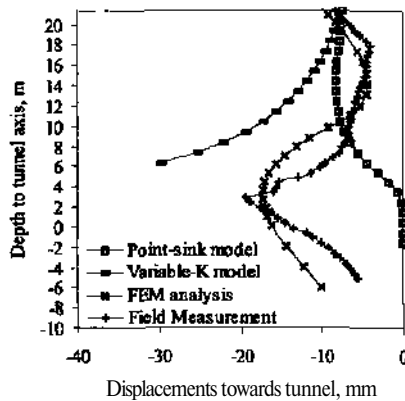


Figure 6. Horizontal movements 7.28m from tunnel centreline.

5 CONCLUSIONS

From this research, the following major conclusions can be made:

1. The finite element analyses, when compared with the stochastic models, produced much better results for horizontal movement transverse to the tunnel axis. Moreover, patterns for both horizontal and vertical movements predicted by FEM analysis are in good agreement with the field measurements. Therefore, FEM analysis incorporated with an appropriate constitutive law which will reflect material behaviour as closely as possible can be used for horizontal movement analysis.

2. Use of the Modified Cam-clay model incorporated with the Hypothetical Modulus of

Elasticity (HME) approach produced very good predictions in the FEM analysis. Thus, this methodology can be used for any ground like London Clay to investigate ground response to tunnelling.

3. The analysis of the empirical models showed that these models could be used to estimate the far-field settlement profiles, but they could not be used for the near-field ground response to tunnelling. Thus, it is considered that these models cannot be used for assessment of building damage in the near-field zone.

4. Considering that the empirical models are mainly based on past experience, these models are conservative for ground that has not undergone a tunnelling process.

ACKNOWLEDGEMENT

The author would like to express his gratitude to Dr. RJ Fowell reader in the Mining and Mineral Engineering Department at Leeds University, UK, for his valuable comments on the research.

REFERENCES

- Attewell, P. 1978. Ground movements caused by tunnelling in soil, *Proc. Conf. Large Ground Movements and Structures*, Cardiff, Pentech Press, pp. 812-948.
- Atzl, G.V. & Mayr, J.K. 1994. FEM-analysis of Heathrow NATM trial tunnel, *Numerical Methods in Geotechnical Engineering*. Balkema Rotterdam, pp. 195-201.
- Bishop, A.W., Webb, D.L. & Lewin, P.I. 1965. Undisturbed samples of London Clay from the Ashford Common shaft: strength-effective stress relationships, *Geotechnique*, Vol. 15, pp. 1-31.
- Bowers, K.H. 1997. An Appraisal of the New Austrian Tunnelling Method in Soil and Weak Rock, PhD Thesis, The University of Leeds, 254p.
- Hibbitt, Karlson & Sorensen Inc. 1997. ABAQUS Standard User's Manual, Version 5.7, Vol. 1., Rhode Island.
- Karakuş, M. (2000). Numerical Modelling for NATM in Soft Ground. PhD Thesis, The University of Leeds, 235p.
- Mair, R.J., Taylor, R.N. & Bracegirdle, A. 1993. Subsurface settlement profiles above tunnels in clays, *Geotechnique*, Vol. 43, No. 2, pp.315-320.
- New, B.M. & Bowers, K.H. 1994. Ground movement model validation at the Heathrow Express trial tunnel, *Tunnelling'94*, IMM, London, pp.301-329.
- New, B.M. & O'Reilly, M.P. 1978. Tunnelling induced ground movements; predicting their magnitude and effects, *Proc. Conf. Large Ground Movements and Structures*, Cardiff, Pentech Press, pp. 671-693.
- O'Reilly, M.P. & New, B.M. 1982. Settlements above tunnels in the United Kingdom - their magnitude and prediction. *Tunnelling'82*, IMM, London, pp. 173-181.
- O'Reilly, M.P. 1988. Evaluating and predicting ground settlements caused by tunnelling in London Clay, *Tunnelling'88*, IMM, London, pp. 231-241.
- Peck, R.B. 1969. Deep excavations and tunnelling in soft ground, *Proc. 7th International Conference on Soil Mechanics and Foundation Engineering*, Mexico, pp. 225-290.
- Powell, D.B., Sigl, O. & Beveridge, J.P. 1997. Heathrow-Ex press-design and performance of platform tunnels at Terminal 4. *Tunnelling '97*, IMM, London, pp. 565-593.
- Roscoe, K.H. and Burland, J.B. 1968. On the generalised stress-strain behaviour of 'wet' clay. *Engineering Plasticity Conference held in Cambridge*, pp. 535-607.
- Ryley, M.D. & Carder, D.R. 1995. The performance of push-in spade cells installed in stiff clay, *Geotechnique*, Vol. 45, No. 3, pp. 533-539.
- TRL Factual Report 1992. Heathrow Express Trial Tunnel: Surface-installed instrumentation and measurements, Technical paper GE/TP/183.

Evaluation of Slope Stability by Numerical Methods

A.Kourdey, M.Alheib & J.-P.Piguet
LAEGO - Nancy School of Mines-France

T.Korini
Polytechnical University of Tirana-Albania

ABSTRACT: Numerical methods are relatively recent compared to the analytical methods of slope stability analysis known as "limit equilibrium". Numerical techniques are used to obtain stress and strain distribution at any point of a defined grid. They are particularly useful for the analysis of slope stability when it is subject to various types of loading or when it has complex geometry. In this paper, we present a means of combining a numerical method using a finite difference code and circular failure analysis by the method of limit equilibrium. The state of stress is calculated by a finite difference code and then used in a program based on the limit equilibrium method for the calculation of the safety factor. We applied this new approach to a finite difference code (Itasca-FLAC^{2D}). For this purpose, we used a parameter called the global safety factor. This safety factor is defined as the average of local safety factors, which are calculated by two methods: the method known as "surface of failure locally imposed", and the method known as "surface of failure locally optimized". A computer program integrated in FLAC makes it possible to find the critical failure surface automatically, and it displays the corresponding safety factors. We applied this development to a real case.

1 INTRODUCTION

The most widely accepted methods of analyzing slope stability problems are based on limit equilibrium and experimental data. The stability of slopes has been traditionally evaluated using a variety of two-dimensional limit equilibrium methods (Merrien-Soukatchoff & Omraci, 2000):

Simplified methods: representative of this group is the Fellenius method (1936); it is the basic method of limit equilibrium.

A second group, to which Taylor's method (Taylor, 1937) belongs, satisfies all equilibrium requirements. Taylor's method is based on the assumption that the kinematical function represents a circular arc.

Generalized methods of slices: this group consists mainly of variations of the approach presented by Morgenstern and Price (1965), and Janbu (1954). In this group, the kinematical function is left unspecified. In order to provide a computation scheme that enables the determination of the critical slip surface, a variational reasoning has been applied to the generalized methods of slices (Revilla and Castillo, 1977). A similar type of analysis had been carried out earlier (Donnan, 1965; Garber, 1973). An improved variational formulation of the slope stability problem was presented by Baker and Garber (1977).

The numerical methods, on the other hand, are widely accepted for analyzing stress and displacements and are, therefore, seldom accepted for analyzing the safety problem. They require much longer times to make just one safety factor calculation. However, recent advances in the computational speed of personal computers now permit safety factor calculations with numerical models to be made routinely. Several attempts have been made in this area, such as the research of Merrien-Soukatchoff (2000), Korini (1999), Stanley (1996), Fry and Brunet (1999) and Itasca (1996).

In this paper, a new method based on both the finite difference method and the limit equilibrium analysis with the objective of better simulation and interpretation of slope failure is given.

2 GLOBAL FACTOR OF SAFETY

We define the global factor of safety as the average value of the local factors of safety:

$$FS_{\text{global}} = f(FS_{\text{local}_1}, FS_{\text{local}_2}, \dots, FS_{\text{local}_n}) \quad (1)$$

n: number of elements on the considered surface of failure;

f: function binding the local safety factors to the global factor; for example, the average in our case.

Normally, we can adopt different forms of failure surface. In this paper, we assume a circular surface.

3 APPROACHES TO CALCULATING THE LOCAL FACTOR OF SAFETY

In order to obtain the global factor of safety, we must determine the values of local safety factors for each point (element) of the slope (model). For slopes and embankments, the factor of safety is traditionally defined as the ratio of the soil's actual shear stress to the minimum shear strength required to prevent failure.

Two approaches to compute this factor of safety with a numerical method are used.

3.1 Surface of failure locally imposed

In our study, we adopt a linear failure criterion like Mohr-Coulomb. This criterion is defined by two constants: the cohesion c and the friction angle ϕ .

The state of stress for any zone can be expressed in terms of the principal stresses σ_1 and σ_3 . This stress state, in general, could be plotted as a circle on a Mohr diagram (Fig. 1). Failure occurs if this circle touches the failure envelope. Drawing the line BE, this tangents the MoV's circle at point B. The line is also parallel to the failure line (Stanley, 1996). By geometric analysis, we obtain (Fig. 1):

$$\text{From } \triangle AFD : \tan \phi = AD / FD = \tau_a / FD \Rightarrow \tau_a = FD \cdot \tan \phi$$

where τ_a is the shear stress of the considered element.

$$\begin{aligned} \text{We also have:} \\ FD = c \cdot \tan \phi + (CO - CD) \\ FD = c / \tan \phi + 0.5 \times (\sigma_1 + \sigma_3) - 0.5 \times (\sigma_1 - \sigma_3) \times \sin \theta \end{aligned}$$

Then:

$$\tau_a = [c / \tan \phi + 0.5 \times (\sigma_1 + \sigma_3) - 0.5 \times (\sigma_1 - \sigma_3) \times \sin \theta] \tan \phi \quad (1)$$

σ_1, σ_3 : principal stresses are the results of the numerical model.

$$\text{From } \triangle ABCD: \cos \theta = BD / BC = \tau_a / 0.5 \times (\sigma_1 - \sigma_3)$$

τ_a - the developed shear stress on the possible failure surface.

The value of the ratio (τ_a / τ_f) is defined as the local factor of safety of an element with a given stress state:

$$FS = \frac{\tau_a}{\tau_f} = \left\{ \frac{[c / \tan \phi + 0.5 \times (\sigma_1 + \sigma_3)]}{0.5 \times (\sigma_1 - \sigma_3) \cos \theta} - \frac{0.5 \times (\sigma_1 - \sigma_3) \times \sin \theta \tan \phi}{0.5 \times (\sigma_1 - \sigma_3) \cos \theta} \right\} \quad (2)$$

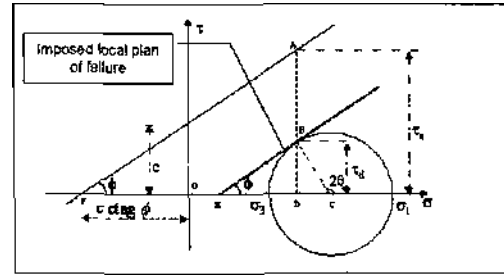


Figure 1 Stress state on Mohr's circle-imposed local plan of failure

A post-processor integrated in the FLAC code makes it possible to find the critical failure surface automatically and to display the corresponding safety factor.

3.2 Surface of failure locally optimized

Let us consider a unit element of slope with properties c, ϕ subjected to a given system of normal and shear stresses (Fig. 2). Assume that the failure surface is a straight line at slope angle θ . Based on the definition of the factor of safety, we can write:

$FS = \text{Resisting Shear Force} / \text{Driving Shear Force}$

$$FS = \frac{c \cdot l \cdot \cos \theta + \sigma_f \cdot l \cdot \cos \theta \cdot \tan \phi}{\tau_f \cdot l \cdot \cos \theta} \quad (3)$$

$$FS = \frac{c + \sigma_f \cdot \tan \phi}{\tau_f} \quad (4)$$

with:

- c = cohesion;
- ϕ = friction,
- θ = angle of failure;
- σ_1, σ_3 = principal stresses;
- FS = local safety factor.

The values of τ_f, τ_a are related to principal stresses σ_1, σ_3 ; substituting into the Equation 4, we get:

$$FS = \frac{c + \left(\frac{\sigma_1 + \sigma_3}{2} + \frac{\sigma_1 - \sigma_3}{2} \cdot \cos 2\theta \right) \cdot \tan \phi}{\frac{\sigma_1 - \sigma_3}{2} \cdot \sin 2\theta} \quad (5)$$

where σ_n , τ_f are normal and shear stresses on the failure surface (Fig. 2).

In order to obtain the minimum value of FS, 9 must yield Equation 6:

$$\frac{dFS}{d\theta} = 0 \quad (6)$$

Equation 6 is complicated and we used MATHEMATICA (Wolfram, 1999) (Fig. 3) to find the exact solution of 9 (surface of failure). The following expression was obtained:

$$\theta = 0.5 \text{ arc cot} \left[\frac{(\sigma_1 - \sigma_3) \sec \phi (2c \cos \phi + (\sigma_1 + \sigma_3) \sin \phi) \tan \phi}{2\sqrt{(c + \sigma_1 \tan \phi)(c + \sigma_3 \tan \phi)} \sqrt{(2c + (\sigma_1 + \sigma_3) \tan \phi)^2}} \right] \quad (7)$$

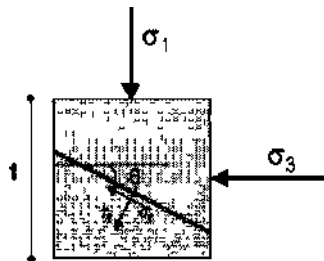


Figure 2. Stresses acting on a unit element.

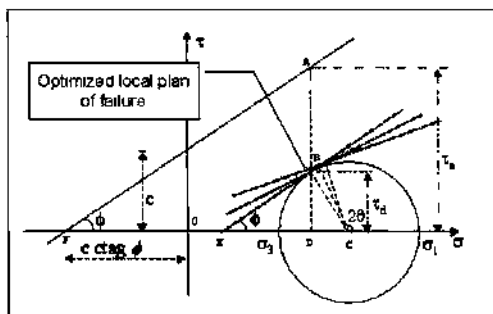


Figure 3. Stress state on Mohr's circle-optimized local plan of failure

If G from Equation 7 is substituted into Equation 5, we obtain the minimum factor of safety for a particular element corresponding to a stress tensor or point with a given stress state.

A simple program with MATHEMATICA was used to compare the results of the two approaches.

4 FLAC CODE PRESENTATION

The FLAC code, developed by ITASCA (1996), is an explicit finite difference code which simulates rock or soil structures which undergo plastic flow when their yield limit is reached. Materials are represented by two-dimensional grid elements which, in response to applied forces or constraints, follow a linear or non-linear stress/strain law. If stresses are high enough to cause the material to yield and flow, the grid elements deform and move with the material it represents. The Lagrangian calculation scheme used is well suited to modeling large distortions. In addition, the time-stepping approach to the solution of the equations of motion at each element node allows the user to examine the development of yield (or material collapse) as it develops instead of visualising the end (equilibrium) state only.

5 PROGRAM INTEGRATED IN FLAC

This program is developed with the FISH programming language (associated with FLAC), based on the "imposed failure surface" approach for slope stability analysis through a circular failure. It can be used for the determination of the safety factor using the stress state computed from the finite difference method.

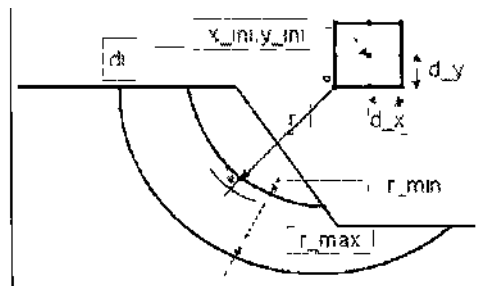


Figure 4. Input data into program integrated in FLAC

Some features of this program are:
 the input data of the stress state is determined by FLAC calculation,
 it realizes the calculation of the minimum factor of safety through a procedure of automatic calculation according to a user's defined grid (Fig-4),
 a graphic plot showing the failure surface is provided.

6 APPLICATION TO A REAL CASE

6.1 Description of the site

The example corresponds to a slope of an open pit mine in France. The site is the Antoinette pit located south of the square of Mercoirol under the old Departmental Path 906. The exploitation of this pit started in May 1992 and stopped in 1993. Its surface is 26 hectares with a maximum depth of 90m. It has a rectangular form, being approximately 400m in length and 300m in width. After the end of mining, the water level was established at the bottom of the pit with the same dimensions (Hadadou & Alheib, 1999).



Figure 5 Antoinette Pit

6.2 FLAC Model and stability analysis

We obtained a representative open pit cut, in a direction perpendicular to the slope. It is representative of the pit. This cut is considered geometrically the most unfavorable. The average slope angle is close to 50° . The slope is composed of hard stratified rock beds.

A 110x66 grid was used as shown in Figures 6 and 7. No horizontal displacement was allowed on the vertical boundaries, while the bottom boundary was completely fixed in both vertical and horizontal directions. A Mohr-Coulomb constitutive model was assigned as described to all zones with the following properties (Table 1):

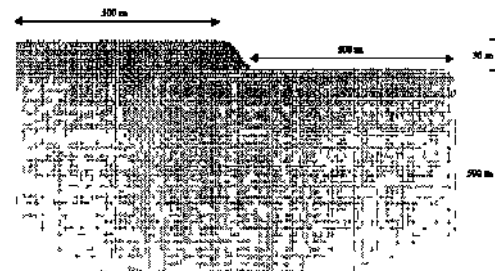


Figure 6 FLAC zone geometry

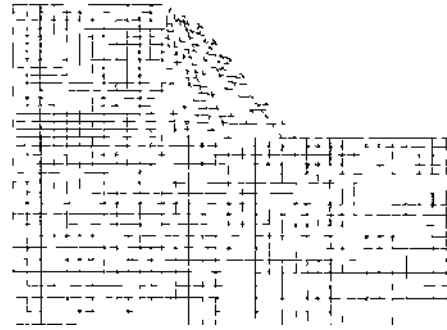


Figure 7. Finite difference mesh for the slope analyzed

Table 1. Material properties

Property	Value
density (kN/m ³)	27
friction angle (°)	35
cohesion (kPa)	100

Our objective was to study the long-term behavior of the slope.

6.3 Results and discussion

Below are the results of the calculation of the local and global safety factors; the failure mechanism for the pit is illustrated in Figure 8, which also shows the circle of failure corresponding to a factor of safety equal to 1.33 (Tables 2 and 3).

The contour lines of the local factors of safety are illustrated in Figure 9, which shows that a localized area of weak zones is developed within the model.

This same example was solved with the limit equilibrium method in order to compare the results obtained with the solution of Bishop (Hunger, 1988).

Table 2. Results of FLAC code

FS - global	1.33
x-coordinate of the center of the circle	574 m
y-coordinate of the center of the circle	570 m
diameter of the circle	75 m

Table 3. Minimal and maximal values of the local factor of safety

FS - local minimum	1.005
FS - local maximum	5.490

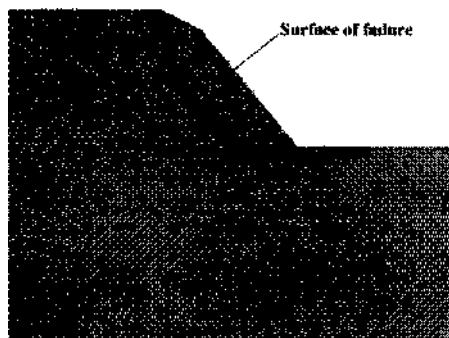


Figure 8. Sliding surface giving the minimum factor of safety.

the choice of element size and shape are significant parameters in the simulation.

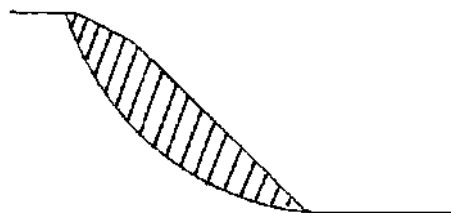


Figure 10 Circle of failure by Bishop method (CLARA program)

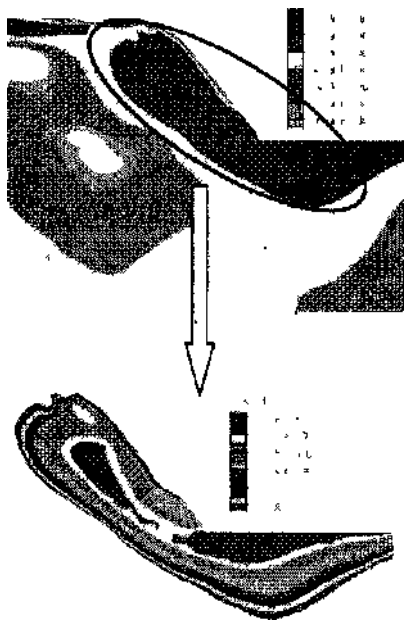


Figure9. Isocontours of the local factor of safety (ex_3 _local FS)

Figure 10 below illustrates the circle of failure corresponding to the minimum factor of safety, which is equal to 1.5.

In both cases, the analysis of the stability of the pit in the long term shows that the slope does not present a major problem of instability. The safety factors obtained are largely higher than 1. On the other hand, the difference in global FS (=11%) values may be explained by the nature of the two approaches: the Bishop simplified method tends to be conservative because it neglects internal strength.

It is more reliable to use a numerical method than sliced segments, and accurate stress results were achieved. The boundary condition assumptions and

7 CONCLUSIONS

Limit equilibrium is the basis for most of the stability analysis procedures used in geotechnical engineering. For more complicated problems, it is appropriate to perform limit equilibrium analysis using a numerical method. The development has a number of advantages over slope stability analysis:

- more complex phenomena can be modeled (effect of water, dynamic, discontinuity, etc.);
- capacity to introduce constitutive models;
- factor of safety is not constant along the slip surface;
- the factor of safety of a slope can be computed with FLAC by reducing the soil shear strength in stages until the slope fails, but this does not show a well-defined surface of failure. The program developed can display two-dimensional plots of die sliding plans, Isozones of local factors of safety, in addition to calculating the global factor of safety.

In the future, progress is expected in improving the method of examining failure surfaces without assuming a failure mode in advance.

REFERENCES

- Baker R & Garber M 1978 Theoretical analysis of stability of slopes, *Géotechnique* 28, No.4. pp 395-411
- Fry J J & Brunei C. 1999 Comparison of classical and elastoplastic methods for the evaluation of safety factor against failure of an embankment dam. *Document', de EOF. Centre National d'Équipement Hydraulique*, pp 1-13
- Hadadou R & Alheib M 1999 Rehabilitation de la Découverte de Mercoirrol "Analyse de la stabilité des talus", *Rapports définitifs. Laboratoire Cêotechnique-Dêpaiement Sol - Sous-sol - Ecosi-stême.s*, pp 1-16
- Hunger O Geotechnical Research Inc 1988 Slope Stability Analysis in Two or Three Dimensions for IBM Compatible Microcomputers, CLARA's Documents.
- ITASCA Consulting Group, Inc 1996 Documents du code FLAC^{3D} V 3.4
- Konni T 1999 Slope stability analysis using FESSTA, *International Symposium on Mine planning and Equipment Selection*, June 15-18 1999, Dnepropetrovsk, Ukraine, pp 239-245

- Memmen-Soukatchoff V & Omracı K 2000 Determination des conditions aux limites pour un calcul de stabilité de talus, *Rev Franc Geoteck*, No 92
- Stanley Z H 1996 Analyzing of two-dimensional slope and foundation problems considering soil-structure interaction effect, *ASCE Congress for Computing in Civil Engineering*, Anaheim, June 20, pp 832-837
- Wolfram S 1999 MATHEMATICA V04, Edition 4em, *WOLFRAM Research*

A Mathematical Model of Simple Flotation Circuits

L.Samoila, S.Arad & M.Marcu
 Petrosani University. Petrosani, Romania

ABSTRACT: This paper presents our results concerning the elaboration of a mathematical model of simple flotation circuits based on material balance equations. We identified the general form of the concentrate and waste quantities as well as the content expressions in different points of the circuits. We elaborated the general program, which makes it possible to calculate any simple flotation circuit. Using this program, comparative studies of different configurations can be made in a very short time and the optimum configuration may be chosen.

1 INTRODUCTION

In order to calculate a flotation technological scheme, we should know beforehand the following elements:

- The quantities of material in the feeding, output products and all intermediate points,
- Useful mineral contents in all of the formerly mentioned products,
- Water quantities, that is dilution, for each product.

It becomes necessary to calculate technological schemes in the following situations:

- To design an installation or a new section in an installation;
- To know the product characteristics all along a technological line for a certain functioning regime.

From time to time, we must know the characteristics of an installation in order to be able to modify or to correct the existing technological scheme without supplementary investments and in order to improve the technical and economical indexes. This may be needed when the raw material quality has been changed or the customers' requirements are different.

2 SIMPLE FLOTATION CIRCUITS MODEL

Using the balance equations [1] written for different types of monometallic mineral simple flotation circuits, we tried to evaluate the useful metal quantities and contents at each point of the circuit.

We expressed these parameters only depending on extractions in weight for each operation (v^* , v_c),

total extraction in weight (v), feed quantity (A) and contents in: feed (a), concentrate (c), floated products of each enriching operation (d^*) and cleaning operation (g).

From our point of view, a flotation circuit can be represented as in Figure 1, where:

- k - enriching operations number;
- j - cleaning operations number;
- (X_k) - vector of enriching operation parameters;
- (y_j) - vector of cleaning operation parameters.

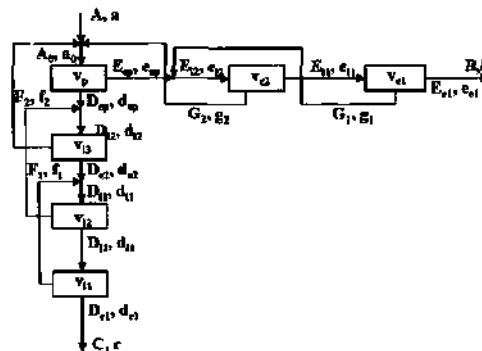


Figure 1. A floabon circuit

Analysing the calculation results, we observed the existence of some general relations. This was possible by noting the input and the output parameters in each block representing a flotation operation as in Figure 2.

The indexes are:
 - "i" means "input";
 - "e" means output.

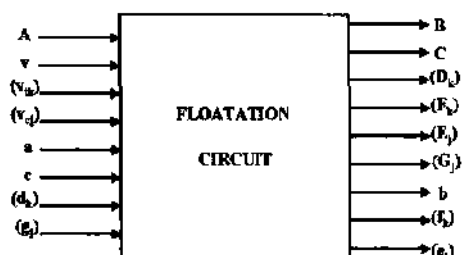


Figure 2 Input and output parameters in a flotation operation.

It must be said that the operations were numbered from the circuit end to the beginning, in order to express the relations in a simpler form.

The relation between the output and the input material quantity for an enriching block is:

$$D_k = \frac{100 D_{tk}}{v_k} \quad (1)$$

The recirculated quantity in the enriching circuit is:

$$F_k = D_k - D_{ek} \quad (2)$$

The output quantity for the primary flotation is:

$$D_{ep} = D_{t,k-1} - F_{k-2} \quad (3)$$

The output material quantities from enriching blocks 2 and 3 (if they exist) are:

$$D_{e2} = D_{t1}; \quad D_{e3} = D_{t2} - F_1 \quad (4)$$

The relation between the input quantity for a cleaning block and the output quantity for the same block, k, is:

$$E_k = \frac{100 E_{ek}}{100 - v_{ek}} \quad (5)$$

The floated material quantity in the cleaning circuit, which is recirculated, is:

$$G_k = \frac{v_{ek} E_k}{100} \quad (6)$$

If there are two cleaning operations, output 2 is equal to input 1 and the waste quantity from the primary flotation is:

$$E_{e2} = E_{t1}; \quad E_{ep} = E_{t,k-1} - G_{k-2} \quad (7)$$

The waste content and the input content in an enriching operation are:

$$f_k = \frac{D_{tk} d_k - D_{ek} d_{ek}}{F_k} \quad (8)$$

$$d_{ik} = \frac{D_{e,k+1} d_{e,k+1} + F_{k-1} f_{k-1}}{D_{ik}} \quad (9)$$

The input content for a cleaning operation is:

$$e_{ik} = \frac{E_{ek} e_{ek} + G_k g_k}{E_k} \quad (10)$$

The waste content from the primary flotation, when there are one or two cleaning operations, is:

$$e_{ep} = \frac{E_{t1} e_{t1} - G_1 g_1}{E_{ep}} \quad (11)$$

3. RESULTS

Using Turbo Pascal, we wrote a program, named SLOT, for calculating the specific values of contents and quantities all along a simple flotation circuit. It was verified for different kind of circuits, with different number of cleaning and enriching operations.

In table 1, we present the characteristics of 5 types of raw material from Rosia Poieni mining area.

Table 1 Characteristics of 5 types of raw material from Rosia Poieni mining area

Product	%Cu ₁	%Cu ₂	%Cu ₃	%Cu ₄	%Cu ₅
Concentrate	6.710	13.91	8.94	11.66	14.53
Waste	0.075	0.095	0.085	0.080	0.112
Feeding	0.310	0.310	0.309	0.370	0.330
Extraction	3.542	1556	2.769	2.504	1512

Table 2. Input parameters for 5 types of raw material from Rosia Poieni mining area

Input	Material				
	1	2~	3	4	5
A	240	240	240	240	240
v	3.542	1.556	2.769	2.504	1.512
v ₁	60	55	60	60	60
v ₂	45	45	45	45	45
v ₃	0	0	0	0	0
v _{ei}	25	25	25	25	25
v _{e2}	0	0	0	0	0
a	0.31	0.31	0.309	0.37	0.33
c	6.71	13.91	8.94	11.66	14.53
<L _i	4.7	10.2	6.5	8.7	10.5
d*	0	0	0	0	0
d*	2.8	4.5	4.2	4.5	5.1
g _l	0.5	0.6	0.5	0.5	0.9
&	0	0	0	0	0

Table 3. Computed parameters for 5 types of raw material from Rosia Poieni mining area

Computed parameters	Material				
	1	2	3	4	5
B	231.499	236.266	233.354	233.990	236.371
C	8.501	3.734	6.646	6.010	3.629
b	0.0750	0.0950	0.0632	0.0800	0.1120
Dei	8.501	3.734	6.646	6.010	3.629
Drf	14.168	6.790	11.076	10.016	6.048
D _{ei}	25.817	12.033	20.183	18.251	11.021
Du	14.168	6.790	11.076	10.016	6.048
D _!	31.484	15.088	24.613	22.258	13.440
D_!	0.000	0.000	0.000	0.000	0.000
F _!	5.667	3.055	4.430	4.006	2.419
Fi	17.316	8.299	13.537	12.242	7.392
F _!	0.000	0.000	0.000	0.000	0.000
E.1	231.499	236.266	233.354	233.990	236.375
Ec	0.000	0.000	0.000	0.000	0.000
Et	308.666	315.021	311.139	311.987	315.162
E _!	0.000	0.000	0.000	0.000	0.000
G _!	77.166	78.755	77.785	77.997	78.790
Gi	0.000	0.000	0.000	0.000	0.000
D*	25.817	12.033	20.183	18.251	11.021
E _!	308.666	315.021	311.139	311.987	315.162
pp	0.181	0.221	0.172	0.185	0.309
d _!	4.700	10.200	6.500	8.700	10.500
du	2.599	4.736	3.955	4.457	4.984
du	0.000	0.000	0.000	0.000	0.000
fi	1.685	5.666	2.840	4.260	4.455
F _!	0.881	0.266	1.873	0.985	0.471
fj	0.000	0.000	0.000	0.000	0.000
e _!	0.181	0.221	0.172	0.185	0.309
e _!	0.000	0.000	0.000	0.000	0.000
e _!	0.075	0.095	0.063	0.080	0.112
e _!	0.000	0.000	0.000	0.000	0.000

The flotation circuit from Rosia Poieni has two enriching and one cleaning operations.

We mention that this is only one example, but the program was tested on more practical situations.

4 CONCLUSIONS

In order to use computers in flotation circuits calculation, we elaborated the mathematical model for simple circuits which made it possible to determine the relations between the material quantities and between the metal contents. We also wrote the programme to calculate any kind of circuit. As any real flotation circuit, no matter how complicated, may be decomposed in simple circuits, like the types we

studied, the calculation can be simpler and faster using this programme.

In attempting to identify the algorithm, we found some new general relations between parameters, as well as restrictive conditions in the circuit calculation. We this programme, we created new possibilities for analysing and optimising the flotation circuit configuration and operations number.

REFERENCE

- L. Samoila. *Introducerea tehnicii de calcul in conducerea procesului de flotatie a substanelor minerale utile* Doctoral thesis, Petrosal^e University, 1999.

Computer Simulation of Truck/Shovel System at Tuncbilek Coal Mine Using GPSS/H

N.Cetin, ICerarslan & A.Okuducu

Dumlupinar University, Department of Mining Engineering, Kutahya, Turkey

ABSTRACT: In this study, the material handling system at Tuncbilek surface coal mine operated by Garp Lignite Enterprise (G.L.I.) is simulated. In the district, material handling is performed as a truck/shovel operation. The simulation model is developed using a well-known simulation language, GPSS/H. The goal of the study is to determine the optimum number of trucks to have in the mine using probabilistic cycle times. The input data is collected by observation of actual system operation and analyzed by using Goodness of Fit Test with Minitab statistical software package. To find the optimum number of trucks, the developed simulation model is run by changing the number of trucks for maximum shovel productivity.

1 INTRODUCTION

Computer simulation is now an ever-increasingly used design tool by engineers in many scientific disciplines. It enables them to solve or evaluate a wide variety of technical problems rapidly and inexpensively without even actually changing the system under consideration. That is, through simulation, various operating policies which are impractical to experiment can be tested before they are implemented in reality. It has been used extensively for automotive designs, design of large factories and production lines in industrial applications. In fact, most situations in which the effect of changes in the operating system policy are to be evaluated can be considered as simulation opportunities. In its broadest sense, computer simulation is the process of designing a mathematical/logical model of a real system and conducting experiments with this model on a computer for the purpose of either understanding its behavior or evaluating various strategies for its operation (Law and Kelton, 1991).

The present paper presents the results of using the GPSS language for simulation of truck/shovel system performance at G.L.I. (Garp Lignite Enterprise) Tuncbilek Coal Mine located in western part of Turkey. The model is used for optimizing the number of trucks using probabilistic cycle times taken from an actual operating mine site.

2 DESCRIPTION OF THE MINE

Tuncbilek Lignite Reserve operated by Garp Lignite Enterprise (G.L.I.) is located at western part of Turkey and is one of the most important lignite deposits being in production since 1940*s. The property has an area of 13,477 hectares, with mineable open pit reserve of over 70 million tons and an underground mine reserve of about 265 million tons. Annual amount of waste stripping is 60 million m³ and surface mine coal production of around 9 millions tons/year. The waste stripping is done with a mixed fleet of 65-ton and 85-ton trucks and 10,17 and 20 cu-yd capacity shovels.

3 DETERMINATION OF OPTIMUM NUMBER OF TRUCKS

Simulation can readily identify the point at which the shovels are over-trucked. This involves a trade-off between truck idle time and shovel idle time. The identification of this point determines the optimum number of trucks required to maintain the operational goals of the mine.

A computer program was written in the GPSS/H language to simulate the load, haul, dump and return cycles. By changing the number of trucks on the haulage run, the optimal number of trucks to be used for maximum shovel utilization is determined.

4 INPUT DATA USED IN THE SIMULATION MODEL

For the purpose of simulating an actual truck/shovel operation, it is important to obtain data that closely describe reality. The input data are often very difficult to gather because many surface mines operate with a mixed fleet of trucks and shovels. Thus, data collection and analysis is one of the most important aspects in the implementation of any simulation model since any simulator is as good as the input data it receives (i.e.: "Garbage-In Garbage-Out") (Banks et al. 1984).

In time studies, it is very important to clearly define the duration of each element of the operation. In order to simulate the truck/shovel production system, the times required to load the truck, haul the coal, dump the coal and return to the shovel have to be known. These times were determined from actual measurements using a stopwatch. An analysis of these time study data using goodness of fit test with Minitab software package have resulted in the statistical distributions which will be used as input data into the simulation program. Goodness of Fit Tests showed that the cycle times from actual mine data collected can reasonably be well modeled by normal distributions for all load, haul and dump times (Rasche and Sturgul, 1991). The mean and standard deviations of these times were needed in the simulation model. However, GPSS/H simulation language can easily handle any statistical distributions. Table 1 shows the mean and standard deviations of these times in seconds.

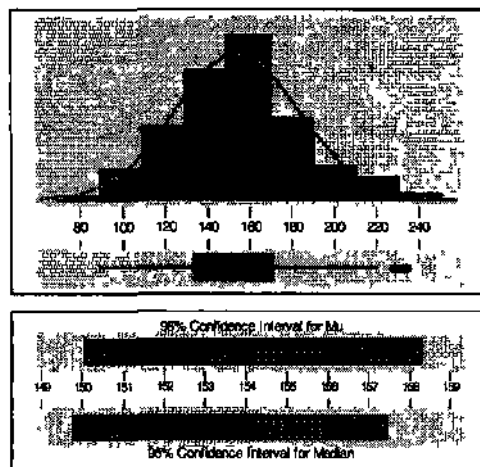
One of the primary problems when dealing with operational data obtained from time studies is that of outliers, which are defined as those points that do not belong to the same population as the bulk of observed data. There is no hard and fast rule to determine which observed values are outliers. As a rule of thumb, Tu and Hucks (1985) suggest that all data points should lie within 3.5 times standard deviations of the mean and this rule is also applied in this study.

Table 1 Time Study Data Used in Simulation Model (Seconds)

	Mean	Std. Dev.
Truck Loading Time	155	30
Truck Dumping Time	55	10
Truck Hauling Time	265	45
Truck Return Time	165	30

By running the simulation program with the number of trucks currently used on the haulage route for the mine, a comparison was made between the actual number of loads and the predicted number from the simulation model. The difference was within a few percentage points and it was felt that the simulation model would accurately represent the mine for other possible combinations of trucks and haul routes.

Descriptive Statistics



Variable, load

Andersen-Darling Nonnormality Test	
A-Square	0.555
p-value	0.150
Mean	155.177
St. Dev.	29.560
Variance	873.804
Skewness	0.265
Kurtosis	0.049
n of data	200000
Minimum	89.310
First Quartile	134.329
Median	152.633
Third Quartile	171.050
Maximum	233.446
95% Confidence Interval for Mean	
Lower	150.055
Upper	158.298
95% Confidence Interval for Sigma	
Lower	26.919
Upper	32.780
95% Confidence Interval for Median	
Lower	149.829
Upper	157.432

Figure 1 Density/Histogram Plot For Truck Loading Time

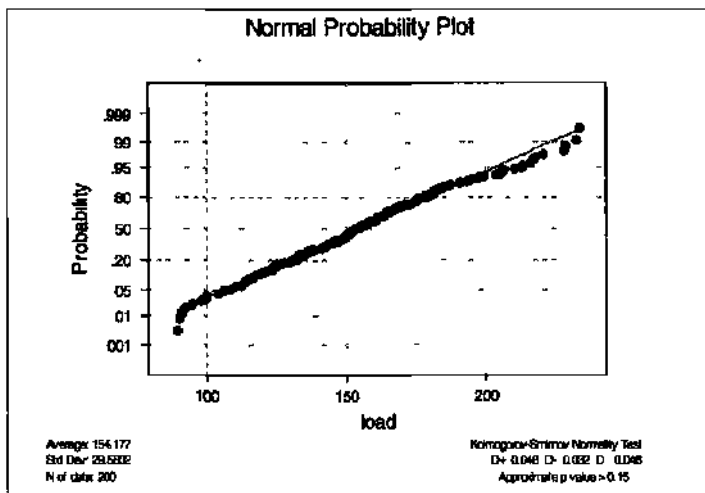


Figure 2 Normal Probability Plot For Truck Loading Time (Sec)

5 RESULTS OF SIMULATION

Table 2 summarizes the most important results and statistics of the simulation runs performed for the mine haulage. The optimal number of trucks to be used is clearly limited by the best possible utilization of the loading unit. The output from GPSS/H program supplies the engineer with all relevant statistical information and assist in forming the

correct decision as to how many trucks should be matched to the loader.

From analysis of figures 3,4 and 5, and table 2, it is seen that the best operating policy for this shovel location is to utilize a fleet of 5 trucks in regard to shovel productivity. A more objective analysis could be performed by using cost-per-ton figures obtained by dividing the total equipment costs by total tons hauled (Cross and Williamson 1969).

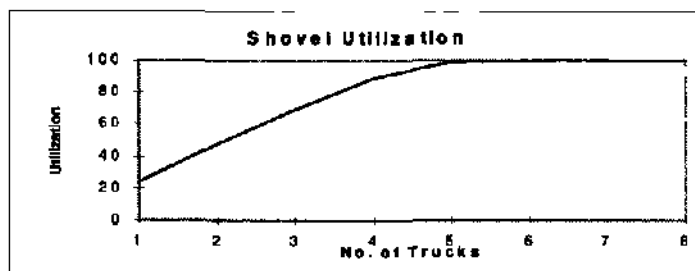


Figure 3 Shovel Utilization vs. Number of Trucks

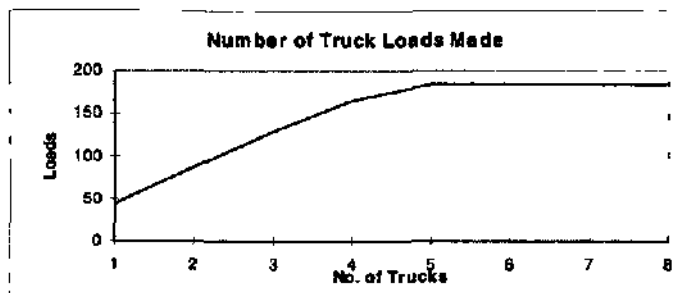


Figure 4. Truck Loads vs. Number of Trucks

Figure 4. Truck Loads vs. Number of Trucks.

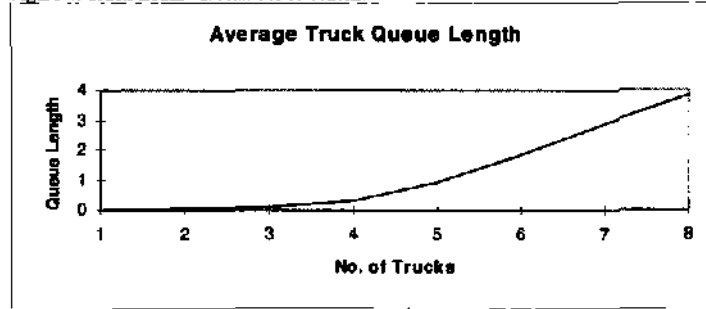


Figure 5. Average Truck Queue Length vs. Number of Trucks.

Table 2. Results of Simulations (Average of 100 Replications).

FTrucks	Shovel Utilization (%)	Truck Loads	Average Queue Length
1	24.2	44	0.00
2	47.8	88	0.03
3	69.8	130	0.10
4	89.5	166	0.29
5	99.3	184	0.90
6	100.0	185	1.86
7	100.0	185	2.86
8	100.0	185	3.86

6 CONCLUSIONS

The use of GPSS/H computer simulation language at a typical surface coal mine in Turkey was presented. It was used to evaluate the current performance of truck fleet at G.L.I. Tuncbilek coal mine. Simulations were performed to find the optimal number of trucks for the haulage routes.

REFERENCES

Banks, J., Carson, J.S. and Nelson, B.L. 1984. Discrete-Event System Simulation, Prentice Hall, Upper Saddle River, NJ, USA.

Law, A-M. and Kelton, W.D. 1991. Simulation modeling and analysis. McGraw-Hill Inc. USA.

Cross, B. and Williamson, G. 1969. Digital Simulation of an open pit truck haulage system. APCOM, Salt Lake City, USA: 384-100.

Rasche, T. and Sturgul, J.R. 1991. A simulation to assist a small mine: A case study. International Journal of Surface Mining and Reclamations : 123-128.

Tu, H. and Hucka, V. J. 1985. Analysis of open - pit truck haulage system by use of a computer model. CIM Bulletin ,78(879): 53-59.

Schriber, J. Thomas, 1991. An introduction to simulation using GPSS/ H. John Wiley & Sons., NY, USA.

Optimum Blending of Coal by Linear Programming for the Power Plant at Seyitömer Coal Mine

K.Erarslan, H.Aycul, H.Akçakoca & N.Çetin

Dumlupınar University, Department of Mining Engineering, 43100, Kütahya, Turkey

ABSTRACT: In this study, a linear programming model is developed to determine the optimum coal blend in terms of quality and quantity. Coal with various features is mined from different panels of Seyitömer Lignite Coal District and fed to a nearby power plant. The quality of the coal is extremely variable through the horizontal and vertical directions, which entails the precise planning of coal blending during the mining and stockpiling stages. Otherwise, a large penalty has to be paid to the power plant. In this study, the objective is to match the calorific values required by the power plant. The quality features and production capacities of coal from different panels are determined and are used in quality constraints. The power plant requires coal in two groups, which are of different qualities and quantities. Therefore, two linear programming models complementing each other are developed in order to determine the blending conditions that satisfy the needs of the plant. The models are introduced and solved in the LINDO package program. Reasonable solutions are obtained and optimal amounts of blending are handled. The model also allows the evaluation of coal panels of low quality.

1 INTRODUCTION

Linear Programming (LP) is one of the most widely used methods of operation research for decision problems. This method is a reasonable and reliable procedure for determining the optimum distribution of resources, optimal production, minimum cost, maximum profit, etc., which comprise the objectives (Öztürk, 1997). In this method, decision parameters to make the objective optimal are linear or assumed to be linear (Taha, 1992, Hillier and Liebermann, 1995).

The general form of the problem is formed by objective function and subjected constraints;

$$\max/\min Z = c_1X_1 + c_2X_2 + \dots + c_nX_n \quad (1)$$

Subjected to

$$\begin{aligned} a_{11}X_1 + a_{12}X_2 + \dots + a_{1n}X_n &\leq b_1 \\ a_{21}X_1 + a_{22}X_2 + \dots + a_{2n}X_n &\leq b_2 \\ \square & \quad \square & \quad \square & \quad \square \\ a_{m1}X_1 + a_{m2}X_2 + \dots + a_{mn}X_n &\leq b_m \end{aligned} \quad (2)$$

where;

Z= objective of the model

c_j = coefficient of j^{th} decision variable ($j=1,2,\dots,N$)

X_j = j^{th} decision variable

a_{ij} = i^{th} coefficient of j^{th} decision variable ($i=1,2,\dots,m$)

b_i = limited resource for i^{th} constraint

LP approximation is widely used in mining as well as in other industrial fields. Open pit limits, production scheduling, material flow in processing plants, blending, equipment selection, method selection, transportation, etc., are its main applications (Chanda and Wilke, 1992, Dijilani and Dowd, 1994, Huang, 1993, Mann and Wilke, 1992, Meyer, 1969, Smith and You, 1995). However, investment, planning, or selection, in other words any actions requiring decision, can be optimized.

Especially in open pit mines and underground mines feeding coal to power plants, the quality and quantity of coal is crucial because the burner blocks of power plants are designed according to specific features of coal. Inability to match coal quality and quantity to these specific features results in either penalty costs for the coal enterprise or a decrease in the power plant's efficiency. In addition, inconsistent coal features lead to wear in the power plant's burning units and all integrated components. In this respect, coal-producing enterprises try to match their coal features to power plants' specifications by blending and homogenizing coal extracted from different panels and levels. Satisfying the requirements of the plant is achieved by selective

mining and/or blending. In this study, a relevant case is considered. Seyitömer coal enterprise in Kütahya, Turkey has problems of quality and quantity in supplying the nearby power plant. A well-planned and organized blending procedure and, accordingly, production plan is necessary. In this paper, the problem, is modeled in terms of linear programming and reasonable solutions are obtained.

2 SEYİTÖMER COAL ENTERPRISE AND ITS PROBLEM

Seyitömer Lignite Enterprise (SLE) is located 20 km. northwest of Kütahya city center. The basin is characterized as Late Miocene-early Pliocene. The lignite seams in Seyitömer basin consist of two horizontal levels (0-7° S), referred to as A and B seams, according to their depths. The seams are separated from each other by waste interbedded formations whose thickness vary from 10 to 50 m. These two seams may exhibit variation according to their occurrence in three sub-regions (Seyitömer, Aslanlı, Ayvalı), where the geological coal formation has been determined by drill holes. The thickness of the A seam, located at the top level of the basin, varies in the range of 5-25 m. (Sofrelec, 1967). The thickness of B seam varies in the range of 2-30 m. In the basin, these two seams are rarely observed together. The seam defined as A is deposited only in the Seyitömer region and the coal occurrences in the Aslanlı and Ayvalı regions. The B seam consists of 3 different sublevels, referred to, from Üie top to the base of the seam, as B₁, B₂, B₃. Their calorific values decrease towards to the seam base as the interbedded layers get thicker. The upper level coal seams B₁ and B₂, which have a high calorific value and are produced in sorted size and quality (+100 mm), have supplied the market for public heating. The B₃ coal, which is of low quality and contains fine coal (-100 mm) from the processing plant, is sold to the power plant.

At the enterprise, production is performed by the open pit mining method. The overburden, whose thickness varies from 35 to 60 m., is loosened by drilling and blasting. The stripping method is the excavator and truck and dragline method. The electrical excavators have a 10-yd³ bucket volume and the dragline has a 70-yd³ bucket capacity. Production and transportation are also by excavator-truck and loader-truck methods. It is impossible to process the coal with wet washing techniques. For this reason, only crushing, sieving and sorting can be applied to the coals of the region. There are three plants working for the power plant and three plants working for the market in the enterprise. The coal is dispatched to the market or the power plant according to its quality.

Recently, in terms of quality and quantity the demands of the plant have not been fulfilled and in order to overcome the problem selective mining has been used. Consequently, there is an increasing tendency to use ripping and bulldozers and loaders (Aykul, 2000).

3 APPLICATION OF LINEAR PROGRAMMING IN SLE

3.1 Definition of the Problem

In Seyitömer Coal Mine, six different coal types produced from different panels and levels are treated. The terms for these coals, their average calorific values and annual quantity to be extracted according to İdeal planning are shown in Table 1. These coals need to be blended in accordance with the specifications required by the power plant's burning units.

Seyitömer power plant has four burning units. The operating conditions of these units are shown in Table 2. The annual coal requirement of the power plant is 6,000,000 tons: the first three burning units (Unit 1, Unit 2 and Unit 3), with the same requirements, need 4,500,000 tons, while the last burning unit (Unit 4) requires 1,500,000 tons.

Table 1. Determined features of coal types according to ideal planning in SLE

Coal Type	Calorific Value (kcal/kg)	Amount (ton/year)
FineCoal(-100)		
(From Plants)	1675	2,000,000
Stock of Kizik	1750	800,000
Stock of Marl	1428	> 250,000
B ₁ Level	2000	< 600,000
B ₂ Level	1800	< 600,000
B ₃ Level	1600	> 1,500,000

Table 2. Operating Conditions of Power Plant

Power Plant Units	Base Heat Content (Kcal/kg)	Grain Size (mm)
Unit 1	1750± 100	0-200
Unit2	1750+100	0-200
Unit3	1750± 100	0-200
Unit 4	1600 ± 100	0-200

The blending requirements of the coal are as follows:

- i. Coal coming from the processing plants (fine coal), and that produced from the stock of Kizik, stock of marl, the B₃ level, B₂ level and B₁ level can supply Unit 1, Unit 2 and Unit 3.
- ii. Coal produced from the stock of Kizik, stock of marl and B₃ level can supply Unit 4.

Two different linear models were developed since there are two design specifications in the power plant. Therefore, first, the amount of coal of the B3 level and stock of Kızık are determined for Unit 4 with the help of the first linear program, and then the rest of the determined amounts are used in the second linear program developed for Unit 1, Unit 2 and Unit 3.

After determining these conditions, the main aim is to obtain coal blends that have the maximum heating calorific value in the range of specifications (Kaya, 2000).

3.2 Constitution of the Model

The objective function for Unit 4 maximizing the first blend's calorific value, which has a maximum limitation by the constraints, is shown in Equation 1:

$$\text{Max } Z = \frac{1750 \cdot X_2 + 1428 \cdot X_3 + 1600 \cdot X_6}{1,500,000} \quad (3)$$

Subjected to Equations 4 to 11:

$$X_2 + X_3 + X_6 = 1,500,000 \quad (4)$$

$$\frac{1750 \cdot X_2 + 1428 \cdot X_3 + 1600 \cdot X_6}{1,500,000} > 1500 \quad (5)$$

$$\frac{1750 \cdot X_2 + 1428 \cdot X_3 + 1600 \cdot X_6}{1,500,000} < 1700 \quad (6)$$

$$X_2 < 800,000 \quad (7)$$

$$X_2 > 300,000 \quad (8)$$

$$X_3 > 250,000 \quad (9)$$

$$X_6 < 1,500,000 \quad (10)$$

$$X_2, X_3, X_6 \geq 0 \quad (11)$$

Here,

X_2 : Amount of coal from stock of Kızık, t.

X_3 : Amount of coal from stock of marl, t.

X_6 : Amount of coal from B3 level, t.

The objective function for Unit 1, Unit 2 and Unit 3 maximizing the second blend's calorific value restricted by a subjected constraint is shown in Equation 12.

$$\text{max } Z = \frac{1675 X_1 + 1750 X_2 + 2000 X_4 + 1800 X_5 + 1600 X_6}{4,500,000} \quad (12)$$

The restrictions are shown in Equations 13 to 21.

$$X_1 + X_2 + X_4 + X_5 + X_6 = 4,500,000 \quad (13)$$

$$\frac{1675 X_1 + 1750 X_2 + 2000 X_4 + 1800 X_5 + 1600 X_6}{4,500,000} > 1650 \quad (14)$$

$$\frac{1675 X_1 + 1750 X_2 + 2000 X_4 + 1800 X_5 + 1600 X_6}{4,500,000} < 1850 \quad (15)$$

$$X_1 = 2,000,000 \quad (16)$$

$$X_2 = 300,000 \quad (17)$$

$$X_4 < 600,000 \quad (18)$$

$$X_5 < 600,000 \quad (19)$$

$$X_6 > 750,000 \quad (20)$$

$$X_1, X_2, X_4, X_5, X_6 \geq 0 \quad (21)$$

where,

X_1 : Amount of fine coal from processing plants, t.

X_2 : Amount of coal from stock of Kızık, t.

X_4 : Amount of coal from B1 level, t.

X_5 : Amount of coal from B2 level, t.

X_6 : Amount of coal from B3 level, t.

3.3 Solutions of Models

The LINDO package program is used to solve the models. The optimum quality and quantity results of the final tables for Unit 4 are shown in Table 3 (Kaya, 2000).

Table 3 Final results of model for Unit 4

Coal Types	Coal Amount (ton/year)	Heat Content (kcal/kg)
Stock of Kızık (X_2)	500.000*	1750
Stock of marl (X_3)	250.000*	1428
B ₁ Level (X_4)	750.000*	1600
Blend of Coals	1,500.000	1620.5*

*Optimum values at 7th iteration

As it may be seen in Table 3, the blend quality of the coal is found to be 1620 kcal/kg. This value is within the range of the specific design values of Unit 4. The final tables for Unit 1, Unit 2 and Unit 3 are shown in Table 4.

Table 4. Final results of model for Unit 4

Coal Types	Coal Amount (ton/year)	Heat Content (kcal/kg)
Fine coal (Xi)	2,000,000*	1675
Stock of Kızık		
x_1	300,000*	1750
B ₁ Level	600,000*	2000
B ₂ Level	600,000*	1800
B ₃ Level (X*)	750,000*	1600
Blend of Coals	4,500,000	1721.8*

* Optimum values 7th iteration

As it may be seen in Table 4, the quality of the blended coal is found to be 1721.8 kcal/kg. This value is within the calorific value range of Unit 1, Unit 2 and Unit 3.

If the results of these tables are considered together, it can be seen that the production goals are reached. In addition, it is crucial that the production of 1,750,000,000 tons of coal from B₃ allows the utilization of low quality coal and high productivity.

4 CONCLUSIONS

In this study, the blending problem of the Seyitömer coal region is modeled and solved by the linear programming method. The district has coal seams with coal of different quality and quantity, which results in an inability to fulfill the requirements of the nearby power plant. By considering the needs of the plant, together with the availability and physical structure of the region, the optimum coal blend, satisfying both quality and quantity provisions, is calculated. The models are solved by the LINDO operations research software package. It is possible for the B3 seam, which contains low quality coal, to be utilized in the blending process rather than be

treated as waste material. Less coal from the B₁ and B₂ seams is used with the addition of B₃ coal. The models reveal concrete and reasonable results.

REFERENCES

- Aykol, H., 1999, The Selection of Selective Mining Methods and Equipment at Coal Seams Containing Inter-burden, Ph.D. Thesis, Dokuz Eylül University, Izmir.
- Chanda, E.K. and Wilke, F.L., 1992. "An EPD Model of Open Pit Short Term Production Scheduling Optimization for Stratiform Ore Bodies", 23rd APCOM, SME, Colorado, pp. 759-768.
- Dijilani, M.C. and Dowd, P.A., 1994. "Optimal Production Scheduling in Open Pit Mines", Leeds University Mining Association Journal, pp. 133-141.
- Hillier, F. and Liebermann, G. 1995. "Dynamic Programming", Introduction to Operations Research, Chapter 11, McGraw Hill Pub. Co.
- Huang, S., 1993. "Computer-Based Optimization of Open-Pit Mining Sequences", IMM, Vol. 102, May, pp. A125-A133.
- Kaya, C., 2000. "Optimization by Linear Programming at SLE", License Thesis, DPU, Mining Eng. Dept., Kütahya, p. 20.
- Mann, C. and Wilke, F.L., 1992. "Open Pit Short Term Mine Planning for Grade Control-A Combination of CAD-Techniques and Linear Programming-", 23rd APCOM, SME, Colorado, pp.487-497.
- Meyer, M., 1969. "Applying Linear Programming to the Design of Ultimate Pit Limits", Management Science, Vol. 16, No. 2, October, pp. B121-B135.
- Öztürk, A., 1997, Yöneyem Araştırması (Operations Research), Ekin Kitabevi (Publications), Bursa.
- Smith, M.L. and You, T., 1995. "Mine Production Scheduling for Optimization of Plant Recovery in Surface Phosphate Operations", Int. J. of Surface Mining and Reclamation, Balkema, pp. 41-46.
- Sofrelec, 1967, Seyitömer Power Plant Project, Turkish Republic Electricity Affairs Institute, Ankara.
- Taha, H.A., 1992. "Dynamic (Multistage) Programming", Operations Research, An Introduction, 5th ed., Chap. 10, MacMillan Pub. Co., New York, pp. 345-382.